

Spring 2019

## **Impact of Glutathione Transporters on Subcellular Glutathione Pools and Cell Survival in *Saccharomyces Cerevisiae***

Crystal Conaway McGee

Follow this and additional works at: <https://scholarcommons.sc.edu/etd>



Part of the [Chemistry Commons](#)

---

### **Recommended Citation**

McGee, C. C.(2019). *Impact of Glutathione Transporters on Subcellular Glutathione Pools and Cell Survival in *Saccharomyces Cerevisiae**. (Doctoral dissertation). Retrieved from <https://scholarcommons.sc.edu/etd/5133>

This Open Access Dissertation is brought to you by Scholar Commons. It has been accepted for inclusion in Theses and Dissertations by an authorized administrator of Scholar Commons. For more information, please contact [digres@mailbox.sc.edu](mailto:digres@mailbox.sc.edu).

IMPACT OF GLUTATHIONE TRANSPORTERS ON SUBCELLULAR GLUTATHIONE  
POOLS AND CELL SURVIVAL IN *SACCHAROMYCES CEREVISIAE*

by

Crystal Conaway McGee

Bachelor of Science  
Albany State University, 2011

---

Submitted in Partial Fulfillment of the Requirements

For the Degree of Doctor of Philosophy in

Chemistry

College of Arts and Sciences

University of South Carolina

2019

Accepted by:

Caryn E. Outten, Major Professor

Thomas M. Makris, Chairman, Examining Committee

John J. Lavigne, Committee Member

Norma Frizzell, Committee Member

Cheryl L. Addy, Vice Provost and Dean of the Graduate School

© Copyright by Crystal Conaway McGee, 2019  
All Rights Reserved.

## DEDICATION

To my first child, Jerrod Kentrell McGee Jr., thank you for giving my life purpose. Before your conception, the choices I made were on a whim. I felt as if my dreams could not affect anyone other than me. For every new life adventure, I was bright-eyed and bushy-tailed. Though, I lacked serious focus. Each goal set was only done with the consideration of a few years. To most people my choices were not inherently flawed. However, I had a narrowed life vision. Having you in my life makes me want to pursue greater things, even if those things come at some risk. You have inspired me to be bold and take unconventional routes. Whenever I felt like giving up hope, your kicks reminded me that someone was depending on me. After your birth, I would look down at your little face and knew that I wanted you to have a mother that you can be proud of. Even though you are just a baby, you have given me the strength to keep pushing forward. For those reasons, I am dedicating this dissertation to you. It is my hope that the motivation that you have given me to complete my PhD will inadvertently motivate you to pursue your life goals.

## ACKNOWLEDGEMENTS

Dr. Caryn E. Outten, thank you for allowing me to be a member of your research group. You have been incredibly patient and supportive in my growth as a scientist. The critical thinking skills obtained under your guidance helped me become an independent thinker and to thoroughly examine details. Both skills will be beneficial in my career endeavors. The networking experiences you afforded me through conference travels are also sincerely appreciated. I cannot thank you enough for your dedication to mentoring me as a graduate student. I, too, wish to thank my committee members Dr. Thomas Makris, Dr. John Lavigne, Dr. Lewis Bowman, and Dr. Norma Frizzell for taking the time to assess my work. Your suggestions helped me better evaluate data and solve difficult questions. In addition to serving as my committee chair, Dr. Thomas Makris, you have always been a wealth of knowledge. Throughout my studies, you allowed me to use your lab's equipment and supplies when needed. I just want to express thanks for your generosity.

My colleagues in biochemistry have been wonderful friends. I want to thank each of you for helping me with the ups and downs of graduate research. First, I would like to thank William Booth. You guided me through graduate life since interviewing for the Integrated Biomedical Science Program to selecting a lab in the Department of Chemistry and even currently notifying me of opportunities. I am sure we will be friends for life. Many students from Dr. Makris's group have offered great conversation and help whenever I came to their lab. Hence, I would like to thank the entire group. Though, an extra thanks

goes to Jason Hsieh. Without hesitation you have helped me with troubleshooting experiments, the proposal examination, and even potential job opportunities. From Dr. Wayne Outten's group, I would like to thank Naimah Ogunleye and Matthew Blahut. You have been great to talk with when I needed encouragement during failed experiments. You were also very helpful if I needed to use equipment or supplies. My lab-mates within the Caryn Outten group, past and current, have all been a boundless resource. I am glad to have worked with such wonderful people. I especially would like to thank Malini, T.T., and Debolina for your expertise in your fields and for the friendly conversation. Our memories as graduate students will always be special to me.

My dear husband, Jerrod McGee, our love story began with me in graduate school. Since, you have brought so much joy to my life. You have always believed in me through this entire process, particularly when I felt discouraged. I am grateful to have you as a husband. I love you dearly and cannot wait to see what our future holds. To my family, I want to thank you for always being there for me. Because of you, there was never a point in life where I questioned my worthiness or felt unloved. If ever I needed to talk about graduate life, I could always count on one of you to listen with care and compassion. Each conversation would end with words of encouragement. You were a huge driving force for me completing my PhD. It is my hope that by obtaining this degree, I will bring you honor and make you proud.

## ABSTRACT

Thiol-disulfide redox homeostasis is integral for maintaining the redox status of proteins and other thiol-containing molecules within cells. Mitochondria are particularly vulnerable to disruptions in redox balance, due to production of reactive oxygen species (ROS) during oxidative metabolism. Among the many antioxidants and detoxifying enzymes existing in mitochondria, glutathione (GSH) has proven to be critical for the preservation of function and structural integrity of the organelle. Therefore, our studies are aimed at elucidating the factors that control mitochondrial GSH metabolism in the model eukaryote *Saccharomyces cerevisiae* (baker's yeast). A critical component of understanding subcellular GSH homeostasis is identifying routes of entry into the organelle. Using genetic modifications combined with targeted redox-sensitive green fluorescent protein-based probes, previous studies found that GSH enters the mitochondrial intermembrane space (IMS) through porins located in the outer mitochondria membrane via passive diffusion. These studies demonstrated that reduced (GSH) and oxidized glutathione (GSSG) pools of the cytosol and IMS are interconnected. On the contrary, the GSH redox potential ( $E_{\text{GSH}}$ ) of the mitochondrial matrix was found to be separate from that of the cytosol. While attempts have been made to uncover a mitochondrial GSH/GSSG importer, none have been confirmed with certainty. Our current studies are aimed at identifying a mitochondrial transporter specific for GSH and biological processes that affect mitochondrial GSH/GSSG pools. Furthermore, we tested the effects of GSH and

GSSG overaccumulation on the mitochondria of yeast cells overexpressing the high affinity GSH/GSSG transporter, Hgt1. We also explored the possibility that plasma membrane-localized Hgt1 exhibits dual localization to the mitochondrial membrane. We find that *HGT1* overexpression in strains incubated with GSH and GSSG leads to GSH and GSSG accumulation in mitochondria as well as the cytosol. However, Hgt1 does not appear to be localized to mitochondria. Intercompartmental cross-talk is also thought to regulate subcellular GSH:GSSG pools. Therefore, we investigated if vacuolar storage of excess GSH could affect mitochondrial GSH concentrations. Our subcellular GSH measurements imply that *HGT1* overexpression affects mitochondrial GSH pools and the vacuole acts as a buffering compartment during GSH and GSSG overaccumulation.

The physiological role of GSH depletion on cellular function and subcellular redox status has been well characterized. Mitochondrial GSH has been reported to be critically important because of its roles in redox homeostasis and iron metabolism. High intracellular GSH has also been shown to be toxic to cells, yet it has not been determined how cells depleted of GSH (*gsh1Δ*) respond to increased GSH uptake. To study this, we employed a *gsh1Δ* yeast strain engineered to overexpress *HGT1*. Interestingly, our results show that *HGT1* overexpression alone can partially rescue growth in cells devoid of GSH and reverse some of the iron-related phenotypes. We demonstrate that cysteine is a key amino acid for rescue, suggesting that cysteine may partially substitute for GSH in *gsh1Δ* cells. However, we did not find significantly increased cysteine levels in *HGT1* overexpressing strains, leaving open the specific mechanism whereby *HGT1* overexpression compensates for the lack of GSH.

## TABLE OF CONTENTS

DEDICATION .....	iii
ACKNOWLEDGEMENTS .....	iv
ABSTRACT .....	vi
LIST OF TABLES .....	xi
LIST OF FIGURES .....	xii
LIST OF ABBREVIATIONS .....	xiv
CHAPTER 1: Introduction and Scope of Thesis .....	1
Thiol Redox Pathways/Regulation .....	1
Biosynthesis and Regulation of GSH .....	5
Subcellular Distribution of GSH.....	8
GSH Transporters .....	9
Mitochondrial GSH.....	12
Iron Regulation and GSH Metabolism in <i>Saccharomyces cerevisiae</i> .....	17
Scope of Thesis.....	22
References.....	25
CHAPTER 2: Exchange of Glutathione Between Vacuolar and Mitochondrial Pools with GSH or GSSG Overaccumulation in <i>Saccharomyces cerevisiae</i> .....	37
Abstract.....	37

Introduction.....	38
Experimental Procedures .....	41
Results.....	43
Discussion.....	50
References.....	53
<b>CHAPTER 3: Identifying a Mitochondrial Glutathione Transporter in <i>S. cerevisiae</i>.....</b>	<b>56</b>
Abstract.....	56
Introduction.....	57
Experimental Procedures .....	60
Results.....	66
Discussion.....	73
References.....	79
<b>CHAPTER 4: Overexpression of the Yeast High Affinity Glutathione Transporter, Hgt1, Rescues Growth in Cells Lacking <math>\gamma</math>-Glutamylcysteine Synthetase .....</b>	<b>83</b>
Abstract.....	83
Introduction.....	84
Experimental Procedures .....	87
Results.....	90
Discussion.....	114
References.....	117
<b>CHAPTER 5: Supplementary Methods .....</b>	<b>121</b>
Introduction.....	121
Small Scale Mitochondria Isolation .....	122

GSH/GSSG Assay Using Synergy H1 Plate Reader .....	125
Large Scale Mitochondria Isolation and Purification .....	128
Extraction of Plasma Membrane Proteins from Whole Cells.....	132
GSH Uptake in Isolated Yeast Mitochondria .....	133
Chromosomal Replacement-Cloning of the <i>GSH1</i> Deletion Plasmid .....	135
Growth Curve Assay- Synergy H1 Plate Reader .....	137
References.....	139

## LIST OF TABLES

TABLE 3.1 Primers used to check for <i>HGT1</i> deletion.....	61
TABLE 3.2 Primers used to make pGSH1KO .....	62

## LIST OF FIGURES

FIGURE 1.1 Thiol-Disulfide Redox Systems .....	2
FIGURE 1.2 Trx Fold Proteins Architecture .....	4
FIGURE 1.3 GSH Biosynthesis Pathway .....	7
FIGURE 1.4 Schematic of Known and Predicted GSH Transporters in <i>Saccharomyces Cerevisiae</i> .....	13
FIGURE 1.5 Mitochondrial GSH Transport .....	16
FIGURE 1.6 Model For Regulation of Aft1/2 By Fe-S Cluster Binding in <i>S. cerevisiae</i> .	21
FIGURE 2.1 Disruption in Vacuolar Storage Causes Increased Mitochondrial Accumulation of GSH in <i>HGT1</i> Expressing Strains.....	44
FIGURE 2.2 GSH Overaccumulation Increases GSSG Steady-State Levels in the Cytosol and Mitochondria of WT and <i>ycf1Δ</i> Strains Overexpressing <i>HGT1</i> .....	46
FIGURE 2.3 Disruption in Vacuolar Storage Causes Accumulation of Cytosolic and Mitochondrial Total GSH in High GSSG Stress .....	48
FIGURE 2.4 GSSG Overaccumulation in <i>HGT1</i> Strains Increases GSSG Steady-State Levels in the Cytosol and Mitochondria of WT and <i>ycf1Δ</i> Strains .....	49
FIGURE 3.1 Incubation of 100 μM GSH in Yeast Overexpressing <i>HGT1</i> Increases Cytosolic and Mitochondrial GSH.....	67
FIGURE 3.2 Deletion of <i>HGT1</i> Impairs Uptake of Cytosolic GSH But Has No Effect on Mitochondrial GSH.....	69
FIGURE 3.3 Hgt1-HA is Localized to Crude Mitochondrial Fractions .....	70
FIGURE 3.4 Hgt1-HA is Localized to Purified Mitochondrial Fractions.....	72
FIGURE 3.5 Plasma Membrane Contamination of Purified Mitochondria is Not Due to Num1 Mito-ER Tethering.....	74

FIGURE 3.6 <i>HGT1</i> Overexpression in <i>gsh1Δ</i> Strains Does Not Increase GSH Uptake into Isolated Mitochondria .....	75
FIGURE 4.1 Confirmation of <i>gsh1Δ</i> + Vector and <i>gsh1Δ</i> + <i>HGT1</i> Phenotypes.....	91
FIGURE 4.2 <i>HGT1</i> Overexpression Rescues the Growth Defect in <i>gsh1Δ</i> Cells and Causes Increased Sensitivity to GSH.....	93
FIGURE 4.3 WT and <i>gsh1Δ</i> Strains Overexpressing <i>HGT1</i> Are Sensitive to Extracellular GSSG .....	94
FIGURE 4.4 Overnight Incubation of <i>gsh1Δ</i> Strains With Increasing GSH Concentrations Led to Less GSH Accumulation in <i>gsh1Δ</i> + <i>HGT1</i> .....	96
FIGURE 4.5 Kinetic Measurements of GSH Content in <i>gsh1Δ</i> + Vector and <i>gsh1Δ</i> + <i>HGT1</i> .....	97
FIGURE 4.6 <i>HGT1</i> Overexpression Partially Rescues the Growth Defect of <i>gsh1Δ</i> Strains .....	99
FIGURE 4.7 Cysteine is a Key Amino Acid for Rescue of <i>gsh1Δ</i> When <i>HGT1</i> is Overexpressed.....	101
FIGURE 4.8 Cysteine Improves Growth of <i>gsh1Δ</i> + <i>HGT1</i> Cells in SC Media .....	102
FIGURE 4.9 DTT Restores Growth of <i>gsh1Δ</i> + <i>HGT1</i> Strains on Minimal 6AA/B Media .....	103
FIGURE 4.10 <i>gsh1Δ</i> + <i>HGT1</i> Strains Are Viable After 48 Hours Without GSH Supplementation .....	105
FIGURE 4.11 Cysteine Uptake Is Not Responsible For Growth of <i>gsh1Δ</i> + <i>HGT1</i> Strains in SC Media .....	106
FIGURE 4.12 Subcellular GSH Measurements of <i>gsh1Δ</i> + Vector and <i>gsh1Δ</i> + <i>HGT1</i> Strains Grown in Various GSH Concentrations .....	108
FIGURE 4.13 <i>gsh1Δ</i> + <i>HGT1</i> Cells Can Grow on Fermentable, Partially Fermentable, and Non-Fermentable Carbon Sources .....	110
FIGURE 4.14 Deletion of <i>glr1</i> Does Not Impact the Rescue of <i>gsh1Δ</i> by <i>HGT1</i> Overexpression .....	112
FIGURE 4.15 Defects in Iron Regulation Are Partially Rescued by <i>HGT1</i> Overexpression in a <i>gsh1Δ</i> Strain.....	113

## LIST OF ABBREVIATIONS

ABC	ATP-binding cassette
Aft	activator of ferrous transport
ARN	Aft1 regulon
Atm1	ABC transporter, mitochondrial
Bcl2	B-cell lymphoma 2
Bpt1	bile pigment transporter 1
Cys	cysteine
DIC	dicarboxylate carrier
DNA	deoxyribonucleic acid
DTT	dithiothreitol
ER	endoplasmic reticulum
Fe-S	iron-sulfur
G1	Gap 1
Gex	glutathione exchanger
GFP	green fluorescent protein
GLR	glutathione reductase
Gpx	glutathione peroxidase
GRX	glutaredoxin
GSH	reduced glutathione

Gsh1 .....  $\gamma$ -glutamyl cysteine synthase  
 Gsh2 ..... glutathione synthetase  
 GSSG ..... oxidized glutathione  
 GS-S-SG ..... GSH polysulfide  
 Gxa1 ..... glutathione export ABC protein  
 HA ..... hemagglutinin  
 Hgt1 ..... high affinity glutathione transporter  
 H<sub>2</sub>O<sub>2</sub> ..... hydrogen peroxide  
 IMS ..... intermembrane space  
 mGSH ..... mitochondrial glutathione  
 MnSOD ..... manganese superoxide dismutase  
 MRP1 ..... multidrug resistance protein 1  
 NADPH ..... nicotinamide adenine dinucleotide  
 O<sub>2</sub><sup>•-</sup> ..... superoxide anion  
 OGC ..... 2-oxoglutarate carrier  
 •OH ..... hydroxyl radical  
 OMM ..... outer mitochondrial membrane  
 Opt ..... oligopeptide transporter  
 PMS ..... post-mitochondrial supernatant  
 Por ..... porin  
 PRX ..... peroxiredoxin  
 roGFP ..... redox-sensitive green fluorescent protein  
 ROS ..... reactive oxygen species

rxYFP..... redox-sensitive yellow fluorescent protein  
SC..... synthetic complete  
SDS..... sodium dodecyl sulfate  
6AA/B..... six amino acids and bases  
SOD..... superoxide dismutase  
SSA..... 5-sulfosalicylic acid  
TMD..... transmembrane domain  
TRR..... thioredoxin reductase  
TRX..... thioredoxin  
YCT1..... yeast cysteine transporter

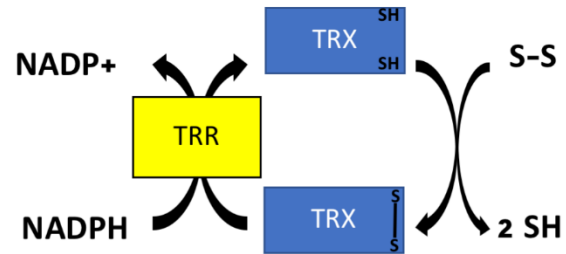
## CHAPTER 1

### INTRODUCTION AND SCOPE OF THESIS

#### **Thiol Redox Pathways/Regulation**

Thiol redox biochemistry is assumed to play a pivotal role in understanding cellular processes such as oxidant-dependent signaling and cell fate decisions (1). Oxidants in the form of reactive oxygen species (ROS) have potentially toxic effects and are linked to neurodegenerative disorders, aging, and cancer (2). To prevent hyper-oxidation, cells depend on the concerted efforts of antioxidants and detoxifying enzymes (3). For instance, the thioredoxin (TRX) and glutathione (GSH)/ glutaredoxin (GRX) pathways are conserved thiol-reductase systems that maintain cellular redox homeostasis via disulfide-exchange reactions (4). TRXs and GRXs are small oxidoreductases (usually 9-15 kDa) of the Trx-fold oxidoreductase superfamily that reduce disulfides via the CXXC cysteine (Cys) residues in their active sites. TRXs donate electrons to reduce protein disulfides resulting in oxidation of the CXXC active site. Oxidized TRXs are reduced back to the dithiol form by the flavoenzyme TRX reductase (TRR) using NADPH as a reducing equivalent. GRXs are also capable of catalyzing the reduction of disulfide-oxidized protein substrates or GSH mixed disulfides. GSH also serves as a reducing agent and cofactor for oxidized GRXs. Oxidized GSH (GSSG) is reduced and regenerated to GSH by GSSG reductase (GLR) at the expense of NADPH (Fig. 1.1) (5, 6).

### TRX System



### GSH/GRX System

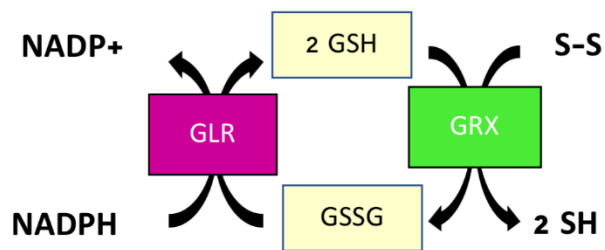


**Figure 1.1 Thiol-Disulfide Redox Systems.** Model illustrating the TRX and GSH/GRX redox regulatory pathways. TRR= TRX reductase, GLR= GSSG reductase.

The first TRX discovered was isolated from *E. coli* and identified as an electron donor for ribonucleotide reductase, the enzyme providing deoxyribonucleotides for DNA replication (7). In later studies involving mutants lacking TRXs, GRXs were also found to effectively reduce ribonucleotide reductase. Cells rely on ribonucleotide reduction for not only DNA synthesis but also sulfate reduction to generate reduced sulfur in the form of cysteine and reduction of methionine sulfoxide (8, 9). Further research revealed that the biological activities in which TRXs and GRXs are involved have grown considerably beyond DNA replication.

TRX and GRX share a very similar structural identity and are conserved throughout evolution. The TRX protein family is defined by a structural motif named the TRX fold which consists of four stranded  $\beta$ -sheets flanked by three  $\alpha$ -helices on either side of the  $\beta$ -sheets (Fig. 1.2) (7, 9). Proteins within the TRX family share a common Cys-X-X-Cys active-site motif. Interestingly, amino acids between the two cysteines vary between the TRX and GRX proteins. The active site motif of TRXs is Cys-Gly-Pro-Cys, whereas GRXs are subdivided into two subfamilies: dithiol and monothiol GRXs. Dithiol GRXs contain Cys-Pro-Tyr-Cys or Cys-Pro-Phe-Cys active site motifs and monothiol GRXs have a Cys-Gly-Phe-Ser motif. Despite variations in the active sites, monothiol and dithiol GRXs share the TRX-fold structure (10, 11).

The primary role of the TRX or GSH/GRX pathways in *E. coli* is their involvement in ribonucleotide reduction (12). TRX and GRX functionally overlap in prokaryotes. Therefore, *E. coli* is viable if either pathway is deleted while inactivation of both pathways is lethal (13). *S. cerevisiae* contain a complete set of the TRX and GSH/GRX pathways in the

## Thioredoxin fold

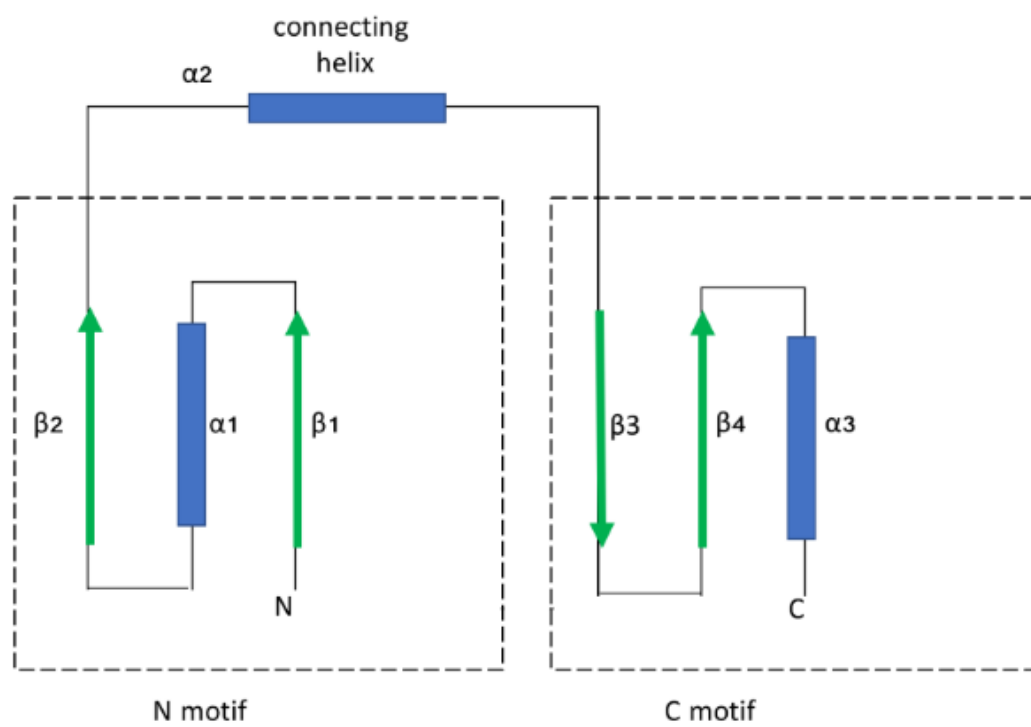


**Figure 1.2 TRX fold proteins architecture.**  $\beta$ -sheet strands are depicted as arrows and  $\alpha$ -helices as rectangles. The dashed lines indicate separation of the fold into N-terminal ( $\beta\alpha\beta$ ) and C-terminal ( $\beta\beta\alpha$ ) motifs which are connected by the  $\alpha 2$  helix (14).

cytosol and mitochondrial matrix. The cytosolic TRX pathway consists of two TRX isoforms (Trx1 and Trx2) and a TRR (Trr1). The mitochondrial matrix contains a TRX (Trx3) and TRR (Trr2). Similarly, the cytosolic GSH/GRX pathway is comprised of two dithiol GRXs (Grx1, Grx2) and GLR (Glr1). In the mitochondrial matrix, there exists Glr1 and Grx2. Dual localization of Glr1 and Grx2 to the cytosol and mitochondria is due to an alternative start site upstream of the canonical one, thereby creating a N-terminal mitochondrial targeting sequence (15–17). Inactivation of Glr1 together with cytoplasmic TRXs or with Trr1 in yeast is synthetically lethal (18, 19). On the contrary, deletion of both cytoplasmic TRXs or the dithiol GRXs does not affect viability. Yeast containing a single gene deletion of the gene encoding  $\gamma$ -glutamylcysteine synthetase (*GSH1*), the rate-limiting enzyme in GSH biosynthesis, are unable to survive without GSH supplementation (20). This essential nature of GSH in yeast and higher organisms has made determining its contribution to thiol-redox control challenging and thus the primary function of GSH has been a topic of debate (12).

### **Biosynthesis and Regulation of GSH**

GSH is the most abundant small intracellular thiol (–SH) molecule in eukaryotic cells. Its high intracellular concentration (between 3 and 10 mM) and negative redox potential (–240 mV) enables GSH to provide reducing capacity for a number of biological reactions (21, 22). As an antioxidant, GSH serves as an electron donor for GSH peroxidases that detoxify hydrogen peroxide by catalyzing its reduction to water (23). Furthermore, glutathione S-transferases (GSTs) are able to rid the cell of xenobiotics by forming GSH-dependent conjugates (24). In addition to its function as a thiol-redox buffer,

GSH is involved in iron-sulfur (Fe-S) cluster biogenesis, redox signaling, apoptosis, and metabolism of heavy metals (25, 26).

GSH is synthesized in the cytosol from the amino acids glutamate, cysteine, and glycine via two conserved ATP-dependent steps catalyzed by the enzymes  $\gamma$ -glutamylcysteine synthetase (Gsh1) and GSH synthetase (Gsh2) (27). In the first step, cysteine and glutamate are linked by Gsh1 to form  $\gamma$ -glutamylcysteine. The first reaction is the rate-limiting step and is regulated by cysteine availability. GSH is formed in the second reaction by Gsh2, which covalently links glycine to  $\gamma$ -glutamyl-cysteine (Fig. 1.3) (28). While GSH is only made in the cytosol, its functions are required in other organelles such as the nucleus, endoplasmic reticulum, and mitochondria. In the nucleus, GSH maintains the redox state of critical protein sulfhydryls involved in DNA repair and expression, and functions as a hydrogen donor for ribonucleotide reductase as mentioned previously (29). GSH is also found in the ER and mitochondrial intermembrane space (IMS) where thiol-containing proteins are oxidatively folded by disulfide oxidases and members of the protein disulfide isomerase (PDI) family. In these compartments, GSH is thought to function in disulfide proofreading by reducing mismatched disulfide bonds to ensure proper oxidative folding of imported proteins (30–33). Fe-S cluster biogenesis within the mitochondrial matrix also relies on distinct GSH pools within the organelle (34, 35). Variations in GSH requirement in each organelle is accompanied by differences in total GSH concentration and the reduced to oxidized ratio. For instance, the GSH:GSSG ratio in the endoplasmic reticulum (ER) is <7:1 suggesting that the ER is relatively oxidizing (36). On the contrary, the cytosol and nucleus are very reducing with a GSH:GSSG ratio of 3000:1, while the mitochondrial matrix has a GSH:GSSG ratio of 900:1 (4).

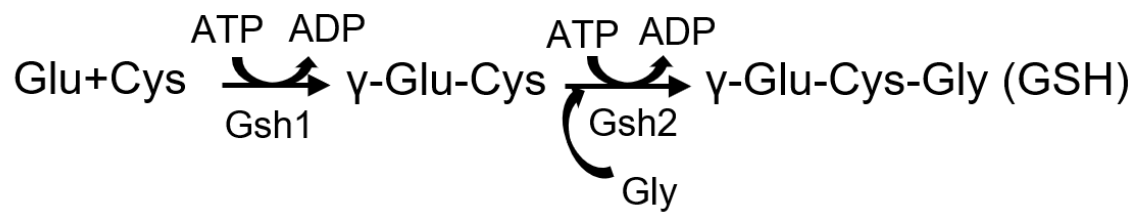


**Figure 1.3 GSH biosynthesis pathway.** GSH is synthesized in the cytosol via a two-step ATP-dependent enzymatic process. In the first step,  $\gamma$ -glutamylcysteine is formed by  $\gamma$ -glutamylcysteine synthetase (Gsh1). In the second step, glycine is added to the peptide via GSH synthetase (Gsh2).

## **Subcellular Distribution of GSH**

Intracellular GSH pools are composed of GSH that is either synthesized in the cytosol or imported from the extracellular environment. Therefore, distribution of GSH to subcellular compartments is thought to occur through permeable pores and GSH-specific transporters. Targeted fluorescent probes genetically engineered to equilibrate with GSH have made it possible to study redox control pathways and transport into organelles. Hu and coworkers were the first to look at GSH equilibration between the cytosol and IMS of yeast. In this study, they used a redox-sensitive yellow fluorescent protein (rxYFP) localized to the IMS. They discovered that the GSH:GSSG redox potential ( $E_{\text{GSH}}$ ) measured by IMS-rxYFP (-255 mV) is distinct from redox measurements in the cytosol (-286 mV) and mitochondrial matrix (-296 mV), since it was more oxidized than the other compartments (37). A subsequent study demonstrated that the oxidizing environment previously measured in the IMS is due to limiting amounts of GRXs available to catalyze equilibration of GSH with IMS disulfides (38). Evidence of GSH permeation via pores in the outer mitochondrial membrane (OMM) was later established by Kojer et al. The authors also used a redox-sensitive fluorescent protein (roGFP2) targeted to the IMS; however, in this study human Grx1 was fused to roGFP2 to facilitate rapid equilibration with local GSH:GSSG pools. By monitoring the dynamic changes in  $E_{\text{GSH}}$  of cells that were exposed to oxidants which were subsequently removed, they were able to explore interplay between subcellular compartments. They found that GSH pools of the IMS equilibrate with the cytosol. Furthermore, evidence for the role of porins in mitochondrial GSH import was found using strains lacking Por1 (*por1* $\Delta$ ). The OMM contains two porins, Por1 and Por2.

Deletion of Por1, the predominant isoform, caused the IMS GSH redox pool to be more oxidized and therefore no longer in equilibrium with the cytosol (39).

Free diffusion of GSH from the cytosol to the nucleus is thought to occur via the nuclear pore complex. The connections between cytosolic and nuclear GSH was established in plant *Arabidopsis thaliana*. It was discovered that GSH was recruited to the nucleus during G1 phase of cell growth. The accumulation of GSH in the nucleus is, therefore, critical for cellular proliferation (40, 41). Increased GSH in nucleus was also linked to severe depletion of cytoplasmic GSH pools (40). In mammalian cells, the anti-apoptotic protein Bcl2, which promotes cell survival, has been identified as a candidate GSH-recruiting protein to the nuclear envelope. Bcl2 was suggested to form a pore-like structure which may be responsible for GSH sequestration to the organelle (41, 42).

### **GSH Transporters**

The transport of GSH across many different membranes within a variety of organisms has been well documented. However, only a few GSH transporters have been identified. The first known GSH transporters were the mammalian multidrug resistance protein and yeast Ycf1 belonging to the ATP-binding cassette (ABC) transporter superfamily. The proteins were found to efflux excess GSH out of the cytoplasm at the plasma membrane of mammalian cells and vacuolar membrane in *S. cerevisiae*, respectively (43, 44). These transporters have a broad range of substrates and a relatively low affinity for GSH with a  $K_m$  of approximately 15 mM (45, 46). Furthermore, they were shown to facilitate excretion from the cytosol and subsequent degradation of GSH and

GSSG (45). Thus, the first identification of proteins that transport GSH, although with low affinity, were not representative of GSH uptake.

More recently, a yeast genomic search for candidate GSH transporters in *S. cerevisiae* led to the discovery of the plasma membrane-localized Hgt1/Opt1 as the first high affinity GSH transporter. Hgt1 belongs to a novel and structurally uncharacterized oligopeptide transporter (OPT) family. The OPT family of transporters are known to mediate the uptake of tetra- and pentapeptides such as endogenous opioids leucine enkephalin (Tyr-Gly-Gly-Phe-Leu) and methionine enkephalin (Tyr-Gly-Gly-Phe-Met). However, the affinity for these peptides was relatively low, with a  $K_m = 310 \mu\text{M}$  compared to reduced GSH ( $K_m = 54 \mu\text{M}$ ) and oxidized GSSG ( $K_m = 91 \mu\text{M}$ ). Homologues of Hgt1 can be found in fungi, plants, bacteria, and archaea. The importance of GSH transport across the plasma membrane of mammalian cells has been established, yet no Hgt1 human homologues have been identified (47–49).

Many structural and mechanistic aspects of members of the OPT family are unknown. However, the dependency of the OPT members on proton-coupled transport has been established. In efforts to identify the substrate binding residues of Hgt1, an alanine scanning mutagenesis of polar or charge residues was done in the putative transmembrane domain. This study revealed four transmembrane domains (TMD1, TMD4, TMD9, TMD12) and a proline rich intracellular loop (537-568) that are critical for GSH transport. Residues N124 of TMD1, Q222 of TMD4, Q526 of TMD9 and K562 of the intracellular loop were found to directly or indirectly interact with GSH. A later analysis of residues important for substrate recognition revealed that both Q526 and F523 of TMD9 are required. Both residues are also conserved among OPT members known to uptake GSH

(50). Characterization of Hgt1 has been an important step as it provides a model for how transporters bind and transport GSH across membranes (51).

Intercompartmental transport of GSH and GSSG is hypothesized to be a key contributor to the regulation of GSH homeostasis in subcellular compartments. Therefore, many studies have been designed to explore factors that influence organelle specific GSH pools and identify subcellular transporters. For instance, Ycf1 has been known to help regulate cytosolic GSH:GSSG ratio by sequestering excess GSSG to the vacuole that has not been reduced by thiol-reductase systems (52). A second vacuolar GSH transporter Bile pigment transporter 1, Bpt1, has been identified in *S. cerevisiae*. This protein has a higher affinity for GSH ( $K_m = 3$  mM) compared to Ycf1 ( $K_m = 15$  mM). Yet, Bpt1 is less capable of transporting GSH (53). Glutathione Exchanger (Gex1) and its paralogues Gex2 are confirmed GSH transporters belonging to the Aft1 regulon (ARN) family. Gex1/2 are mostly at the plasma membrane in early exponential growth phase and at the vacuolar membrane in late exponential phase. When on the plasma membrane, Gex1/2 mediates cytosol acidification and the expulsion of GSH. The authors hypothesized that the lower pH in the cytosol induces the targeting of Gex1 to the vacuolar membrane resulting in GSH import and export of  $H^+$ . Unlike other members of the ARN family, Gex1/2 are not regulated by the activator of ferrous transport protein 1 (Aft1). Instead, the transporters are regulated by its paralog Aft2. Gex1/2 also differ from members of the ARN family because they are not involved in the transport of known iron-binding siderophores, but instead support GSH intercompartmental exchange (54). Along with Gex1/2, yeast is thought to possess another GSH export protein, Gxa1, belonging to the ABC family. The suggestion that Gxa1 is a GSH exporter was based on a study showing that overexpression of *GXA1*

leads to a significant increase in intracellular GSH in yeast defective in extracellular GSH utilization (55). Another example of how intercompartmental cross-talk could potentially affect the subcellular environment can be seen in the Opt2 transporter, a close homolog of Hgt1/Opt1. Opt2 was determined to be dually localized to the plasma membrane and peroxisomes of yeast. Interestingly, Opt2 was found to not only affect cytosolic and peroxisomal GSH:GSSG but mitochondrial GSH:GSSG as well (56).

In reference to other organelles, the endoplasmic reticulum (ER) is more oxidizing and early reports suggest that GSSG is selectively imported into the ER lumen (30). A subsequent study using rat liver microsomal vesicles found that reduced GSH is selectively imported into hepatic endoplasmic reticulum while GSSG is virtually nonpermeable. A portion of imported GSH is converted into GSSG by the intraluminal oxidation of GSH. Interestingly, GSSG generated in the microsomal lumen scarcely exited from the vesicles. Therefore, retention of GSSG in the ER may be responsible for an oxidizing environment (57). In a recent search to identify a candidate ER GSH transporter, Ponsero et al. screened null and temperature-sensitive mutants of genes encoding ER transmembrane proteins. As a result, protein-conducting channel Sec61 was found to transport GSH into the ER of *S. cerevisiae* by facilitated diffusion (58). The discovery of an ER transporter has added to the list of already identified GSH-specific transporters located in various membranes in *S. cerevisiae* (Fig. 1.4).

### **Mitochondrial GSH**

Mitochondria are a major source of energy in eukaryotic cells and the primary site of ROS production. Under normal physiological conditions, oxygen consumption in the

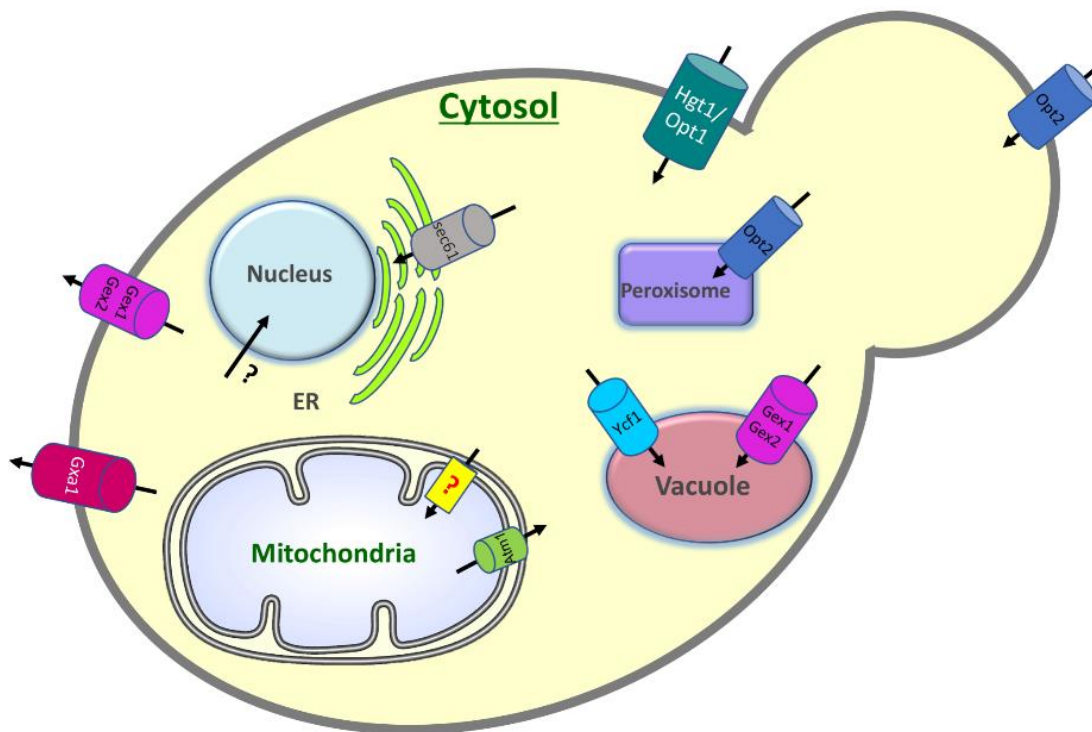


**Figure 1.4. Schematic of known and predicted GSH transporters in *Saccharomyces cerevisiae*.** GSH is exclusively made in the cytosol or may be imported from the extracellular environment. GSH synthesized and imported in the cytosol must be transported into subcellular compartments. The illustration shows known GSH transporters and organelles predicted to contain GSH transporters.

mitochondria involves four-electron reduction of molecular oxygen to water. However, incomplete transfer of electrons results in the formation of superoxide anion ( $O_2^{\cdot-}$ ) and hydrogen peroxide ( $H_2O_2$ ). In addition to the ROS generated during respiration, other toxic or pathological conditions can lead to an impairment of mitochondrial function causing an increase in ROS. Thus, mitochondria are constantly exposed to potentially damaging oxidant species. Yet, the organelle remains functional due to the existence of myriad antioxidant enzyme systems such as manganese superoxide dismutase (MnSOD), and the GSH/GRX and TRX pathways. Collectively, these enzymes and thiol redox systems combat deleterious ROS production. Evidence over recent years has demonstrated that mGSH is of particular importance in regulating the thiol redox environment (3, 59–61).

Mitochondrial GSH is mainly found in the reduced state and represents a small fraction of the total GSH pool (10–15%). Given the size of the mitochondrial matrix, however, the concentration of mGSH is similar to that of the cytosol (10–14 mM) (3). The primary form of ROS generated during mitochondrial respiration is superoxide ( $O_2^{\cdot-}$ ), a free radical with moderate reactivity. Superoxide can be dismutated to  $H_2O_2$  by SOD, which is the first line of antioxidant defense in the mitochondrial matrix.  $H_2O_2$  is a relatively mild oxidant. However, in the presence of transition metals such as  $Fe^{2+}$  and  $Cu^+$  it can be converted into the highly reactive hydroxyl radical ( $\cdot OH$ ) by the Fenton reaction (62). To rid the mitochondria of  $H_2O_2$ , cells rely on GSH peroxidase (Gpx) to rapidly reduce  $H_2O_2$  to water using reducing equivalents from GSH. Reduced mGSH becomes oxidized through the process of detoxification and is recycled back by the NADPH-dependent GSSG reductase (GLR). GSSG is not readily exported out of the mitochondria. Thus, GLR in this organelle is critical for maintaining redox homeostasis (63, 64).

Selective depletion of GSH in the mitochondria results in oxidant sensitivity, mitochondrial dysfunction, and disruption of iron regulation. Therefore, understanding factors that regulate mitochondrial GSH pools and identifying a mitochondrial GSH transporter is vital to our understanding of diseases characterized by low mitochondrial GSH (mGSH) (35). Evidence for distinct GSH pools in the mitochondrial matrix has prompted studies aimed at finding a GSH transporter on the mitochondrial membrane. Two members of the superfamily of anion carriers have been identified as potential mGSH transporters: dicarboxylate carrier (DIC) and 2-oxoglutarate carrier (OGC). Direct evidence of GSH uptake was shown when DIC and OGC were partially purified and reconstructed into proteoliposomes. In a separate study, using rat renal mitochondria, the transport of GSH by the anionic transporters was found to contribute to approximately 50% of observable transport (65, 66). On the contrary, research conducted by Booty et al. was unable to confirm GSH transport by OGC and DIC (67). The model used to study transport was created by first expressing human OGC and *S. cerevisiae* DIC in *Lactococcus lactis*. Uptake activity and substrate specificity was then assessed in *L. lactis* membranes containing OGC or DIC proteins that were fused with liposomes. These experiments were carried out in a simpler model compared to previous reports where the characterization of the individual transport processes can be difficult. Therefore, the authors believe that the *L. lactis* model system is better to explore GSH transport than previous systems because observed transport could have been due to secondary consequences of metabolite redistribution between the mitochondria and the cytosol (67). Neither of the yeast homologues of DIC or OGC has been determined to transport GSH. Therefore, an unambiguous mGSH transporter is yet to be confirmed (Fig. 1.5).

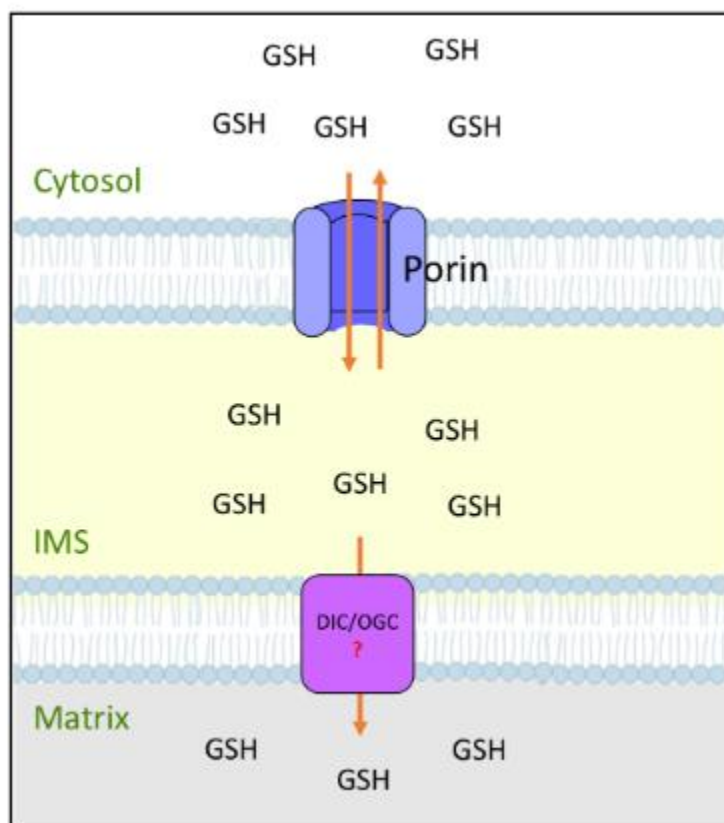


**Figure 1.5 Mitochondrial GSH transport.** Transport of GSH into the IMS of the mitochondria is dependent upon porins in the OMM. Dicarboxylate carrier (DIC) and the 2-oxoglutarate carrier (OGC) have been established as candidate transporters involved in the import of cytosolic GSH inside the mitochondria in mammalian cells but not in yeast cells. Modified from a figure generated by C. Outten.

As stated previously, yeast mitochondria possess a full set of TRX and GSH/GRX pathways. Currently, the only known function these pathways have are to assist mitochondrial peroxiredoxin (PRX) Prx1 and perhaps Gpx2 in protecting mitochondria against respiratory ROS as well as exogenous peroxide (68). GSH fulfills an additional role separate from its connection to the thiol-reductive systems, which is its involvement in iron metabolism. A recent report provides evidence that the role of GSH in regulating iron homeostasis may be the reason for the requirement of GSH for viability (12).

### **Iron Regulation and GSH Metabolism in *Saccharomyces cerevisiae***

Tight regulation of intracellular iron levels is important for eukaryotic cells as high iron can be toxic due to its role in catalyzing the formation of hydroxyl radicals via Fenton chemistry. Yet, it is indispensable for a variety of biological functions as a cofactor for several essential proteins such as Fe-S cluster proteins and hemoproteins. A few examples of important Fe-S proteins include DNA polymerases, nicotinamide adenine dinucleotide (NADH)-dehydrogenases, ferredoxins, and aconitases (26). Hemoproteins contain a heme prosthetic group allowing them to carry out oxidative functions. One famous example of this is hemoglobin, a protein within red blood cells that is responsible for transporting oxygen to tissues. Other important hemoproteins include cytochromes, myoglobin, catalases, and peroxidases (69). Therefore, it comes as no surprise that disturbances in iron homeostasis or Fe-S cluster biogenesis are linked to many iron-related diseases such as Parkinson's disease and anemia (11).

Regulation of iron in *S. cerevisiae* occurs primarily at the transcriptional level via the transcription factor Aft1 and its paralog Aft2 (70, 71). The iron sensing proteins

regulate iron by controlling iron-responsive genes that are responsible for acquisition, compartmentalization, and utilization of iron. Low iron conditions results in Aft1 transport from the cytosol into the nucleus where it binds to the conserved promoter sequence motif (T/CG/ACACCC) in the 5'-upstream regions of target genes. As a result, expression of genes involved in iron uptake (*FET3*, *FTR1*, and *FRE1,2*), siderophore uptake (*ARN1-4* and *FIT1-3*), and Fe-S cluster formation (*ISU1,2*) are induced (72–76). Iron-replete conditions causes Aft1 to become disassociated from target promoters and translocated back to the cytosol by the nuclear exporter Msn5. Aft2 is assumed to function in a similar manner due to its close homology to Aft1 (77).

Iron regulation by Aft1 is impacted by Fe-S cluster biogenesis occurring in the mitochondrial matrix of *S. cerevisiae*. This process happens in two distinct stages. In the first step, Fe<sup>2+</sup> and sulfur are joined on a scaffold protein (Isu). Sulfur is acquired through its release from cysteine by the cysteine desulfurase Nfs1. The function of Nfs1 is dependent on its complex with Isd11. Nfs1-Isd11 generates sulfane sulfur (S<sup>0</sup>) by persulfide formation. For Fe-S cluster synthesis to occur, sulfur (S<sup>0</sup>) must be reduced to sulfide (S<sup>2-</sup>) (78). This reduction is thought to occur in yeast via electron transfer by the ferredoxin-ferredoxin reductase pair Yah1 and Arh1 using electrons from NADPH (79–81). Yfh1, the yeast homologue of human frataxin, is proposed to deliver iron to the Isu protein (82). In the second stage, a chaperone helps release the newly synthesized Fe-S cluster from the scaffold and assist in its binding to the ISC transfer protein Grx5 (83). The synthesis of cytosolic and nuclear Fe-S proteins is dependent on the mitochondrial export of a still unknown compound via the mitochondrial inner membrane transporter Atm1 (84).

Direct links between iron metabolism and thiol-redox metabolism have been established in various reports. For instance, GSH polysulfide (GS-S-SG) has been identified as a substrate for Atm1. This discovery suggests that GSH may be involved in extramitochondrial Fe-S cluster assembly by assisting in the transport of activated persulfide ( $S^0$ ) from the mitochondria to the cytosol (34). Additionally, depletion of GSH leads to constitutive activation of the Aft1/2 iron regulon and disruption in the synthesis of extramitochondrial Fe-S clusters (12, 85). This effect is also seen in strains lacking Atm1 (85). Interestingly, Kumar et al. found that toxic levels of GSH in yeast cells leads to Aft1 accumulation in the nucleus and inhibits cytoplasmic Fe-S cluster maturation. Therefore, maintaining intracellular GSH levels is critical for cytosolic Fe-S-containing proteins.

Monothiol GRXs, Grx3 and Grx4, localized in the cytosol have also been identified as regulators of Aft1 activity and Fe-S cluster biosynthesis. The dissociation of Aft1 from its target promoters under iron-replete conditions was found to be dependent on its interaction with Grx3 and Grx4 (11). Ueta et al. reported that binding of Grx3 and Grx4 to an Fe-S cluster is a prerequisite for interactions with Aft1. The Atm1 transporter was also determined to be necessary for iron binding to Grx3 and dissociation of Aft1 from its target promoters (86). Using a genetic screen to find mutants that were involved in iron regulation, Kumánovics et al. discovered two unexpected cytosolic proteins, Fra1 and Fra2, that when deleted activated the iron regulon. Fra1 and Fra2 were shown to bind Grx3 and Grx4 in an iron-dependent manner. This complex inhibits Aft1 from entering the nucleus. Individual deletions of Fra1/2 or Grx3/4 causes Aft1 to be constitutively active and thereby nuclear localized (87–89).

The connection between Fe-S clusters biogenesis and Aft1 regulation has been well established. However, it was not until a study conducted by Poor et al. that the molecular mechanism for such regulation was unveiled. In this study, a crystal structure of Aft2 bound to DNA revealed a Zn finger motif that was essential for DNA binding. In addition, an [2Fe-2S] cluster was shown to bind Aft2 at the conserved CDC motif leading to its dimerization. Using UV-visible absorption and circular dichroism spectra, the authors were able to show that Aft2 receives a [2Fe-2S] cluster via direct Fe-S cluster transfer from [2Fe-2S]-bridged Grx3-Fra2 heterodimers. This study also revealed that the [2Fe-2S]-bridged Aft2 homodimer has a lower DNA binding, resulting in deactivation of the iron regulon. Collectively, these findings have allowed researchers to develop a mechanism for Aft1 regulation by Fe-S cluster biogenesis and a proposed model for iron regulation in *S. cerevisiae* has been created (Fig. 1.6) (90).

Molecular and genetic manipulation of yeast has proven to be a powerful tool in the understanding of iron regulation in eukaryotic cells. While significant progress has been made, there are still many gaps in our understanding in iron regulation and its role in thiol-redox control. For instance, we have yet to conclusively identify the sulfur-containing substance that is transported out of the mitochondria that is critical for the biogenesis of Fe-S proteins in the cytosol and nucleus. Identification of residues that are critical for binding of complex proteins responsible for Fe-S cluster transfer and determining factors that influence the efficiency of Fe-S transfer is still ongoing in the field of iron regulation. These details are vital as they can be used to uncover therapeutic targets in treating diseases related to disruptions in iron and thiol-redox homeostasis.

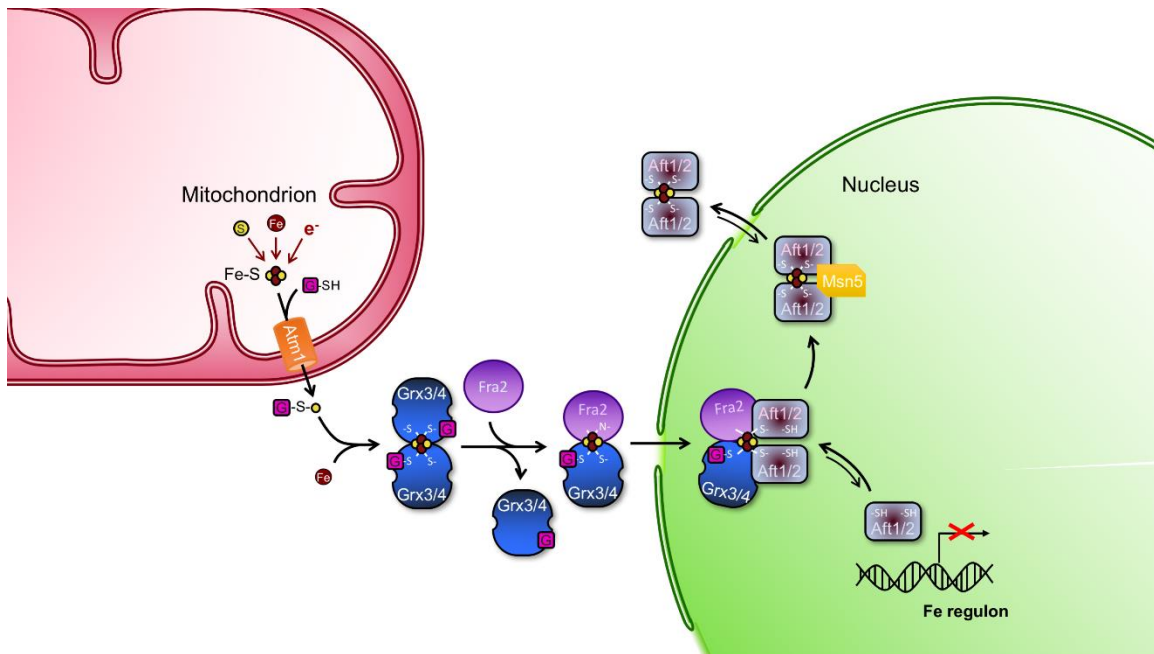


**Figure 1.6. Model for regulation of Aft1/2 by Fe-S cluster binding in *S. cerevisiae*.** Fe-S clusters are synthesized in the mitochondrial matrix by proteins in the Fe-S cluster assembly pathway. Once assembled, an unknown sulfur-containing substance is transported out of the mitochondria by the Atm1 transporter. GSH is required for the export process. Grx3 and Grx4 use GSH to help coordinate Fe-S clusters. This Grx3/4- [2Fe-2S] complex is thought to form a heterodimer with Fra2 that then relays a signal to Aft1/2 and promotes its dissociation from target DNA. Aft1/2 is therefore deactivated and transported out of the mitochondria by the Msn5 exportin. Figure created by C. Outten.

## **Scope of Thesis**

The tripeptide glutathione (GSH) is an essential and multifaceted thiol-containing molecule found in all eukaryotic cells. Due to its role in cell signaling, detoxification, protein folding, and iron homeostasis, maintenance of GSH pools and redox balance is crucial to the overall health of cells. The biosynthesis of GSH occurs exclusively in the cytosol. However, distinct GSH pools can be found in subcellular compartments. The development of targeted GFP-based probes and intracellular measurements of GSH have contributed to our understanding of regulatory processes that affect the subcellular environment. Although, there remains many gaps in our understanding of organelle-specific GSH regulation.

Mitochondria are the hub for energy production and consequently the primary site of ROS generation that can lead to oxidant-induced damage. Evidence points to GSH as the primary defense against the harmful effects of increased oxidation in the mitochondria. GSH limitation also causes mitochondrial dysfunction, such as respiratory incompetency and loss of mitochondrial DNA. Cells depleted of GSH or containing very high GSH concentrations have a similar phenotype characterized by redox imbalance, an iron starvation-like response, and eventual cell death. In this dissertation we look at factors that influence subcellular GSH pools, such as intercompartmental cross-talk and increased GSH or GSSG uptake. We also explore how yeast cells cope with extreme changes in intracellular GSH.

Vacuolar storage was found to be important in regulating cytosolic redox homeostasis. Since the cytosol and mitochondria possess similar redox regulatory mechanisms and GSH concentrations are similar within each compartment, in Chapter 2

we discuss the involvement of a vacuolar GSH transporter in regulating mitochondrial GSH levels. We show that yeast cells lacking vacuolar storage accumulate more mitochondrial GSH when exposed to excess GSH. Additionally, elevated cytosolic and mitochondrial GSH was observed in cells grown under oxidative stress caused by excess GSSG. Surprisingly, our data suggests that vacuolar storage may act to remove GSH in the cytosol prior to its transport to the mitochondria. Therefore, we conclude that vacuole storage may be an additional regulatory pathway for the mitochondria to combat redox stress.

Opt2, an oligopeptide transporter protein and homologue of the *S. cerevisiae* high affinity GSH transporter protein Hgt1, was discovered to be dually localized to the plasma membrane and peroxisomes of yeast. Therefore, in Chapter 3 we investigated the potential of Hgt1 to be localized to subcellular organelles by specifically testing for its presence on the mitochondrial membrane. Secondly, we examined the effect of deletion and overexpression of *HGT1* on mitochondrial GSH. We found that while Hgt1 does not appear to be a mitochondrial GSH transporter, its overexpression in cells treated with extracellular GSH increases mitochondrial GSH pools. This is likely due to the high GSH in the cytosol diffusing into the mitochondria via other unknown transporters. Deletion of *HGT1*, on the other hand, had no effect on GSH accumulation in this compartment.

GSH depletion in strains has been extensively studied in efforts to understand which of the many roles of GSH is essential for viability. These studies revealed that GSH is essential for maintaining mitochondrial integrity and maturation of extra-mitochondrial Fe-S cluster proteins. Interestingly, high intracellular GSH also impacts iron metabolism in addition to protein folding in the ER. Together, these studies shed light on how cells

handle low and high levels of GSH. However, we wanted to examine GSH trafficking more closely by monitoring subcellular GSH metabolism in a GSH-depleted strain that is engineered to accumulate extracellular GSH. In Chapter 4, we developed a model to explore the effects of GSH fluctuations by creating a *gsh1Δ* strain that overexpresses *HGT1* (*gsh1Δ + HGT1*). Surprisingly, we found that *HGT1* overexpression rescues the exogenous GSH dependence of a *gsh1Δ* strain without GSH supplementation. We also tested whether a similar phenomenon occurs in minimal media that only contains the necessary amino acids for wild type yeast to grow. We find that under these conditions *HGT1* is unable to sustain growth of *gsh1Δ* cells. By investigating which amino acids are important for rescue, we discovered that cysteine restores growth of *gsh1Δ + HGT1* cells. This effect is more pronounced under anaerobic conditions, suggesting that rescue is redox-dependent. Our results also confirm that *HGT1* overexpression in *gsh1Δ* partially rescues the iron starvation response associated with GSH depletion. Therefore, we conclude that *HGT1* overexpression helps cells with low GSH to regulate redox and iron metabolism, although the specific mechanism behind the rescue is unclear.

Techniques developed or modified for our research needs are described in Chapter 5. The procedures were adapted from published protocols to obtain the reported results. The methods discussed are small-scale mitochondrial isolation, GSH/GSSG plate reader assay, GSH uptake into isolated yeast mitochondria, mitochondrial purification, construction of deletion plasmids, and monitoring growth of yeast using the Synergy H1 plate reader. Collectively, these experiments have allowed us to genetically modify intracellular GSH and assess the consequences of these changes in whole cell, cytosolic, and mitochondrial compartments.

## References

1. Aller, I., Rouhier, N., and Meyer, A. J. (2013) Development of roGFP2-derived redox probes for measurement of the glutathione redox potential in the cytosol of severely glutathione-deficient *rm11* seedlings. *Front. Plant Sci.* 4, 506
2. Rahman, I., Kode, A., and Biswas, S. (2006) Assay for quantitative determination of glutathione and glutathione disulfide levels using enzymatic recycling method. *Nat. Protoc.* 1, 3159-3165
3. Marí, M., Morales, A., Colell, A., García-Ruiz, C., and Fernández-Checa, J. C. (2009) Mitochondrial Glutathione, a Key Survival Antioxidant. *Antioxid. Redox Signal.* 11, 2685-2700
4. Toledano, M. B., Delaunay-Moisan, A., Outten, C. E., and Igarria, A. (2013) Functions and Cellular Compartmentation of the Thioredoxin and Glutathione Pathways in Yeast. *Antioxid. Redox Signal.* 18, 1699-1711
5. Pai, H. V., Starke, D. W., Lesnefsky, E. J., Hoppel, C. L., and Mieyal, J. J. (2007) What is the Functional Significance of the Unique Location of Glutaredoxin 1 (GRx1) in the Intermembrane Space of Mitochondria? *Antioxid. Redox Signal.* 9, 2027-2033
6. Gibson, L. M., Dingra, N. N., Outten, C. E., and Lebioda, L. (2008) Structure of the thioredoxin-like domain of yeast glutaredoxin 3. *Acta Crystallogr. Sect. D Biol. Crystallogr.* 64, 927-932
7. Vlamis-Gardikas, A., and Holmgren, A. (2002) Thioredoxin and glutaredoxin isoforms. *Methods Enzymol.* 347, 286-296
8. Lloyd G. Wilson, Tadashi Asahi, A. R. S. B. (1961) Yeast sulfate-reducing system.

- I. Reduction of sulfate to sulfite. *J. Biol. Chem.* 236, 1822–1829
9. Holmgren, A. (1989) Thioredoxin and Glutaredoxin Systems. *J. Biol. Chem.* 264, 13963–13966
  10. Herrero, E., Ros, J., Tamarit, J., and Bellí, G. (2006) Glutaredoxins in fungi. *Photosynth. Res.* 89, 127-140
  11. Berndt, C., and Lillig, C. H. (2017) Glutathione, Glutaredoxins, and Iron. *Antioxid. Redox Signal.* 27, 1235-1251
  12. Kumar, C., Igarria, A., D’Autreaux, B., Planson, A. G., Junot, C., Godat, E., Bachhawat, A. K., Delaunay-Moisan, A., and Toledano, M. B. (2011) Glutathione revisited: A vital function in iron metabolism and ancillary role in thiol-redox control. *EMBO J.* 30, 2044-2056
  13. Toledano, M. B., Kumar, C., Le Moan, N., Spector, D., and Tacnet, F. (2007) The system biology of thiol redox system in Escherichia coli and yeast: Differential functions in oxidative stress, iron metabolism and DNA synthesis. *FEBS Lett.* 581, 3598-3607
  14. Martin, J. L. (1995) Thioredoxin -a fold for all reasons. *Structure.* 3, 245-250
  15. Outten, C. E., and Culotta, V. C. (2004) Alternative Start Sites in the Saccharomyces cerevisiae GLR1 Gene Are Responsible for Mitochondrial and Cytosolic Isoforms of Glutathione Reductase. *J. Biol. Chem.* 279, 7785-7791
  16. Pedrajas, J. R., Porras, P., Martinez-Galisteo, E., Padilla, C. A., Miranda-Vizuete, A., and Barcena, J. A. (2002) Two isoforms of Saccharomyces cerevisiae glutaredoxin 2 are expressed in vivo and localize to different subcellular compartments. *Biochem. J.* 364, 617-623

17. Porras, P., Padilla, C. A., Krayl, M., Voos, W., and Bárcena, J. A. (2006) One single in-frame AUG codon is responsible for a diversity of subcellular localizations of glutaredoxin 2 in *Saccharomyces cerevisiae*. *J. Biol. Chem.* 281, 16551-16562
18. Muller, E. G. (1996) A Glutathione Reductase Mutant of Yeast Accumulates High Levels of Oxidized Glutathione and Requires Thioredoxin for Growth. *Mol. Biol. Cell.* 7, 1805-1813
19. Trotter, E. W., and Grant, C. M. (2003) Non-reciprocal regulation of the redox state of the glutathione-glutaredoxin and thioredoxin systems. *EMBO Rep.* 4, 184-188
20. Grant, C. M., MacIver, F. H., and Dawes, I. W. (1996) Glutathione is an essential metabolite required for resistance to oxidative stress in the yeast *Saccharomyces cerevisiae*. *Curr. Genet.* 29, 511-515
21. Glutathione, reduced (GSH) (2001) *Altern. Med. Rev.* 6, 601-607
22. Schafer, F. Q., and Buettner, G. R. (2001) Redox environment of the cell as viewed through the redox state of the glutathione disulfide/glutathione couple. *Free Radic. Biol. Med.* 30, 1191-1212
23. Dalvi, S. M., Patil, V. W., and Ramraje, N. N. (2012) The roles of glutathione, glutathione peroxidase, glutathione reductase and the carbonyl protein in pulmonary and extra pulmonary tuberculosis. *J. Clin. Diagnostic Res.* 6, 1462-1465
24. Couto, N., Wood, J., and Barber, J. (2016) The role of glutathione reductase and related enzymes on cellular redox homeostasis network. *Free Radic. Biol. Med.*

95, 27-42

25. Aquilano, K., Baldelli, S., and Ciriolo, M. R. (2014) Glutathione: New roles in redox signalling for an old antioxidant. *Front. Pharmacol.* 5, 196
26. Lill, R. (2009) Function and biogenesis of iron-sulphur proteins. *Nature.* 460, 831-838
27. Ribas, V., Garcı-a-Ruiz, C., and Fernandez-Checa, J. C. (2014) Glutathione and mitochondria. *Front. Pharmacol.* 5, 151
28. Pompella, A., Visvikis, A., Paolicchi, A., De Tata, V., and Casini, A. F. (2003) The changing faces of glutathione, a cellular protagonist. in *Biochemical Pharmacology*, 66, 1499-1503
29. Valko, M., Leibfritz, D., Moncol, J., Cronin, M. T. D., Mazur, M., and Telser, J. (2007) Free radicals and antioxidants in normal physiological functions and human disease. *Int. J. Biochem. Cell Biol.* 39, 44-84
30. Hwang, C., Sinskey, A. J., and Lodish, H. F. (1992) Oxidized redox state of glutathione in the endoplasmic reticulum. *Science.* 257, 1496-1502
31. Bien, M., Longen, S., Wagener, N., Chwalla, I., Herrmann, J. M., and Riemer, J. (2010) Mitochondrial Disulfide Bond Formation Is Driven by Intersubunit Electron Transfer in Erv1 and Proofread by Glutathione. *Mol. Cell.* 37, 516-528
32. Chakravarthi, S., and Bulleid, N. J. (2004) Glutathione is required to regulate the formation of native disulfide bonds within proteins entering the secretory pathway. *J. Biol. Chem.* 279, 39872-39879
33. Molteni, S. N., Fassio, A., Ciriolo, M. R., Filomeni, G., Pasqualetto, E., Fagioli, C., and Sitia, R. (2004) Glutathione limits Ero1-dependent oxidation in the

- endoplasmic reticulum. *J. Biol. Chem.* 279, 32667-32673
34. Schaedler, T. A., Thornton, J. D., Kruse, I., Schwarzländer, M., Meyer, A. J., Van Veen, H. W., and Balk, J. (2014) A conserved mitochondrial ATP-binding cassette transporter exports glutathione polysulfide for cytosolic metal cofactor assembly. *J. Biol. Chem.* 289, 23264-23274
  35. Ayer, A., Tan, S.-X., Grant, C. M., Meyer, A. J., Dawes, I. W., and Perrone, G. G. (2010) The critical role of glutathione in maintenance of the mitochondrial genome. *Free Radic. Biol. Med.* 49, 1956-1968
  36. Montero, D., Tachibana, C., Rahr Winther, J., and Appenzeller-Herzog, C. (2013) Intracellular glutathione pools are heterogeneously concentrated. *Redox Biol.* 1, 508-513
  37. Hu, J., Dong, L., and Outten, C. E. (2008) The redox environment in the mitochondrial intermembrane space is maintained separately from the cytosol and matrix. *J. Biol. Chem.* 283, 29126-29134
  38. Kojer, K., Peleh, V., Calabrese, G., Herrmann, J. M., and Riemer, J. (2015) Kinetic control by limiting glutaredoxin amounts enables thiol oxidation in the reducing mitochondrial intermembrane space. *Mol. Biol. Cell.* 26, 195-204
  39. Kojer, K., Bien, M., Gangel, H., Morgan, B., Dick, T. P., and Riemer, J. (2012) Glutathione redox potential in the mitochondrial intermembrane space is linked to the cytosol and impacts the Mia40 redox state. *EMBO J.* 31, 3169-3182
  40. Vivancos, P. D., Dong, Y., Ziegler, K., Markovic, J., Pallardó, F. V., Pellny, T. K., Verrier, P. J., and Foyer, C. H. (2010) Recruitment of glutathione into the nucleus during cell proliferation adjusts whole-cell redox homeostasis in Arabidopsis

- thaliana and lowers the oxidative defence shield. *Plant J.* 64, 825-838
41. Markovic, J., Borrás, C., Ortega, Á., Sastre, J., Viña, J., and Pallardó, F. V. (2007) Glutathione is recruited into the nucleus in early phases of cell proliferation. *J. Biol. Chem.* 282, 20416-20424
  42. Voehringer, D. W., McConkey, D. J., McDonnell, T. J., Brisbay, S., and Meyn, R. E. (1998) Bcl-2 expression causes redistribution of glutathione to the nucleus. *Proc. Natl. Acad. Sci.* 95, 2956-2960
  43. Li, L., Lee, T. K., Meier, P. J., and Ballatori, N. (1998) Identification of glutathione as a driving force and leukotriene C4 as a substrate for oatp1, the hepatic sinusoidal organic solute transporter. *J. Biol. Chem.* 273, 16184-16191
  44. Rebbeor, J. F., Connolly, G. C., Dumont, M. E., and Ballatori, N. (1998) ATP-dependent transport of reduced glutathione in yeast secretory vesicles. *Biochem. J.* 334, 723-729
  45. Rebbeor, J. F., Connolly, G. C., Dumont, M. E., and Ballatori, N. (1998) ATP-dependent transport of reduced glutathione on YCF1, the yeast orthologue of mammalian multidrug resistance associated proteins. *J. Biol. Chem.* 273, 33449-33454
  46. Rappa, G., Lorico, A., Flavell, R. A., and Sartorelli, A. C. (1997) Evidence that the multidrug resistance protein (MRP) functions as a co- transporter of glutathione and natural product toxins. *Cancer Res.* 57, 5232-5237
  47. Bachhawat, A. K., Thakur, A., Kaur, J., and Zulkifli, M. (2013) Glutathione transporters. *Biochim. Biophys. Acta - Gen. Subj.* 1830, 3154-3164
  48. Bourbouloux, A., Shahi, P., Chakladar, A., Delrot, S., and Bachhawat, A. K.

- (2000) Hgt1p, A high affinity glutathione transporter from the yeast *Saccharomyces cerevisiae*. *J. Biol. Chem.* 275, 13259–13265
49. Yen, M. R., Tseng, Y. H., and Saier, J. (2001) Maize Yellow Stripe 1, an iron-phytosiderophore uptake transporter, is a member of the oligopeptide transporter (OPT) family. *Microbiology.* 147, 2881-2883
50. Thakur, A., and Bachhawat, A. K. (2010) The role of transmembrane domain 9 in substrate recognition by the fungal high-affinity glutathione transporters. *Biochem. J.* 429, 593-602
51. Kaur, J., and Bachhawat, A. K. (2009) Gln-222 in transmembrane domain 4 and Gln-526 in transmembrane domain 9 are critical for substrate recognition in the yeast high affinity glutathione transporter, Hgt1p. *J. Biol. Chem.* 284, 23872-23884
52. Morgan, B., Ezeriņa, D., Amoako, T. N. E., Riemer, J., Seedorf, M., and Dick, T. P. (2013) Multiple glutathione disulfide removal pathways mediate cytosolic redox homeostasis. *Nat. Chem. Biol.* 9, 119-125
53. Sharma, K. G., Mason, D. L., Liu, G., Rea, P. A., Bachhawat, A. K., and Michaelis, S. (2002) Localization, regulation, and substrate transport properties of Bpt1p, a *Saccharomyces cerevisiae* MRP-type ABC transporter. *Eukaryot. Cell.* 1, 391-400
54. Dhaoui, M., Auchere, F., Blaiseau, P.-L., Lesuisse, E., Landoulsi, A., Camadro, J.-M., Haguenaer-Tsapis, R., and Belgareh-Touze, N. (2011) Gex1 is a yeast glutathione exchanger that interferes with pH and redox homeostasis. *Mol. Biol. Cell.* 22, 2054-2067

55. Kiriyaama, K., Hara, K. Y., and Kondo, A. (2012) Extracellular glutathione fermentation using engineered *Saccharomyces cerevisiae* expressing a novel glutathione exporter. *Appl. Microbiol. Biotechnol.* 96, 1021-1027
56. Elbaz-Alon, Y., Morgan, B., Clancy, A., Amoako, T. N. E., Zalckvar, E., Dick, T. P., Schwappach, B., and Schuldiner, M. (2014) The yeast oligopeptide transporter Opt2 is localized to peroxisomes and affects glutathione redox homeostasis. *FEMS Yeast Res.* 14, 1055-1067
57. Bánhegyi, G., Lusini, L., Puskás, F., Rossi, R., Fulceri, R., Braun, L., Mile, V., Di Simplicio, P., Mandl, J., and Benedetti, A. (1999) Preferential transport of glutathione versus glutathione disulfide in rat liver microsomal vesicles. *J. Biol. Chem.* 274, 12213-12216
58. Ponsero, A. J., Igarria, A., Darch, M. A., Miled, S., Outten, C. E., Winther, J. R., Palais, G., D'Autréaux, B., Delaunay-Moisan, A., and Toledano, M. B. (2017) Endoplasmic Reticulum Transport of Glutathione by Sec61 Is Regulated by Ero1 and Bip. *Mol. Cell.* 67, 962-973
59. Griffith, O. W., and Meister, A. (1985) Origin and turnover of mitochondrial glutathione. *Proc. Natl. Acad. Sci. U. S. A.* 82, 4668-4672
60. Marí, M., Morales, A., Colell, A., García-Ruiz, C., Kaplowitz, N., and Fernández-Checa, J. C. (2013) Mitochondrial glutathione: Features, regulation and role in disease. *Biochim. Biophys. Acta - Gen. Subj.* 1830, 3317-3328
61. Holley, A. K., Bakthavatchalu, V., Velez-Roman, J. M., and St. Clair, D. K. (2011) Manganese superoxide dismutase: Guardian of the powerhouse. *Int. J. Mol. Sci.* 12, 7114-7162

62. Cadenas, E., and Davies, K. J. A. (2000) Mitochondrial free radical generation, oxidative stress, and aging. *Free Radic. Biol. Med.* 29, 222-230
63. Olafsdottir, K., and Reed, D. J. (1988) Retention of Oxidized Glutathione by Isolated Rat Liver Mitochondria During Hydroperoxide Treatment. *Biochim. Biophys. Acta.* 964, 377-382
64. Yin, F., Sancheti, H., and Cadenas, E. (2012) Mitochondrial Thiols in the Regulation of Cell Death Pathways. *Antioxid. Redox Signal.* 17, 1714-1727
65. Chen, Z., Putt, D. A., and Lash, L. H. (2000) Enrichment and functional reconstitution of glutathione transport activity from rabbit kidney mitochondria. Further evidence for the role of the dicarboxylate and 2-oxoglutarate carriers in mitochondrial glutathione transport. *Arch. Biochem. Biophys.* 373, 193-202
66. Zhong, Q., Putt, D. A., Xu, F., and Lash, L. H. (2008) Hepatic mitochondrial transport of glutathione: Studies in isolated rat liver mitochondria and H4IIE rat hepatoma cells. *Arch. Biochem. Biophys.* 474, 119-127
67. Booty, L. M., King, M. S., Thangaratnarajah, C., Majd, H., James, A. M., Kunji, E. R. S., and Murphy, M. P. (2015) The mitochondrial dicarboxylate and 2-oxoglutarate carriers do not transport glutathione. *FEBS Lett.* 589, 621-628
68. Ukai, Y., Kishimoto, T., Ohdate, T., Izawa, S., and Inoue, Y. (2011) Glutathione peroxidase 2 in *Saccharomyces cerevisiae* is distributed in mitochondria and involved in sporulation. *Biochem. Biophys. Res. Commun.* 411, 580-585
69. Murphy, E. R., Sacco, R. E., Dickenson, A., Metzger, D. J., Hu, Y., Orndorff, P. E., and Connell, T. D. (2002) BhuR, a virulence-associated outer membrane protein of *Bordetella avium*, is required for the acquisition of iron from heme and

- hemoproteins. *Infect. Immun.* 70, 5390-5403
70. Philpott, C. C. (2012) Yeast Iron Metabolism. *Iron Physiology and Pathophysiology in Humans*, pp. 653–667
  71. Outten, C. E., and Albetel, A. N. (2013) Iron sensing and regulation in *Saccharomyces cerevisiae*: Ironing out the mechanistic details. *Curr. Opin. Microbiol.* 16, 662-668
  72. Yamaguchi-Iwai, Y., Dancis, A., and Klausner, R. D. (1995) *AFT1*: a mediator of iron regulated transcriptional control in *Saccharomyces cerevisiae*. *Embo J.* 14, 1231-1239
  73. Yamaguchi-Iwai, Y., Stearman, R., Dancis, A., and Klausner, R. D. (1996) Iron-regulated DNA binding by the *AFT1* protein controls the iron regulon in yeast. *EMBO J.* 15, 3377-3384
  74. Yun, C. W., Ferea, T., Rashford, J., Ardon, O., Brown, P. O., Botstein, D., Kaplan, J., and Philpott, C. C. (2000) Desferrioxamine-mediated iron uptake in *Saccharomyces cerevisiae*. Evidence for two pathways of iron uptake. *J. Biol. Chem.* 275, 10709-10715
  75. Foury, F., and Talibi, D. (2001) Mitochondrial control of iron homeostasis. A genome wide analysis of gene expression in a yeast frataxin-deficient strain. *J. Biol. Chem.* 276, 7762-7768
  76. Garland, S. A., Hoff, K., Vickery, L. E., and Culotta, V. C. (1999) *Saccharomyces cerevisiae* ISU1 and ISU2: Members of a well-conserved gene family for iron-sulfur cluster assembly. *J. Mol. Biol.* 294, 897-907
  77. Rutherford, J. C., Jaron, S., Ray, E., Brown, P. O., and Winge, D. R. (2001) A

- second iron-regulatory system in yeast independent of Aft1p. *Proc. Natl. Acad. Sci.* 98, 14332-14337
78. Nakai, Y., Umeda, N., Suzuki, T., Nakai, M., Hayashi, H., Watanabe, K., and Kagamiyama, H. (2004) Yeast Nfs1p Is Involved in Thio-modification of Both Mitochondrial and Cytoplasmic tRNAs. *J. Biol. Chem.* 279, 12363-12368
79. Lill, R., and Mühlenhoff, U. (2005) Iron-sulfur-protein biogenesis in eukaryotes. *Trends Biochem. Sci.* 30, 133-141
80. Rouault, T. A. (2012) Biogenesis of iron-sulfur clusters in mammalian cells: new insights and relevance to human disease. *Dis. Model. Mech.* 5, 155-164
81. Lill, R., and Mühlenhoff, U. (2008) Maturation of Iron-Sulfur Proteins in Eukaryotes: Mechanisms, Connected Processes, and Diseases. *Annu. Rev. Biochem.* 77, 669-700
82. Subramanian, P., Rodrigues, A. V., Ghimire-Rijal, S., and Stemmler, T. L. (2011) Iron chaperones for mitochondrial Fe-S cluster biosynthesis and ferritin iron storage. *Curr. Opin. Chem. Biol.* 15, 312-318
83. Braymer, J. J., and Lill, R. (2017) Iron-sulfur cluster biogenesis and trafficking in mitochondria. *J. Biol. Chem.* 292, 12754-12763
84. Kispal, G., Csere, P., Prohl, C., and Lill, R. (1999) The mitochondrial proteins Atm1p and Nfs1p are essential for biogenesis of cytosolic Fe/S proteins. *EMBO J.* 18, 3981-3989
85. Rutherford, J. C., Ojeda, L., Balk, J., Mühlenhoff, U., Lill, R., and Winge, D. R. (2005) Activation of the iron regulon by the yeast Aft1/Aft2 transcription factors depends on mitochondrial but not cytosolic iron-sulfur protein biogenesis. *J. Biol.*

*Chem.* 280, 10135-10140

86. Ueta, R., Fujiwara, N., Iwai, K., and Yamaguchi-Iwai, Y. (2012) Iron-Induced Dissociation of the Aft1p Transcriptional Regulator from Target Gene Promoters Is an Initial Event in Iron-Dependent Gene Suppression. *Mol. Cell. Biol.* 32, 4998-5008
87. Ojeda, L., Keller, G., Muhlenhoff, U., Rutherford, J. C., Lill, R., and Winge, D. R. (2006) Role of glutaredoxin-3 and glutaredoxin-4 in the iron regulation of the Aft1 transcriptional activator in *Saccharomyces cerevisiae*. *J. Biol. Chem.* 281, 17661-17669
88. Pujol-Carrion, N., Belli, G., Herrero, E., Nogues, A., and de la Torre-Ruiz, M. A. (2006) Glutaredoxins Grx3 and Grx4 regulate nuclear localisation of Aft1 and the oxidative stress response in *Saccharomyces cerevisiae*. *J. Cell Sci.* 119, 4554-4564
89. Kumánovics, A., Chen, O. S., Li, L., Bagley, D., Adkins, E. M., Lin, H., Dingra, N. N., Outten, C. E., Keller, G., Winge, D., Ward, D. M., and Kaplan, J. (2008) Identification of FRA1 and FRA2 as genes involved in regulating the yeast iron regulon in response to decreased mitochondrial iron-sulfur cluster synthesis. *J. Biol. Chem.* 283, 10276-10286
90. Poor, C. B., Wegner, S. V., Li, H., Dlouhy, A. C., Schuermann, J. P., Sanishvili, R., Hinshaw, J. R., Riggs-Gelasco, P. J., Outten, C. E., and He, C. (2014) Molecular mechanism and structure of the *Saccharomyces cerevisiae* iron regulator Aft2. *Proc. Natl. Acad. Sci.* 111, 4043-4048

## CHAPTER 2

### EXCHANGE OF GLUTATHIONE BETWEEN VACUOLAR AND MITOCHONDRIAL POOLS WITH GSH OR GSSG OVERACCUMULATION IN *SACCHAROMYCES* *CEREVISIAE*

#### **Abstract**

Glutathione (GSH), an abundant low-molecular weight thiol, acts to protect the cell from hyper-oxidation and regulate subcellular redox homeostasis. In *Saccharomyces cerevisiae*, the biosynthesis of GSH occurs in the cytosol or may be imported extracellularly via a high affinity GSH transporter, Hgt1. The biochemical transport of GSH across other membranes has been demonstrated and while advances have been made in identifying mechanisms that control GSH homeostasis, our understanding of GSH distribution from the cytosol to subcellular compartments remain elusive. The ability of cells to regulate GSH pools through subcellular crosstalk has recently been demonstrated. Ycf1, a vacuolar GSH S-conjugate transporter of the ATP-binding cassette family, was shown to facilitate vacuolar storage of oxidized glutathione (GSSG) not immediately reduced by other cytosolic redox pathways. Storage of GSSG in the vacuole was, therefore, determined to be an important mechanism for maintaining a reduced cytosolic environment. Elucidating the fundamental role of subcellular compartmentalization in regulating the cytosolic GSH:GSSG ratio is an important step forward. However, there remains many gaps in our understanding of mechanisms that govern intercompartmental

exchange of GSH. Given that mitochondrial GSH (mGSH) is derived from the cytosol, we hypothesized that vacuolar storage plays a fundamental role in maintaining the redox environment in this compartment. Our current studies are designed to explore the role of vacuolar storage on mGSH pools under GSH or GSSG overaccumulation conditions. To accomplish this, GSH or GSSG was added to the growth media of strains overexpressing *HGT1*. Overaccumulation of GSH and GSSG was measured in wild type (WT) and yeast lacking *YCF1*. We find that disruption of vacuolar storage leads to elevated mitochondrial GSH in cells grown with excess GSH. Addition of excess GSSG in a *ycf1*Δ strain results in elevated cytosolic and mitochondrial total GSH. Interestingly, this increase is not due to GSSG. Overall, our data suggests that vacuole storage is important for maintaining subcellular GSH:GSSG pools under redox stress.

## **Introduction**

An important mechanism that cells use to rid the intracellular environment of toxins is the conjugation of xenobiotics to GSH. This process occurs spontaneously or with the help of GSH transferases. Conjugates are then transferred outside the cell or into vacuoles via GSH S-conjugate pumps belonging to the ATP-binding cassette family of transporters (1). Transporters of the ATP-Binding Cassette (ABC) superfamily are found in all organisms and function in the transport of a wide range of harmful compounds across cellular membranes (2). In *Saccharomyces cerevisiae*, the yeast cadmium factor protein (Ycf1) is a vacuolar-localized member of the ATP-binding cassette class C (ABCC) transporters. *YCF1* was originally isolated due to its critical role in cadmium tolerance. The mechanism of cadmium (Cd) resistance was determined to be a result of Cd sequestration to the vacuole

through the formation of GSH S-conjugates. Surprisingly, reduced GSH itself was also identified as a low affinity ( $K_m$   $15 \pm 4$  mM) substrate of Ycf1. Once inside the vacuole, GSH is degraded by the vacuolar membrane-bound proteins,  $\gamma$ -glutamyl transpeptidase and dipeptidase. This process of eliminating GSH from the cytosol is analogous to that performed on the external surface of the plasma membrane by the human multidrug resistance protein MRP1 of which Ycf1 is a close homolog (3–5). Sequestration of GSSG from human cells by MRP1 has been detected when cells are under oxidative stress. Likewise, uptake of radiolabeled GSSG by Ycf1 has also been directly measured ( $K_m = 290 \pm 50$   $\mu$ M) (1). The ability of MRP1 and Ycf1 to transport unconjugated GSSG or GSH has placed these transporters as potential regulators of the cellular redox status (6).

Evidence for the maintenance of intracellular GSH homeostasis has been reported for Ycf1 using *Saccharomyces cerevisiae*. Studies conducted by Paumi et al. found that salt-induced oxidative stress in *ycf1* deletion (*ycf1* $\Delta$ ) strains increases intracellular reactive oxygen species (ROS) formation and reduces free GSH and GSSG. The ratio of GSH:GSSG was also decreased as a result of oxidative stress. In addition to changes in GSH, Sod1, Sod2, and GSH peroxidase activity were induced in *ycf1* $\Delta$  cells exposed to oxidants. Cytoplasmic Sod1 (Cu/ZnSOD), mitochondrial Sod2 (MnSOD), and GSH peroxidase have all been shown to protect cells against oxygen toxicity and oxidative stress. Therefore, these findings suggest that Ycf1 plays an important role in the regulation of cellular redox balance in cytosolic and mitochondrial compartments (2).

Another indication for the protective role of Ycf1 in redox homeostasis was reported by Morgan et al. The authors investigated the role of vacuolar storage in regulating cytosolic GSH homeostasis as it relates to subcellular distribution of GSSG. Conventional

methods of measuring intracellular GSH and GSSG in combination with monitoring dynamic changes of GSH:GSSG redox potentials using targeted green fluorescent protein based probes revealed discrepancies in whole cell and subcellular GSH:GSSG. The authors report that genetic and chemical elevation of GSSG decreased over time in the cytoplasm while whole-cell GSH was unaffected. These results were an indication that GSSG is transported into another subcellular compartment. Vacuolar membrane localized ABC-transporters were evaluated as potential contributors to GSSG storage under oxidative stress conditions. Ycf1 was shown to be exclusively responsible for GSSG compartmentalization. These findings provided evidence for intercompartmental crosstalk (6).

Compartmentalization of GSH is assumed to play a key role in maintaining GSH redox balance in different subcellular environments. Enzymes responsible for GSH biosynthesis are only found in the cytosol. Yet, GSH is required in other organelles such as the nucleus, endoplasmic reticulum, and mitochondria. Determining the mechanisms that control subcellular transport and distribution of GSH is therefore considered to be critical to our understanding of cellular redox homeostasis. Maintaining mitochondrial GSH is especially important since this organelle is the site of ROS production and changes in mitochondrial GSH levels is associated with pathologies such as aging, diabetes, neurological disorders, liver diseases, and pulmonary diseases (7).

In the current study, we set out to determine the underlying mechanisms that govern intercompartmental exchange of GSH between the cytosol and the mitochondria. Mitochondria contain a distinct pool of GSH with concentrations similar to the cytosol (10-14 mM). Both compartments also rely on GSSG reductase (GLR) to maintain the high

GSH:GSSG ratio (8). Therefore it is plausible that under redox stress, vacuolar storage is important for regulating mitochondrial GSH:GSSG homeostasis. To test this, our lab has employed the *HGT1* overexpression plasmid, which allows GSH and GSSG to overaccumulate in cells when GSH or GSSG is added to the growth media (9). By increasing intracellular GSH and GSSG, a form of redox stress, we are then able to monitor changes in subcellular GSH:GSSG pools. Using targeted GFP-based redox sensors, our previous studies showed that adding GSH and GSSG to the media of *HGT1* strains lacking vacuolar storage protein Ycf1 (*ycf1* $\Delta$ ) alters the mitochondrial GSH:GSSG redox state (10). To correlate these redox changes with direct measurement of subcellular GSH and GSSG levels and elucidate the role of vacuolar storage on mitochondrial GSH, we measured cytosolic and mitochondrial GSH levels in WT and *ycf1* $\Delta$  strains expressing the *HGT1* plasmid. Our results suggest that reductive (excess GSH) and oxidative (excess GSSG) stress cause increased mitochondrial GSH accumulation when vacuolar storage is lacking, whereas only oxidative stress results in elevated cytosolic GSH in *ycf1* $\Delta$  + *HGT1* strains. The observed differences in WT and *ycf1* $\Delta$  GSH accumulation appear to be in the form of reduced GSH.

### **Experimental Procedures**

*Yeast Strains, Plasmids, Media, and Growth Conditions-* The *Saccharomyces cerevisiae* strains used in this study were derivatives of WT BY4742 (*MAT $\alpha$  his3 $\Delta$ 1 leu2 $\Delta$ 0 lys2 $\Delta$ 0 ura3 $\Delta$ 0*). The BY4742 *ycf1::kanMX4* was a kind gift from Dr. Tobias Dick (6). The *CEN* pTEF-416 vector and pTEF-416-HGT1 overexpression plasmids carrying *URA3* selection were inserted into WT and *ycf1* $\Delta$  strains (9, 11). Yeast transformations were

performed using standard lithium acetate transformation protocols (12). Cells were grown in synthetic complete (SC) selection media (0.671% yeast nitrogen base without amino acids and ammonium sulfate (US Biological), 2% glucose) and supplemented with appropriate amino acids. All assays were done using cells grown to mid-log phase.

*Small Scale Mitochondrial Isolation-* Yeast cells were grown aerobically to mid-log phase in SC selection medium with 2% glucose. Cytosolic and mitochondrial fractions were obtained as previously described by converting cells to spheroplasts followed by gentle lysis using a loose fitting Dounce homogenizer and differential centrifugation (13). Incubation with reductant (dithiothreitol) was omitted from fractionation steps to avoid alteration of the GSH:GSSG redox state, and protease inhibitors were omitted since protein integrity was not a concern for the subsequent assays. Protein concentrations were measured using the Bradford method with bovine serum albumin as a calibration standard.

*GSH/GSSG Assay-*Total GSH (GSH and GSSG) was measured in cytosolic and mitochondrial extracts using the 5,5-dithiobis(2-nitrobenzoic acid) (DTNB)-GSSG reductase cycling assay as previously described (14, 15). Subcellular fractions were prepared as described above (13). Samples were incubated with 1% 5-sulfosalicylic acid (SSA) on ice for 30 minutes and fractions were spun at 13000 x g at 4 °C. The supernatant containing total GSH was transferred to sterile microcentrifuge tubes. GSSG samples were prepared by alkylating total GSH samples with 2-vinylpyridine. DTNB reduction was monitored at 412 nm. Absorption measurements were taken every 15 seconds for approximately 2 minutes (15). Standard concentrations of GSH and GSSG are obtained by using known concentrations of GSH or GSSG solubilized in 1% SSA. The reported

GSH/GSSG measurements are the rate of increasing absorbance directly proportional to GSH/GSSG concentration over a range of 2 minutes.

## **Results**

*Disruption in vacuolar storage causes increased mitochondrial accumulation of GSH in HGT1 expressing strains-* To examine how overaccumulation of GSH impacts GSH pools in subcellular compartments, we transformed an *HGT1* overexpression plasmid into WT yeast. After addition of 100  $\mu$ M GSH to the growth medium, total GSH (GSH + GSSG) measurements of subcellular fractions reveal that GSH accumulation occurs in both the cytosol and mitochondria of WT + *HGT1* cells (Fig. 2.1A,B). These data are in agreement with previous studies showing that whole cell GSH significantly increases in WT + *HGT1* strains when GSH is added to the growth media (9). Furthermore, these results demonstrate that the excess GSH is clearly imported into mitochondria.

We next wanted to evaluate how vacuolar storage affects GSH distribution from the cytosol to the mitochondria. To test this, we used a *ycf1* $\Delta$  deletion strain containing *HGT1* overexpression or empty vector control plasmids. Mitochondria were separated from the cytosol and fractions were evaluated for total GSH + GSSG content. WT + *HGT1* and *ycf1* $\Delta$  + *HGT1* cells showed no difference in cytosolic GSH accumulation (Fig. 2.1A). However, *ycf1* $\Delta$  + *HGT1* accumulated 1.6X more total mitochondrial GSH than the WT control (Fig. 2.1B). These data imply that with GSH overaccumulation, mitochondria partially rely on vacuolar storage of GSH to regulate GSH pools.

*GSH overaccumulation increases GSSG steady-state levels in the cytosol and mitochondria of WT and ycf1 $\Delta$  strains overexpressing HGT1-* To access the oxidation state

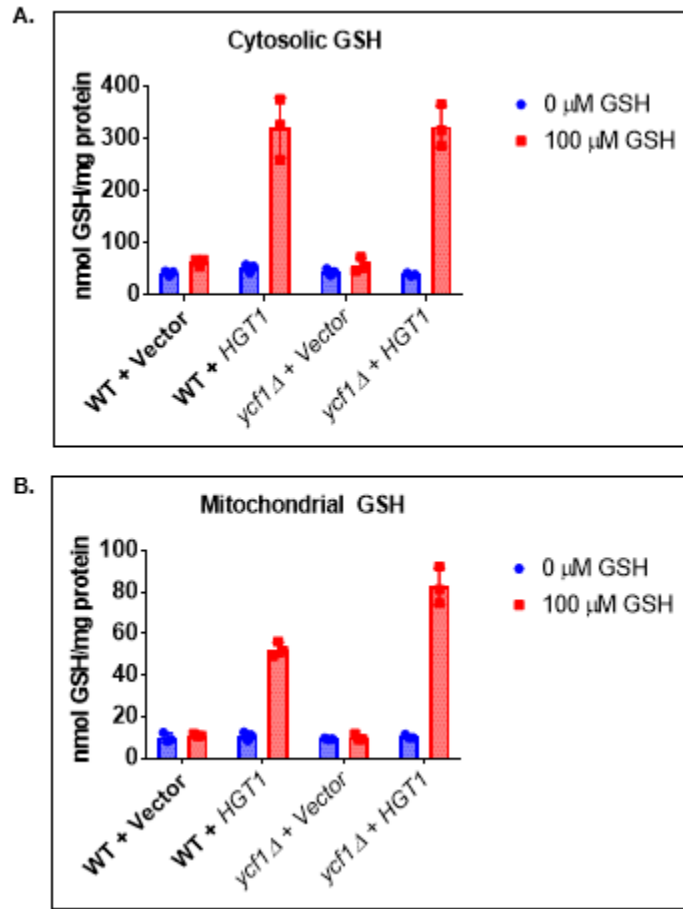


**Figure 2.1 Disruption in vacuolar storage causes increased mitochondrial accumulation of GSH in *HGT1* expressing strains.** Cells were grown overnight at 30 °C to an OD<sub>600</sub> of approximately 1 in SC selection media. Select cells were treated with 100  $\mu$ M GSH for 30 minutes. Cytosolic and mitochondrial fractions were collected and acidified with 1% SSA. The DTNB spectrophotometric assay was used to measure (A) cytosolic and (B) mitochondrial steady-state total GSH (GSH + GSSG) concentrations in WT BY4742 and *ycf1* $\Delta$  strains transformed with vector control and *HGT1* overexpression plasmids. The reported data are from 3 independent experiments with the error bars representing the standard deviation.

of total GSH measured in subcellular compartments, cellular GSH:GSSG extracts were alkylated with 2-vinylpyridine so that only GSSG could be assessed. Our studies measuring cytosolic GSH showed that WT + *HGT1* and *ycf1Δ* + *HGT1* strains accumulated approximately the same amount of total GSH (GSH + GSSG) (see Fig. 2.1A). However, when GSSG was measured alone, we show that WT + *HGT1* cells have 1.7X more GSSG than *ycf1Δ* + *HGT1* (Fig. 2.2A). These data suggest that WT and *ycf1Δ* regulate cytosolic GSH:GSSG differently when subject to GSH overaccumulation. However, the mechanism of regulation is yet to be determined. Next, we looked at GSSG levels in mitochondrial fractions of WT and *ycf1Δ* cells expressing *HGT1* and vector plasmids. Since mitochondria of *ycf1Δ* + *HGT1* cells appear to accumulate more total GSH from the media than WT + *HGT1*, we wanted to determine if GSH pools in this compartment are reduced or oxidized. Previous studies using targeted GFP-based probes have found the mitochondrial matrix to be very reducing (16). Here, we see that the increase of total GSH in *ycf1Δ*+ *HGT1* appears to be mostly reduced GSH (Fig. 2.2B). Therefore, we conclude that vacuolar storage may be important for storing excess reduced GSH in addition to GSSG. However, these experiments should be repeated to confirm that these differences between WT and *ycf1Δ* strains are reproducible and statistically significant.

*Disruption in vacuolar storage causes accumulation of cytosolic and mitochondrial total GSH in high GSSG stress* - Previous studies showing the involvement of Ycf1 in regulating cellular GSH homeostasis were done by increasing GSSG intracellularly and exposing cells to other oxidants. Data evaluating GSH levels and redox changes of the whole cell and cytosol of *ycf1Δ* strains link vacuolar storage to maintaining GSH

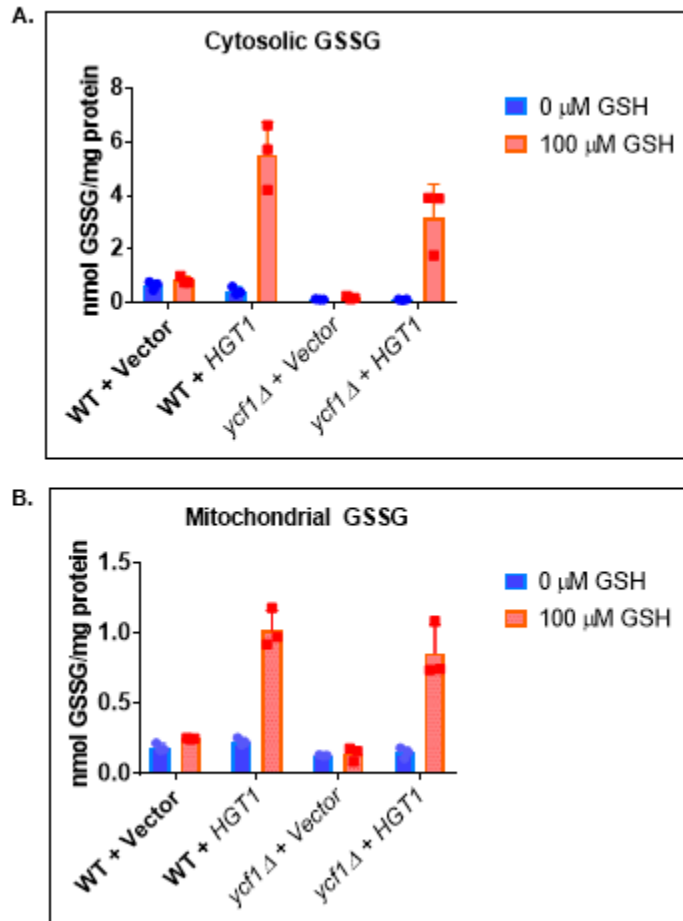


**Figure 2.2 GSH overaccumulation increases GSSG steady-state levels in the cytosol and mitochondria of WT and *ycf1*Δ strains overexpressing *HGT1*.** WT BY4742 and *ycf1*Δ strains expressing vector control and *HGT1* overexpression plasmids were grown overnight at 30 °C to an OD<sub>600</sub> of approximately 1.0 in SC media. Select cells were treated with 100 μM GSH for 30 minutes. DTNB spectrophotometric analysis was used to measure steady state GSSG concentrations of (A) cytosolic and (B) mitochondrial fractions. The reported data are from 3 independent experiments with the error bars representing the standard deviation.

homeostasis (2, 6). To further explore the role of GSH sequestration to the vacuole in regulating GSH at the subcellular level, we directly measured GSH and GSSG levels following GSSG overaccumulation from the extracellular environment of WT + *HGT1* and *ycf1Δ* + *HGT1* strains. Total GSH levels spike in both WT and *ycf1Δ* strains expressing *HGT1* with addition of GSSG to the growth medium. However, *ycf1Δ* + *HGT1* accumulated 1.7X more cytosolic GSH than WT + *HGT1* (Fig. 2.3A). These results corroborate reports by Morgan et al. showing that a *ycf1Δ* strain genetically modified to accumulate GSSG have larger GSSG content in whole cell lysates compared to the control (6). We also checked the effect of vacuolar storage on the mitochondria of strains with enhanced import of extracellular GSSG. Surprisingly, mitochondria of *ycf1Δ* + *HGT1* cells accumulated 1.3X more GSH than the control (Fig. 2.3B). Taken together, these data show that Hgt1 imports large amounts of GSSG from the extracellular environment which causes increased total GSH that is distributed to the mitochondria. Additionally, Ycf1 is not only important for maintaining cytosolic GSH but may also be key in regulating mitochondrial GSH.

*GSSG overaccumulation in HGT1 strains increases GSSG steady-state levels in the cytosol and mitochondria of WT and ycf1Δ strains-* Under GSSG overaccumulation conditions, *ycf1Δ* + *HGT1* was shown to have a larger accumulation of total GSH than the WT control (see Fig. 2.3A,B). Therefore, we investigated the amounts of GSSG in the cytosol and mitochondria of WT + *HGT1* and *ycf1Δ* + *HGT1* cells. We report that WT + *HGT1* strains acquire 2.4X more cytosolic GSSG than *ycf1Δ* + *HGT1* strains (Fig. 2.4A). Interestingly, mitochondrial GSSG increases 3X more in WT cells than *ycf1Δ* strains that overexpress *HGT1* (Fig. 2.4B). Since it appears that the increase in total GSH in *ycf1Δ*

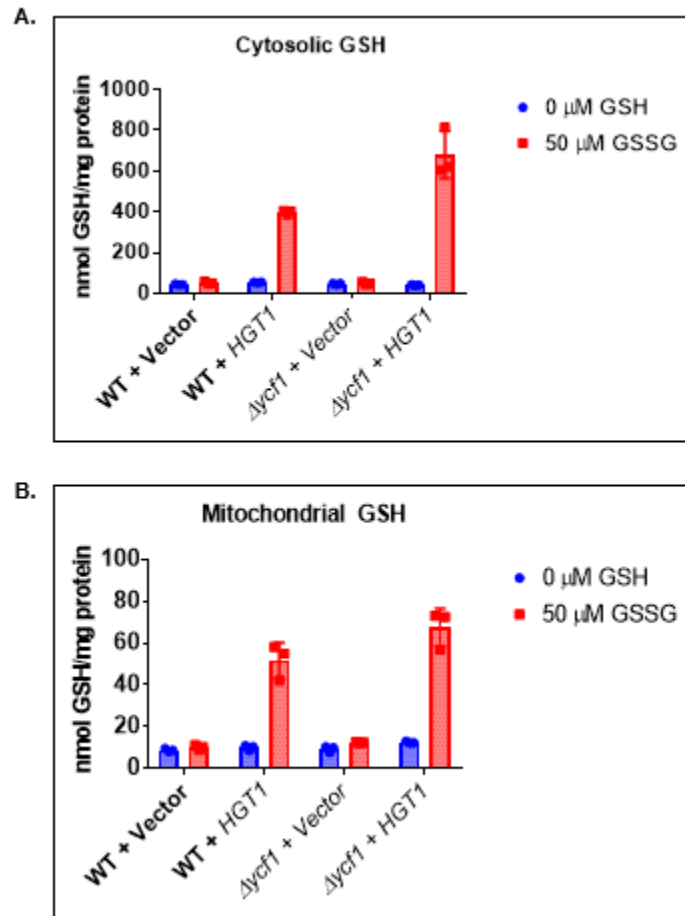


**Figure 2.3 Disruption in vacuolar storage causes accumulation of cytosolic and mitochondrial total GSH in high GSSG stress.** Yeast strains were grown overnight to mid-log phase at 30 °C in SC selection media. Cells were split and select cells were treated with 50  $\mu$ M GSSG for 30 minutes. Acidification of cytosolic and mitochondrial fractions using 1% SSA was done prior to measuring (A) cytosolic and (B) mitochondrial steady state total GSH (GSH + GSSG) concentrations in WT BY4742 and *ycf1* $\Delta$  strains transformed with vector control and *HGT1* overexpression plasmids using the DTNB spectrophotometric assay. The reported data are from 3 independent experiments with the error bars representing the standard deviation.

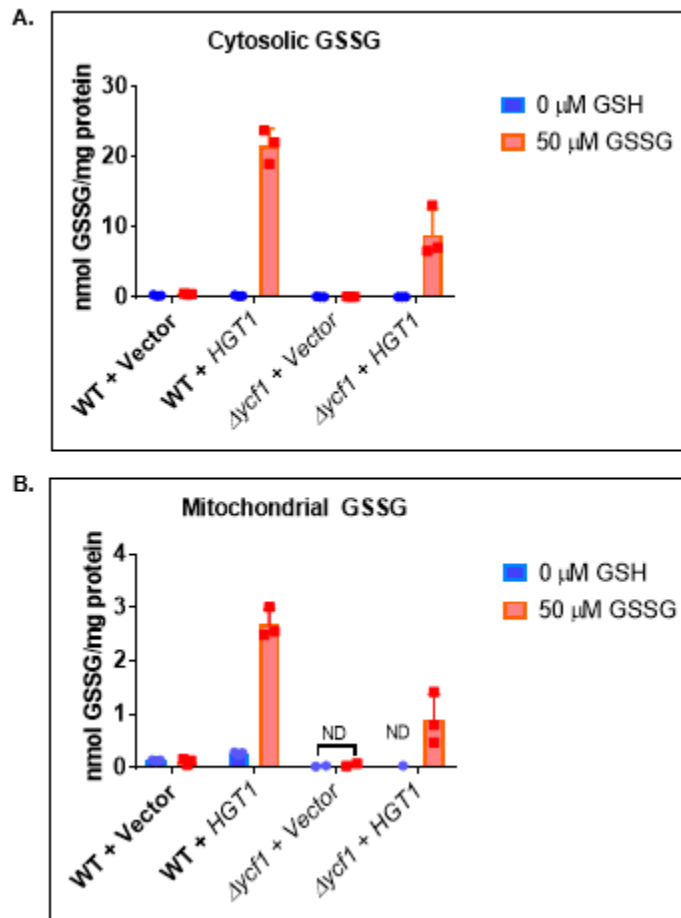


**Figure 2.4 GSSG overaccumulation in *HGT1* strains increases GSSG steady-state levels in the cytosol and mitochondria of WT and *ycf1* $\Delta$  strains.** WT BY4742 and *ycf1* $\Delta$  strains expressing vector and *HGT1* overexpression plasmids were grown overnight at 30  $^{\circ}$ C to mid-log phase in SC media. Select cells were treated with 50  $\mu$ M GSSG for 30 minutes and the steady state GSSG concentrations of (A) cytosolic and (B) mitochondrial fractions were measured using the DTNB colorimetric assay. The reported data are from 3 independent experiments with the error bars representing the standard deviation. ND, not detected due to levels below the assay detection limit.

strains is reduced, it seems that GSSG reductase (GLR) and possibly the TRX and GRX redox systems are likely responsible for the rapid reduction of imported GSSG. These redox regulatory pathways are localized to the cytosol and mitochondria and act to maintain GSH:GSSG. Previous studies found that thiol-reductase systems along with vacuolar storage works together to alleviate oxidative stress from the cytosol caused by elevated GSSG (6). We provide evidence that expression of Ycf1 effects mitochondrial GSH pools as well as cytosolic pools. However, our studies suggest that reduced GSH may also be stored in the vacuole to maintain the redox environment of subcellular organelles. Further genetic and molecular testing is needed to confirm the ways in which vacuolar storage regulates mitochondrial GSH.

## **Discussion**

We investigated the distribution of GSH and GSSG accumulated from the extracellular environment between the cytosol and the mitochondria of strains overexpressing *HGT1*. This study revealed that intracellular overaccumulation of GSH is distributed between subcellular organelles. Specifically, imported GSH and GSSG to the cytosol of *HGT1* strains results in elevated mitochondrial GSH and GSSG. Our ability to selectively look at increased GSH pools in the mitochondria allowed us to investigate the role of vacuolar storage in maintaining mitochondrial GSH levels. Ycf1 is the only vacuolar-localized ABC transporter in *Saccharomyces cerevisiae* identified as a regulator of cellular GSH (6). Therefore, a genetically modified strain where *YCF1* was deleted and transformed with an *HGT1* overexpression plasmid was used to determine the impact of vacuolar storage on mitochondrial GSH and GSSG.

Steady-state levels of accumulated GSH were measured in cytosolic and mitochondrial fractions of *ycf1Δ + HGT1* strains when cells were exposed to GSH. As expected, cytosolic and mitochondrial total GSH + GSSG was elevated in this strain. Interestingly, mitochondrial GSH + GSSG of *ycf1Δ + HGT1* showed increased total GSH accumulation compared to the WT strain. These data suggest that the loss of GSH export to the vacuole affects the amount of total GSH (GSH + GSSG) transported to the mitochondria. On the contrary, no difference in the cytosolic total GSH was measured.

Vacuolar storage was not only found to affect GSH levels but also the GSH:GSSG ratio (2, 6). Therefore, we measured GSSG levels of strains treated with reduced GSH. GSSG measurements showed that while there was no difference in total cytosolic GSH, GSSG levels in the *ycf1Δ + HGT1* strain were found to be lower than the WT strain. Likewise, the mitochondrial GSH accumulated was primarily in the reduced form in *ycf1Δ + HGT1*. Observing a smaller mitochondrial GSSG pool was interesting given that total GSH was elevated in *ycf1Δ + HGT1* compared to WT + *HGT1*. Thus, we conclude that *ycf1Δ* strains regulate both the cytosolic and mitochondrial redox state differently than WT and reductive systems such as GLR, the thioredoxin (TRX) and glutaredoxin (GRX) pathways may be responsible for these variations.

The human homologue of Ycf1, MRP1, has been demonstrated to exhibit GSSG transport activity (17, 18). Ycf1 has also been shown to regulate intracellular GSH when exposed to oxidants (2, 6). Therefore, in this study we directly measured changes in subcellular GSH when *HGT1* cells are grown in the presence of GSSG. We find that the import of GSSG causes cytosolic and mitochondrial total GSH to spike. *HGT1* strains where *ycf1* was deleted have an even greater accumulation of total GSH in both the cytosol

and mitochondria. While Ycf1 has already been shown to affect the cytosol GSH pool of strains with elevated GSSG, we present for the first time evidence that the vacuole may play a role in mitochondrial redox homeostasis. GSSG was also measured in WT + *HGT1* and *ycf1Δ* + *HGT1* cells exposed to GSSG. To our surprise, GSSG was lower in the cytosol and mitochondria of *ycf1Δ* + *HGT1*. Therefore, Ycf1 may be important for storing imported GSSG that had been reduced by cytosolic thiol reductases pathways prior to entering the vacuole. Taken together our studies suggest that vacuolar storage is involved in maintaining mitochondrial GSH and GSSG pools when cells are exposed to high GSH and GSSG levels. The cytosol, however, depends on vacuolar storage under the threat of increased oxidant exposure. These observations are important for our understanding of intercompartmental crosstalk. However, future studies are welcomed so that the relationship between GSH disruption and cellular consequence can be well established.

## References

1. Lazard, M., Ha-Duong, N. T., Mounié, S., Perrin, R., Plateau, P., and Blanquet, S. (2011) Selenodiglutathione uptake by the *Saccharomyces cerevisiae* vacuolar ATP-binding cassette transporter Ycf1p. *FEBS J.* 278, 4112-4121
2. Paumi, C. M., Pickin, K. A., Jarrar, R., Herren, C. K., and Cowley, S. T. (2012) Ycf1p attenuates basal level oxidative stress response in *Saccharomyces cerevisiae*. *FEBS Lett.* 586, 847-853
3. Brechbuhl, H. M., Gould, N., Kachadourian, R., Riekhof, W. R., Voelkerand, D. R., and Day, B. J. (2010) Glutathione transport is a unique function of the ATP-binding cassette protein ABCG2. *J. Biol. Chem.* 285, 16582-16587
4. Lee, T. K., Li, L., and Ballatori, N. (1997) Hepatic glutathione and glutathione S-conjugate transport mechanisms. in *Yale Journal of Biology and Medicine*, 70, 287-300
5. Rebbeor, J. F., Connolly, G. C., Dumont, M. E., and Ballatori, N. (1998) ATP-dependent transport of reduced glutathione on YCF1, the yeast orthologue of mammalian multidrug resistance associated proteins. *J. Biol. Chem.* 273, 33449-33454
6. Morgan, B., Ezeriņa, D., Amoako, T. N. E., Riemer, J., Seedorf, M., and Dick, T. P. (2013) Multiple glutathione disulfide removal pathways mediate cytosolic redox homeostasis. *Nat. Chem. Biol.* 9, 119-125
7. Marí, M., Morales, A., Colell, A., García-Ruiz, C., and Fernández-Checa, J. C. (2009) Mitochondrial Glutathione, a Key Survival Antioxidant. *Antioxid. Redox Signal.* 11, 2685-2700

8. Østergaard, H., Tachibana, C., and Winther, J. R. (2004) Monitoring disulfide bond formation in the eukaryotic cytosol. *J. Cell Biol.* 166, 337-345
9. Kumar, C., Igarria, A., D'Autreaux, B., Planson, A. G., Junot, C., Godat, E., Bachhawat, A. K., Delaunay-Moisan, A., and Toledano, M. B. (2011) Glutathione revisited: A vital function in iron metabolism and ancillary role in thiol-redox control. *EMBO J.* 30, 2044-2056
10. Darch, M. A. (2015) *Subcellular glutathione distribution during severe redox stress and characterizing thiol redox control of human CU, ZN superoxide*. Ph.D. thesis, University of South Carolina
11. Bourbouloux, A., Shahi, P., Chakladar, A., Delrot, S., and Bachhawat, A. K. (2000) Hgt1p, A high affinity glutathione transporter from the yeast *Saccharomyces cerevisiae*. *J. Biol. Chem.* 275, 13259–13265
12. Gietz, R. D., and Schiestl, R. H. (1991) Applications of high efficiency lithium acetate transformation of intact yeast cells using single-stranded nucleic acids as carrier. *Yeast.* 7, 253-263
13. Daum, G., Böhni, P. C., and Schatz, G. (1982) Import of proteins into mitochondria. Cytochrome *b*<sub>2</sub> and cytochrome *c* peroxidase are located in the intermembrane space of yeast mitochondria. *J. Biol. Chem.* 257, 13028-13033
14. Anderson, M. (1985) Glutathione and glutathione disulfide in biological samples. *Methods Enzymol.* 113, 548-555
15. Rahman, I., Kode, A., and Biswas, S. (2006) Assay for quantitative determination of glutathione and glutathione disulfide levels using enzymatic recycling method. *Nat. Protoc.* 1, 3159-3165

16. Toledano, M. B., Delaunay-Moisan, A., Outten, C. E., and Igarria, A. (2013) Functions and Cellular Compartmentation of the Thioredoxin and Glutathione Pathways in Yeast. *Antioxid. Redox Signal.* 18, 1699-1711
17. Minich, T., Riemer, J., Schulz, J. B., Wielinga, P., Wijnholds, J., and Dringen, R. (2006) The multidrug resistance protein 1 (Mrp1), but not Mrp5, mediates export of glutathione and glutathione disulfide from brain astrocytes. *J. Neurochem.* 97, 373-384
18. Hirrlinger, J., König, J., Keppler, D., Lindenau, J., Schulz, J. B., and Dringen, R. (2001) The multidrug resistance protein MRP1 mediates the release of glutathione disulfide from rat astrocytes during oxidative stress. *J. Neurochem.* 76, 627-636

## CHAPTER 3

### IDENTIFYING A MITOCHONDRIAL GLUTATHIONE TRANSPORTER IN *S. CEREVISIAE*

#### **Abstract**

Several mitochondrial functions rely on thiol-disulfide homeostasis and are thus influenced by glutathione (GSH) metabolism. These functions include maintaining the membrane structure and integrity, the activity of various sulfhydryl-dependent enzymes, and ion homeostasis. Despite GSH being exclusively made in the cytosol, mitochondria contain distinct GSH pools. This GSH is thought to originate from the transport of GSH from the cytosol across the mitochondrial inner membrane. However, the specific mitochondrial transporter that imports GSH into mitochondria has not been identified in *S. cerevisiae*. Here we investigated the role of Hgt1/Opt1, the plasma membrane high affinity GSH transporter, in mitochondrial GSH transport. A previous study found that Opt2, a close homolog of Hgt1/Opt1, is dually localized to the plasma membrane and peroxisomes of yeast. To determine if Hgt1 also exhibits dual localization to the plasma and mitochondrial membranes in a similar manner, we overexpressed Hgt1 with a hemagglutinin tag. Subcellular fractionation and western blot analysis suggested that Hgt1 is indeed localized to crude mitochondrial fractions. To elucidate if Hgt1 is specifically localized to the mitochondrial membrane, we further purified crude mitochondrial fractions

in hopes of removing plasma membrane contamination. While purified mitochondrial fractions were devoid of endoplasmic reticulum, vacuolar, and cytosolic fractions; we were unable to separate mitochondria from plasma membrane. Num1, the core component of the mitochondria-endoplasmic reticulum [ER]-cortex anchor (MECA) tethers mitochondria to the plasma membrane. To determine if plasma membrane contamination was due to Num1 expression, we used a *NUM1* deletion (*num1Δ*) strain overexpressing HA-tagged Hgt1. However, plasma membrane contamination was not removed in these strains. We further analyzed Hgt1's role in regulating mitochondrial GSH pools using genetic modifications of genes that influence GSH pools. Here we report that an *HGT1* deletion (*hgt1Δ*) strain does not affect mitochondrial GSH levels. Similarly, incubation of isolated mitochondria in *GSH1* deletion (*gsh1Δ*) strains overexpressing *HGT1* does not result in increased GSH uptake. Taken together, these studies show that cytosolic uptake of GSH by Hgt1 increases mitochondrial GSH. However, Hgt1 does not directly affect mitochondrial GSH pools and is unlikely a mitochondrial GSH transporter.

## **Introduction**

Redox chemistry is thought to play a pivotal role in understanding cellular processes such as oxidant-dependent signaling and cell fate decisions (1). Therefore, characterizing the redox environment within cells is vital to understanding diseases related to redox changes. Previously, research designed to understand cellular redox homeostasis was performed using whole cell measurements. These studies revealed important information regarding redox homeostasis; however, the differences in redox regulation mechanisms between subcellular compartments was not elucidated until recently (2). More recent

studies show that while GSH is exclusively made in the cytosol, it is transported across various membranes and is required for the function of other organelles (3). *Saccharomyces cerevisiae* has been extensively used to study GSH transport. In fact, the first high affinity GSH transporter, Hgt1, was discovered in this organism as well as other transporters localized to subcellular compartments (4, 5).

Redox balance is particularly important in the mitochondria since this organelle contains several proteins involved in redox signaling, apoptosis, and bioenergetics. Mitochondria are also subject to DNA mutations and oxidative damage caused by reactive oxygen species (ROS) produced during oxidative metabolism. To prevent hyper-oxidation, mitochondria rely on an array of antioxidants and detoxifying enzymes, with the redox active tripeptide GSH being the main line of defense. The importance of mitochondrial GSH is highlighted not only by its abundance but its ability to detoxify hydrogen peroxide, lipid hydroperoxides, and xenobiotics by serving as a cofactor to GSH peroxidases or glutathione-S-transferases (6). Further evidence supporting the critical nature of GSH in maintaining mitochondrial redox homeostasis are reports in which chemically depleted mitochondrial GSH, as opposed to cytosolic GSH, led to cellular injury in liver and kidney cells (7, 8).

Many studies using isolated mitochondria along with targeted green fluorescent protein (GFP) based probes have investigated mitochondrial GSH redox potentials and other subcellular pools. While these methods provide insight into the redox state of GSH in this organelle, the molecular mechanisms that control mitochondrial redox balance remain elusive. One key factor that eludes our understanding is the mechanism of GSH transport into this compartment. GSH is thought to freely diffuse through the outer membrane of the

mitochondria via porin channels (9). However, transport of GSH across the mitochondrial inner membrane is energetically unfavorable because it is negatively charged at physiological pH and the mitochondrial matrix is negatively charged. Thus, it is believed that a GSH transporter is required for import. Due to the overall negative charge of GSH, it was proposed that anionic carriers of the mitochondrial inner membrane could import GSH into the matrix (10). Research conducted by Chen et. al. using rat kidney and liver tissue identified two anionic carriers, dicarboxylate and 2-oxoglutarate carriers, as responsible for GSH uptake into the mitochondrial matrix (10, 11). Conversely, a more recent report in which human and yeast dicarboxylate and 2-oxoglutarate carriers were overexpressed in fused membrane vesicles of *Lactococcus lactis*, concluded that these carriers do not transport GSH (12). Therefore, an unambiguous mitochondrial GSH importer has yet to be identified.

Elbaz-Alon et al. discovered via colocalization studies using fluorescently tagged proteins that Opt2 exhibits dual localization to the plasma membrane and peroxisomes of yeast. Additionally, Opt2 was found to not only affect cytosolic and peroxisomal GSH:GSSG but mitochondrial GSH:GSSG homeostasis as well (13). Therefore, our lab set out to determine whether Hgt1 exhibits dual localization to the plasma and mitochondrial membranes. We also wanted to determine how Hgt1 affects subcellular GSH pools. A hemagglutinin (HA)-tagged Hgt1 overexpression plasmid coupled with mitochondrial isolation and purification was used to investigate the localization of Hgt1 to the mitochondrial fraction. Unfortunately, with this method Hgt1 localization to the mitochondria could not be determined with certainty.

Strains overexpressing *HGT1* have been shown to uptake extracellular GSH from the media into the cell, resulting in a 7-10 fold increase in GSH and GSSG (14). Therefore, we wanted to determine if Hgt1 had any effect on mitochondrial GSH pools. Our results showed that while it could not be determined if Hgt1 was localized to the mitochondrial membrane, redox stress caused by GSH uptake from the extracellular environment by Hgt1 does affect mitochondrial GSH pools.

### **Experimental Procedures**

*Yeast Strains, Plasmids, Media, and Growth Conditions*- The *S. cerevisiae* strains used in this study were derived from the wild type (WT) strain BY4741 (*MATa his3Δ1 leu2Δ0 met15Δ0 ura3Δ0*). Deletion strains *num1::kanMX4* and *hgt1::kanMX4* were purchased from Open Biosystems. Deletion of *HGT1* was confirmed by PCR colony screening using primers recommended by the *Saccharomyces* Genome Deletion Project (Table 3.1, primers used for PCR screening) (15). The *gsh1Δ* strain was made by deleting the *GSH1* gene using pGSH1KO (see plasmid construction for more information). Yeast transformations were performed using standard lithium acetate transformation protocols (16). Yeast strains were cultured at 30 °C in synthetic complete (SC) media (US Biological) supplemented with either 2% glucose or 2% galactose as the carbon source with the appropriate amino acids.

*Plasmid Construction*- The *GSH1* deletion plasmid (pGSH1KO) was created by cloning flanking regions of the *GSH1* gene. Briefly, upstream and downstream regions of *GSH1* were amplified using primers engineered with BamHI, Sall, and EcoRI cut sites (Table 3.2). The resulting fragments from PCR amplification were cloned into an empty

Table 3.1 Primers used to check for *HGT1* deletion (15).

<b>Primer Name</b>	<b>Primer Sequence</b>
<b>Hgt1_A_SCRN</b>	GTCACACAAAATCCAGGACAATAG
<b>Hgt1_B_SCRN</b>	TCAAAATGTACATAGCGTATGCAGT
<b>Hgt1_C_SCRN</b>	GCATAATATCGATGGCTTATGTACC
<b>Hgt1_D_SCRN</b>	TTCTTAAAGTCGGAATTTGTTATCG
<b>KanB1</b>	TGTACGGGCGACAGTCACAT
<b>KanC3</b>	CCTCGACATCATCTGCCAGAT

Table 3.2 Primers used to make pGSH1KO (restriction enzyme sites are underlined in primer sequence).

<b>Primer Name</b>	<b>Primer Sequence</b>	<b>Restriction Enzyme</b>
<b>GSH1KO Primer A</b>	GATTATATT <u>GAATTCTT</u> GTGCTGGAG	EcoRI
<b>GSH1KO Primer B</b>	GATTCCAC <u>GGATCCTT</u> AATG	BamHI
<b>GSH1KO Primer C</b>	GATTTGCTG <u>TCGACGTG</u> TGATAG	Sall
<b>GSH1KO Primer D</b>	CTCAGAGATCTTT <u>GAATTCTT</u> GTTC	EcoRI

integrating vector (pRS403) with a *HIS3* selection marker at the BamHI and SalI sites. The yeast integrating plasmid was linearized with EcoRI and inserted into the genome of yeast strains via homologous recombination. The p416-*TEF-HGT1* plasmid (*CEN, URA3*) which allows *HGT1* to be constitutively expressed via the *TEF1* promoter was a kind gift from Anand Kumar Bachhawat (5, 14, 17).

*Small Scale Mitochondrial Isolation*- To separate the cytosolic and mitochondrial fractions, yeast strains were plated on 2% glucose SC media for 2-3 days. Cells were then cultured in SC with 2% galactose at 30 °C overnight until reaching O.D. ~ 1.0. Cells were washed with deionized water followed by SOR buffer (1.2 M sorbitol, 20 mM Hepes, pH 7.5). Pelleted cells were resuspended in SOR buffer and lysed with zymolyase for 30 min to 1 hour. To prevent protein degradation, spheroplasts were placed on ice and resuspended in ice-cold SM buffer (250 mM sucrose, 10 mM MOPS, pH 7.2) containing protease inhibitors. Organelle release was obtained via Dounce homogenization which disrupts the plasma membrane. The homogenate containing cytosol and crude mitochondria was separated from unbroken cells and nuclei by centrifugation at 3000 rpm for 5 min at 4 °C. After saving some of this low-speed centrifugation supernatant, the remainder was centrifuged at 12000 rpm for 10 min at 4 °C, separating the mitochondria from the post-mitochondrial supernatant (PMS) (18). The crude mitochondrial pellet was carefully washed with SM buffer and diluted to desired volume.

*GSH/GSSG Assays*- Spectrophotometric analysis of GSH concentration was determined by creating whole cell lysates of  $2 \times 10^7$  cells for strains with normal GSH levels or  $2 \times 10^9$  cells for GSH-depleted *gsh1Δ* strains. Cell lysates were resuspended in 1% SSA (5-sulfosalicylic acid) and broken in a bead beater with acid-washed glass beads.

The broken cells were centrifugation at 13000 x g for 5 min to pellet out the precipitated protein (19). GSH concentration in the supernatant was determined by mixing 20  $\mu$ L of acidified lysate with 180  $\mu$ L reaction mix (0.1 mM Na-phosphate, pH 7.5, 1 mM EDTA, 2 mM DTNB (5,5'-dithiobis(2-nitrobenzoic acid)), 1 mM NADPH) and 3 U/mL GSSG reductase. The reduction of DTNB to TNB (2-nitro-5-thiobenzoic acid) via GSH was monitored at 412 nm. Absorption measurements were taken every 15 seconds for approximately 2 minutes (20). Standard concentrations of GSH are obtained by using known concentrations of GSH solubilized in 1% SSA. The rate of increasing absorbance is directly proportional to GSH concentration over a range of 2 minutes.

*Large Scale Mitochondrial Isolation and Purification-* Yeast cells were cultured in SC with 2% galactose media (to promote mitochondrial biogenesis) at 30 °C overnight to O.D. ~1.0. The next morning, cells were diluted into large volumes and grown to mid-log phase. Mitochondrial isolation and purification was conducted according to a previously published method (21). In brief, cells were washed with water and incubated with DTT buffer (100 mM Tris-H<sub>2</sub>SO<sub>4</sub>, pH 9.4, 10 mM DTT (dithiothreitol)) at 30°C for 20 min. Pelleted cells were washed with zymolyase buffer (1.2 M sorbitol, 20 mM potassium phosphate, pH 7.4) and lysed with 3 mg of zymolyase per g cells for 30-45 minutes. Spheroplasts were resuspended in ice-cold homogenization buffer (0.6 M sorbitol, 10 mM Tris-HCl, pH 7.4, 1 mM EDTA, 1 mM PMSF, 0.2% BSA) containing protease inhibitors. Organelles were released via Dounce homogenization. Cytosolic and mitochondrial fractions were separated from unbroken cells and nuclei by centrifugation at 4000 g for 5 min at 4 °C. Crude mitochondria were isolated from the cytosol by centrifugation at 12000 g for 10 min at 4 °C. The mitochondrial pellet was washed with SEM buffer (250 mM

sucrose, 1 mM EDTA, 10 mM MOPS-KOH, pH 7.2) and diluted to desired volume (22). Purification of crude mitochondria was done over a sucrose step gradient using 15%, 23%, 32%, and 60% sucrose prepared in EM buffer (1 mM EDTA, 10 mM MOPS-KOH, pH 7.2). Mitochondria were carefully loaded on top of the sucrose gradient and centrifuged at 134000 g (33000 rpm) for 1 hour at 4 °C using a Beckman SW41 Ti Swinging-bucket Rotor. Recovered purified mitochondria from the 60%/32% interface were washed with SEM buffer and diluted to desired volume (21).

*SDS-PAGE and Immunoblotting Techniques-* SDS-PAGE analysis was used to separate protein fractions via electrophoresis on 12% Tris-Glycine gels (Invitrogen). Samples were prepared by treatment with 1X SDS (sodium dodecyl sulfate) loading buffer containing 0.6 M DTT followed by heating at 95 °C prior to sample loading. The separated protein was then transferred to a nitrocellulose membrane and blocked at room temperature for 1 hour in 5% TBST milk blocking buffer (1X TBS, 0.1% Tween-20 with 5% w/v nonfat dry milk). Immunoblotting was performed using HA antibodies (1:1000, rabbit IgG, Santa Cruz Biotechnology), Pgl1 antibodies (1:10,000, mouse IgG monoclonal, Invitrogen), Porin (1:10,000 mouse IgG monoclonal, Invitrogen), Cpy1 (1:10,000 mouse IgG monoclonal, Invitrogen), Dpm1 (1:10,000 mouse IgG monoclonal, Invitrogen), and Pma1 (1:10,000 mouse IgG monoclonal, Invitrogen) in blocking buffer.

*GSH Uptake into Isolated Mitochondria-* GSH uptake into purified mitochondria was performed according to a previously published protocol. Incubation steps with DTT and protease inhibitors or PMSF were omitted (18). Freshly prepared mitochondria were purified according to the small mitochondrial isolation protocol listed above. Crude mitochondria were treated with 15 mM GSH resuspended in SM buffer and untreated cells

were used as a control. A 27% sucrose cushion prepared in EM buffer was layered under the mitochondria using a syringe. Samples were placed in the 30 °C incubator for 30 minutes to allow uptake of GSH. Afterwards, mitochondria were centrifuged through the sucrose cushion at 14000 X g for 10 minutes at 4 °C. Pelleted mitochondria were washed with SM buffer and centrifuged (23). The resulting mitochondrial pellet was acidified with 1% SSA on ice for 30 minutes. Lysates were centrifuged at 13000 x g and the supernatant was transferred to new tube. Total GSH was measured in isolated mitochondria using the GSH/GSSG DTNB cycling assay as previously described (20).

## **Results**

*Incubation of 100 μM GSH in yeast overexpressing HGT1 increases cytosolic and mitochondrial GSH-* In our previous studies, we observed a spike in mitochondrial GSH in yeast strains overexpressing *HGT1*. Therefore, we set out to determine if this increase is a result of excess cytosolic GSH being shuttled into the mitochondria or if Hgt1 is localized to the mitochondrial membrane. Using a spectrophotometric enzyme cycling assay, we measured the steady state concentrations of GSH in cytosolic and mitochondrial fractions of cells treated with 100 μM GSH using untreated cells as a control. Again, we see that intracellular GSH is elevated in both the cytosol and mitochondria. Overexpression of the Hgt1 transporter alone, however, does not affect cytosolic or mitochondrial GSH levels in the absence of added GSH to the media, as seen in untreated cells (Fig. 3.1). These results agree with research done by Kumar et. al. showing that intracellular GSH spikes within an hour of adding GSH to the media when *HGT1* is overexpressed in WT yeast (14). Taken

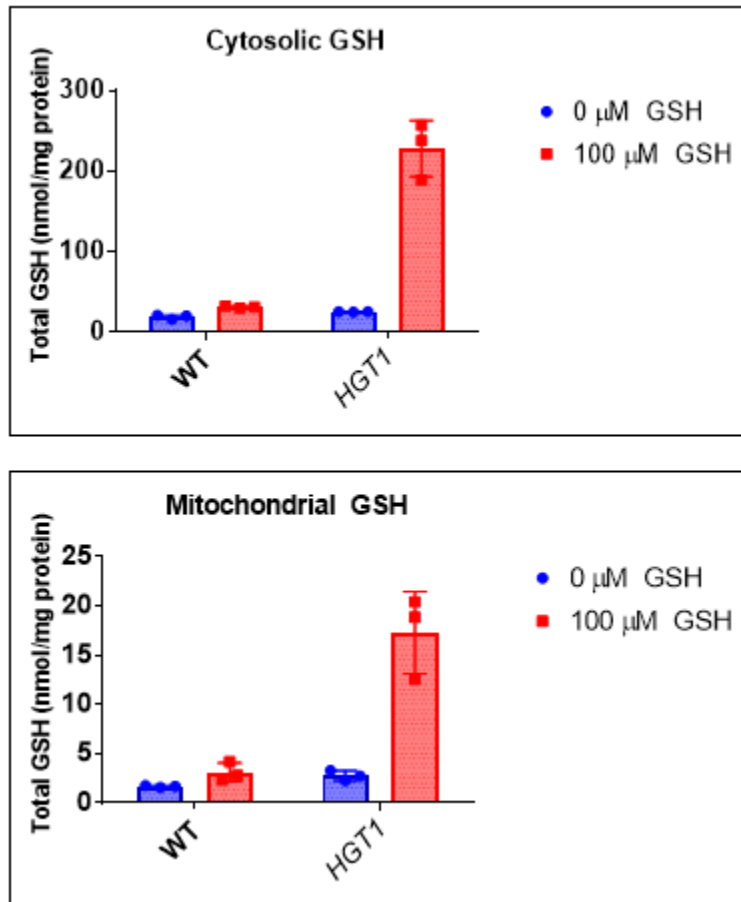


**Figure 3.1 Incubation of 100 μM GSH in yeast overexpressing *HGT1* increases cytosolic and mitochondrial GSH.** *HGT1* overexpression plasmid or the vector control was transformed into WT strain BY4741. Intracellular GSH was determined for cells incubated with extracellular GSH by growing cells overnight to exponential phase and adding 100 μM GSH to media to select cells for 20 min. Cytosolic and mitochondrial fractions were isolated and the total GSH in each extract was measured using the DTNB enzyme cycling assay. Error bars represent the standard deviation for three biological replicates.

together, these results demonstrate that *HGT1* overexpression specifically impacts both cytosolic and mitochondrial GSH levels.

*Deletion of HGT1 impairs uptake of cytosolic GSH but has no effect on mitochondrial GSH-* To further understand if Hgt1 has any effect on mitochondrial GSH pools, we used a genetically modified strain where *HGT1* was deleted. Subsequently, GSH was measured in cytosolic and mitochondrial fractions collected from cells treated with 100  $\mu$ M GSH for 30 minutes as well as from the untreated cells (Fig. 3.2). As expected, *HGT1* deletion lead to lower cytosolic uptake of GSH-treated cells. These data are in agreement with results reported by Bourbonloux et al. that found deleting *HGT1* significantly reduced the ability of yeast cells to import radioactive GSH (5). However, we did not find that mitochondrial GSH uptake was affected in *hgt1* $\Delta$  strains compared to WT strains. These results indicate that Hgt1 is not the primary mitochondrial GSH transporter or may be only partially responsible for GSH uptake if there are multiple GSH entry routes into mitochondria.

*Hgt1-HA is localized to crude mitochondrial fractions-* To explore the possibility that Hgt1 is intracellularly localized, we employed an *HGT1* overexpression plasmid containing a C-terminal HA tag that was gifted to us by Anand Kumar Bachhawat (17). Yeast cells were fractionated and western blot analysis was performed to determine the localization of Hgt1-HA (Fig. 3.3). As expected, Hgt1-HA was found in whole cell lysates that include the plasma membrane. The cytosolic fraction was almost completely devoid of Hgt1-HA. Surprisingly, crude mitochondrial fractions contained the Hgt1-HA protein. The results indicate that Hgt1-HA co-localizes with mitochondrial fractions and could potentially be localized to this organelle. However, since crude mitochondria contain other

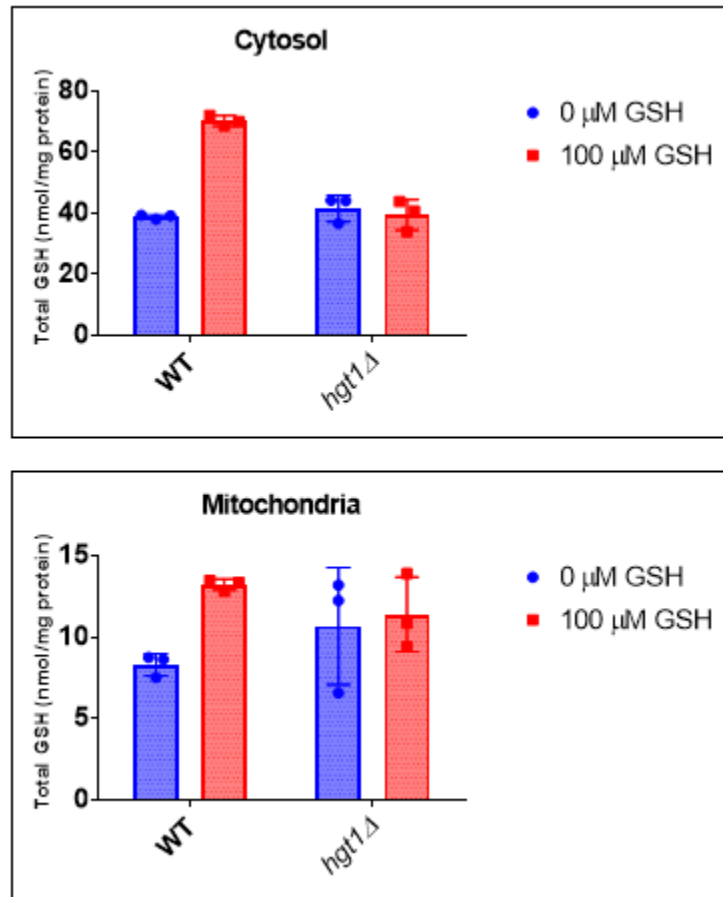


**Figure 3.2 Deletion of *HGT1* impairs uptake of cytosolic GSH but has no effect on mitochondrial GSH.** WT BY4741 and *hgt1Δ* yeast were grown overnight to mid-log phase in SC media. Subsequently, 100 μM GSH was added to the growth media and cells were harvested after 20 minutes. Cytosolic and mitochondrial fractions were isolated and the total GSH in each extract was measured using the DTNB enzyme cycling assay. Error bars are indicative of the standard deviation of three independent experiments.

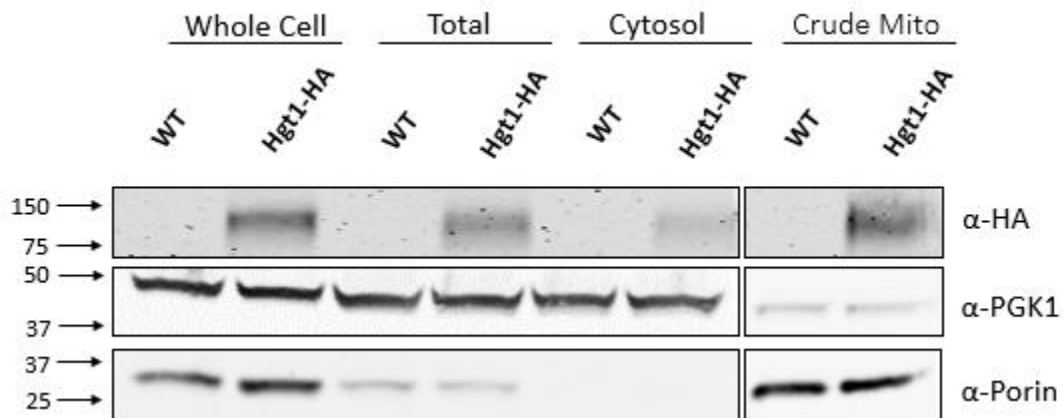


**Figure 3.3 Hgt1-HA is localized to crude mitochondrial fractions.** Cells transformed with empty vector (WT) or *HGT1-HA* plasmid were lysed and fractionated into cytosolic and crude mitochondrial (mito) fractions. Whole cell and total lysates (containing the cytosolic and crude mitochondrial fraction) were saved prior to fractionation and used as controls. 75  $\mu$ g of protein was loaded for whole cell, total, and cytosolic compartments. 15  $\mu$ g of mitochondrial protein was added to the gel. All fractions were analyzed using SDS-PAGE and immunoblotted with HA, PGK1 (cytosolic marker), and Porin (mitochondria marker) antibodies.

subcellular compartments such as ER and vacuole, as well as plasma membrane,(22) the exact localization of the Hgt1-HA protein could not be determined using this method.

*Hgt1-HA is localized to purified mitochondrial fractions-*To determine if Hgt1-HA is truly localized to the mitochondria when overexpressed, we proceeded to purify crude mitochondria using density gradient ultracentrifugation. Western blot analysis was performed on whole cell, cytosolic, crude mitochondria and purified mitochondrial fractions (Fig 3.4). Using this method, we successfully separated the mitochondria from vacuolar and most ER contamination. These results suggest Hgt1-HA in the crude mitochondria fraction was not localized to these compartments. Unfortunately, we were not able to successfully separate the plasma membrane from the purified mitochondrial sample. Therefore, we cannot conclusively state that Hgt1 is dually localized to the mitochondrial and plasma membranes.

*Plasma membrane contamination of purified mitochondria is not due to Num1 mito-ER tethering-* During cell division, mitochondria are inherited from the mother to the daughter cells. This process involves tethering of the mitochondria to the plasma membrane (24). The proper positioning of mitochondria in budding yeast requires the mitochondria-ER cortex anchor (MECA), of which Num1 is the principal component. The C-terminal pleckstrin homology domain of Num1 interacts with the plasma membrane while the N-terminal coiled-coil domain of Num1 interacts with mitochondria (25). This interaction facilitates cluster formation of Num1 dimers, which is essential for tethering of the plasma membrane to the mitochondria (26). Here we investigated whether Num1 tethering was responsible for the plasma membrane contamination that was seen in purified mitochondria. Using a *NUM1* deletion strain (*num1Δ*) to eliminate mitochondria-plasma

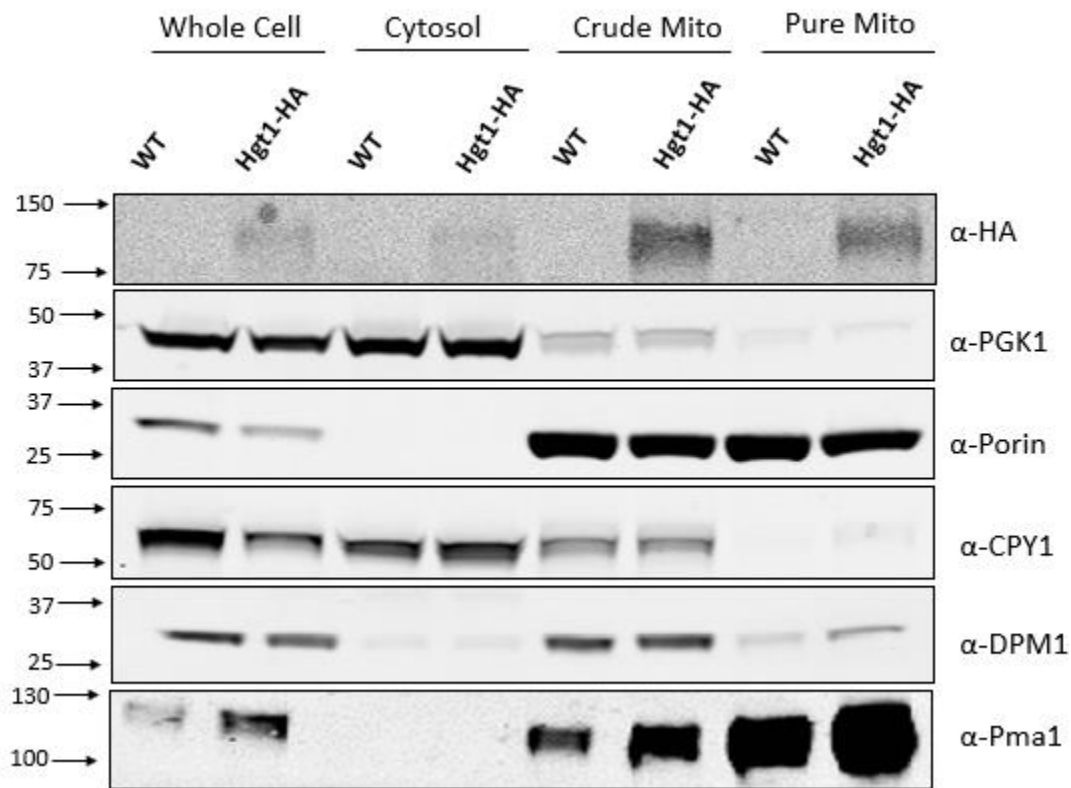


**Figure 3.4 Hgt1-HA is localized to purified mitochondrial fractions.** Yeast were grown to mid-log phase in SC media using 2% galactose as the carbon source. Prior to fractionation, whole cell lysates were prepared and saved as controls. The cytosol was separated from crude mitochondria (mito) by a series of low and high-speed centrifugation steps. Resulting mitochondria were density gradient purified via ultracentrifugation. 75  $\mu$ g of protein was loaded for the whole cell and cytosolic fractions. 15  $\mu$ g of crude and purified mitochondrial protein was added to the gel. Fractions were separated by SDS-PAGE and immunoblotted against HA, Pkg1 (cytosolic marker), Porin (mitochondria marker), Cpy1 (vacuolar marker), Dpm1 (ER marker), and Pma1 (plasma membrane marker) antibodies.

membrane tethering, we fractionated and purified mitochondria (Fig. 3.5). The resulting western blot showed that mitochondria purified from *num1* $\Delta$  yeast still contained some plasma membrane contamination. Thus, it seems that tethering is not responsible for this contamination and that the density gradient purification protocol we used is not effective at purifying mitochondria from plasma membrane.

*HGT1 overexpression in gsh1* $\Delta$  strains does not increase GSH uptake into isolated mitochondria- To determine if Hgt1 is directly involved in GSH accumulation in the mitochondria, we measured the uptake of GSH into isolated mitochondria from GSH depleted cells that overexpress *HGT1* (Fig 3.6). GSH depletion in yeast cells was accomplished by knocking out the  $\gamma$ -glutamylcysteine synthetase gene (*GSH1*), which catalyzes the first step in the GSH biosynthesis pathway (27). The resulting *GSH1* deletion (*gsh1* $\Delta$ ) strain was then transformed with the *HGT1* overexpression plasmid and vector control and grown in GSH-deficient media. Isolated mitochondria were treated with 15 mM GSH or the buffer control for 30 minutes. GSH uptake was determined by the acidification of mitochondrial samples and total GSH measurement via the DTNB enzyme cycling assay. Our results show that the uptake of GSH into purified mitochondria from the surrounding buffer is similar for *HGT1* overexpression strains and the vector control. Taken together with previous studies, we conclude that Hgt1 is not a mitochondrially localized protein and mitochondrial GSH pools are not directly affected by overexpression or deletion of the transporter.

## **Discussion**

GSH participates in several biological functions and reduced GSH is a key factor in protecting cells against damage by toxic xenobiotics, reactive oxygen compounds, and

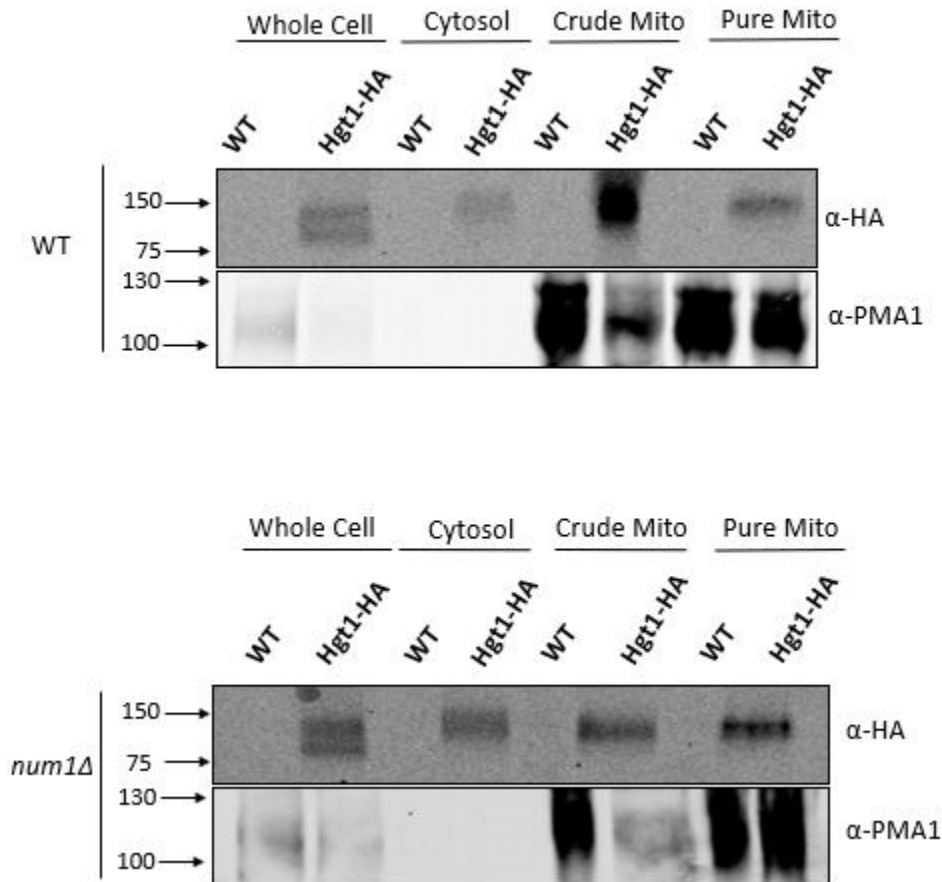


**Figure 3.5 Plasma membrane contamination of purified mitochondria is not due to Num1 mito-ER tethering.** WT and *num1Δ* were transformed with *HGT1* overexpression and vector control plasmids. Cytosolic and crude mitochondria (mito) fractions were separated by a series of low and high-speed centrifugation steps. Resulting mitochondria were layered over a sucrose gradient and purified using ultracentrifugation. 75  $\mu$ g of protein was loaded for the whole cell and cytosolic fractions. 15  $\mu$ g of crude and purified mitochondrial protein was added to the gel. Fractions were separated by SDS-PAGE and immunoblotted against HA and Pma1 (plasma membrane marker) antibodies.

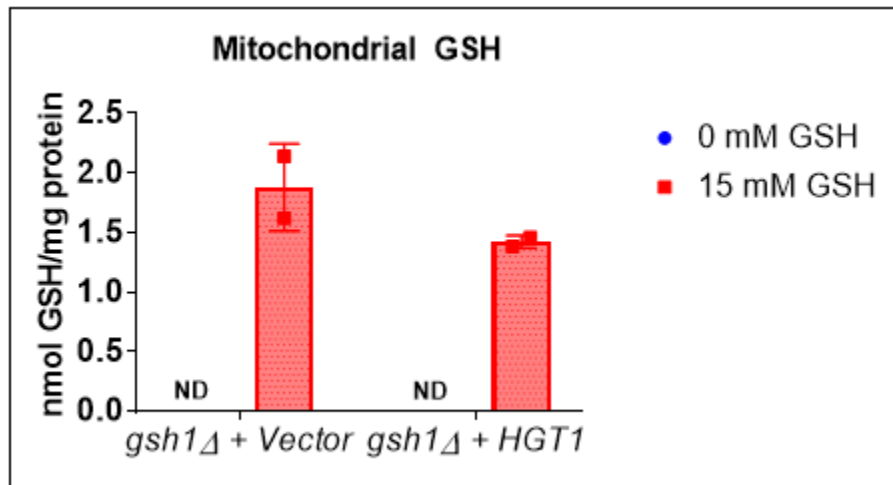


**Figure 3.6 *HGT1* overexpression in *gsh1Δ* strains does not increase GSH uptake into isolated mitochondria.** Crude mitochondria were isolated from *gsh1Δ* strains overexpressing *HGT1* and the vector control. Mitochondria was layered over a 27% sucrose cushion at 2000  $\mu\text{g/mL}$  and treated with 15 mM GSH for 30 minutes at 30  $^{\circ}\text{C}$ . Samples were treated with 1% SSA and GSH concentration was measured using the DTNB enzyme cycling assay. ND, not detected due to levels below the assay detection limit.

heavy metals. Mitochondrial GSH status is particularly important given that selective depletion of mitochondrial GSH leads to cellular injury (28). To understand the mechanisms that regulate mitochondrial GSH levels and redox state, it is critical to understand GSH transport inside the mitochondrial matrix. Two anion transporters, dicarboxylate and 2-oxoglutarate carriers, isolated from renal tissue were found to be responsible for approximately 70-80% of GSH transport into the mitochondria in mammalian cells. These results were based on GSH uptake studies in the presence of known inhibitors of each anionic carrier (10)(11). However, studies overexpressing the dicarboxylate and 2-oxoglutarate carriers in fused membrane vesicles of *Lactococcus lactis* contradict these findings (12). Homologues of the dicarboxylate and 2-oxoglutarate anionic carriers in *S. cerevisiae* have been identified. However, their specific role in GSH transport has not yet been demonstrated.

Due to the conflicting data surrounding the proposed mitochondrial GSH transporters and recent reports that the Hgt1 homologue, Opt2, is dually localized to plasma and peroxisomal membranes, we decided to explore the role of Hgt1 in mitochondrial GSH import. We also set out to determine if Hgt1 is localized to subcellular organelles and specifically the mitochondrial membrane. Localization of Hgt1 was determined by overexpressing HA-tagged Hgt1. Isolation of crude cytosolic and mitochondrial fractions revealed Hgt1 in the mitochondria. While interesting, these data did not definitively mean that Hgt1 is localized to mitochondria, given that crude mitochondria isolates are often contaminated with vacuole, ER, and some plasma membranes. Thus, we proceeded to further purify crude mitochondrial fractions via density gradient ultracentrifugation. This purification procedure removed vacuole contamination and most of the ER found in crude

mitochondria. However, with this method we were not able to separate plasma membrane from mitochondria.

During the cell cycle, mitochondria are partitioned from the mother cells to the daughter cells through a process known as tethering. Tethering plays a critical role in maintaining the shape and position of mitochondria, which is critical for proper function. The cell cortex protein, Num1, is responsible for mitochondrial inheritance and positioning in budding yeast by tethering the mitochondria to the inner face of the plasma membrane (24–26). We hypothesized that plasma membrane contamination of purified mitochondria was due to Num1 tethering. A genetically modified yeast with *NUM1* deleted was fractionated and mitochondria purified. Antibodies for the plasmid membrane H<sup>+</sup>-ATPase Pma1 was used as a plasma membrane marker in purified mitochondria from the *num1Δ* strain. As seen in WT yeast, Pma1 contamination was not removed from the purified mitochondria under these conditions. Therefore, we concluded that Hgt1-HA was not intracellularly localized to the ER or vacuole. Secondly, mitochondrial purification using a sucrose gradient was not effective for determining localization of Hgt1-HA on the mitochondrial membrane.

To further investigate the role of Hgt1 in mitochondrial GSH transport, we created a *GSH1* deletion strain where *HGT1* is overexpressed (*gsh1Δ + HGT1*). *GSH1* deletion results in whole cell GSH depletion when GSH is omitted from the growth media (29). Mitochondria were isolated from the *gsh1Δ + HGT1* strain and treated with 15 mM GSH. Cells devoid of GSH were used so that any measured GSH could be attributed to the uptake by Hgt1 and not cytosolic biogenesis and transport into mitochondria prior to isolation. When compared to the vector control, *HGT1* overexpression strains had similar levels of

GSH uptake into mitochondria. Taken together with our localization studies, we believe that it is unlikely that Hgt1 is a mitochondrial transporter. Given the importance of mitochondrial GSH pools to many cellular functions, future studies identifying the GSH transporter within the mitochondrial matrix would be beneficial for understanding pathologies connected to changes in mitochondrial GSH.

In this study, we also looked at the effect of Hgt1 on mitochondrial GSH pools. First, we employed the *HGT1* overexpression plasmid in WT yeast and measured GSH accumulation in cytosolic and mitochondrial fractions from cells treated with 100  $\mu$ M GSH. We found that cells under reductive stress accumulate both cytosolic and mitochondrial GSH. Therefore, we show that while Hgt1 may not directly import GSH into the mitochondria, a large influx of GSH into the cytosol increases mitochondrial GSH pools.

To further elucidate the impact of *HGT1* on mitochondrial GSH pools we used a *HGT1* deletion strain. Previous reports using a *hgt1* $\Delta$  strain showed that uptake of radiolabeled GSH is significantly reduced (5). Our results confirm these findings as we see that cytosolic GSH of *hgt1* $\Delta$  is lower compared to WT cells treated with 100  $\mu$ M GSH. Interestingly, we find that mitochondrial GSH is unaffected by extracellular GSH compared to the WT control. Thus, it appears that mitochondria can maintain GSH pools in cells that have reduced cytosolic GSH. Overall, our data show that increasing the cytosolic GSH pools can affect GSH pools in subcellular organelles. However, reduced import has no effect of mitochondrial GSH. These results address the topic of subcellular cross-talk, which is thought to be important in maintaining redox homeostasis. Future studies focused on identifying GSH transporters involved in regulating GSH pools would be of interest.

## References

1. Aller, I., Rouhier, N., and Meyer, A. J. (2013) Development of roGFP2-derived redox probes for measurement of the glutathione redox potential in the cytosol of severely glutathione-deficient *rml1* seedlings. *Front. Plant Sci.* 4, 506
2. Morgan, B., Ezeriņa, D., Amoako, T. N. E., Riemer, J., Seedorf, M., and Dick, T. P. (2013) Multiple glutathione disulfide removal pathways mediate cytosolic redox homeostasis. *Nat. Chem. Biol.* 9, 119-125
3. Miyake, T., Hazu, T., Yoshida, S., Kanayama, M., Tomochika, K., Shinoda, S., and Ono, B. (1998) Glutathione transport systems of the budding yeast *Saccharomyces cerevisiae*. *Biosci. Biotechnol. Biochem.* 62, 1858-1864
4. Bachhawat, A. K., Thakur, A., Kaur, J., and Zulkifli, M. (2013) Glutathione transporters. *Biochim. Biophys. Acta - Gen. Subj.* 1830, 3154-3164
5. Bourbouloux, A., Shahi, P., Chakladar, A., Delrot, S., and Bachhawat, A. K. (2000) Hgt1p, A high affinity glutathione transporter from the yeast *Saccharomyces cerevisiae*. *J. Biol. Chem.* 275, 13259–13265
6. Marí, M., Morales, A., Colell, A., García-Ruiz, C., and Fernández-Checa, J. C. (2009) Mitochondrial Glutathione, a Key Survival Antioxidant. *Antioxid. Redox Signal.* 11, 2685-2700
7. Olafsdottir, K., Pascoe, G. A., and Reed, D. J. (1988) Mitochondrial glutathione status during Ca<sup>2+</sup> ionophore-induced injury to isolated hepatocytes. *Arch. Biochem. Biophys.* 263, 226-235
8. Shan, X., Jones, D. P., Hashmi, M., and Anders, M. W. (1993) Selective Depletion of Mitochondrial Glutathione Concentrations by (R,S)-3-Hydroxy-4-pentenoate Potentiates Oxidative Cell Death. *Chem. Res. Toxicol.* 6, 75-81

9. Kojer, K., Bien, M., Gangel, H., Morgan, B., Dick, T. P., and Riemer, J. (2012) Glutathione redox potential in the mitochondrial intermembrane space is linked to the cytosol and impacts the Mia40 redox state. *EMBO J.* 31, 3169-3182
10. Chen, Z., and Lash, L. H. (1998) Evidence for Mitochondrial Uptake of Glutathione by Dicarboxylate and 2-Oxoglutarate Carriers. *J. Pharmacol. Exp. Ther.* 285, 608-618
11. Chen, Z., Putt, D. A., and Lash, L. H. (2000) Enrichment and functional reconstitution of glutathione transport activity from rabbit kidney mitochondria. Further evidence for the role of the dicarboxylate and 2-oxoglutarate carriers in mitochondrial glutathione transport. *Arch. Biochem. Biophys.* 373, 193-202
12. Booty, L. M., King, M. S., Thangaratnarajah, C., Majd, H., James, A. M., Kunji, E. R. S., and Murphy, M. P. (2015) The mitochondrial dicarboxylate and 2-oxoglutarate carriers do not transport glutathione. *FEBS Lett.* 589, 621-628
13. Elbaz-Alon, Y., Morgan, B., Clancy, A., Amoako, T. N. E., Zalckvar, E., Dick, T. P., Schwappach, B., and Schuldiner, M. (2014) The yeast oligopeptide transporter Opt2 is localized to peroxisomes and affects glutathione redox homeostasis. *FEMS Yeast Res.* 14, 1055-1067
14. Kumar, C., Igbaria, A., D'Autreaux, B., Planson, A. G., Junot, C., Godat, E., Bachhawat, A. K., Delaunay-Moisan, A., and Toledano, M. B. (2011) Glutathione revisited: A vital function in iron metabolism and ancillary role in thiol-redox control. *EMBO J.* 30, 2044-2056
15. Saccharomyces Genome Deletion Project
16. Gietz, R. D., and Schiestl, R. H. (1991) Applications of high efficiency lithium

- acetate transformation of intact yeast cells using single-stranded nucleic acids as carrier. *Yeast*. 7, 253-263
17. Thakur, A., and Bachhawat, A. K. (2010) The role of transmembrane domain 9 in substrate recognition by the fungal high-affinity glutathione transporters. *Biochem. J.* 429, 593-602
  18. Daum, G., Böhni, P. C., and Schatz, G. (1982) Import of proteins into mitochondria. Cytochrome *b*<sub>2</sub> and cytochrome *c* peroxidase are located in the intermembrane space of yeast mitochondria. *J. Biol. Chem.* 257, 13028-13033
  19. Anderson, M. (1985) Glutathione and glutathione disulfide in biological samples. *Methods Enzymol.* 113, 548-555
  20. Rahman, I., Kode, A., and Biswas, S. (2006) Assay for quantitative determination of glutathione and glutathione disulfide levels using enzymatic recycling method. *Nat. Protoc.* 1, 3159, 3165
  21. Meisinger, C., Sommer, T., and Pfanner, N. (2000) Purification of *Saccharomyces cerevisiae* mitochondria devoid of microsomal and cytosolic contaminations. *Anal. Biochem.* 287, 339342
  22. Meisinger, C., Pfanner, N., and Truscott, K. N. (2006) Isolation of mitochondria. *Methods Mol. Biol. Clift. Nj.* 313, 33-39
  23. Shen, D., Dalton, T. P., Nebert, D. W., and Shertzer, H. G. (2005) Glutathione redox state regulates mitochondrial reactive oxygen production. *J. Biol. Chem.* 280, 25305-25312
  24. Klecker, T., Scholz, D., Förtsch, J., Westermann, B. (2013) The yeast cell cortical protein Num1 integrates mitochondrial dynamics into cellular architecture. *J. Cell*

*Sci.* 126, 2924-2930

25. Ping, H. A., Kraft, L. M., Chen, W. T., Nilles, A. E., and Lackner, L. L. (2016) Num1 anchors mitochondria to the plasma membrane via two domains with different lipid binding specificities. *J. Cell Biol.* 213, 513-524
26. Kraft, L. M., and Lackner, L. L. (2017) Mitochondria-driven assembly of a cortical anchor for mitochondria and dynein. *J. Cell Biol.* 216, 3061-3071
27. Pompella, A., Visvikis, A., Paolicchi, A., De Tata, V., and Casini, A. F. (2003) The changing faces of glutathione, a cellular protagonist. in *Biochemical Pharmacology*, 66, 1499-1503
28. Lash, L. H., Putt, D. A., and Matherly, L. H. (2002) Protection of NRK-52E cells, a rat renal proximal tubular cell line, from chemical-induced apoptosis by overexpression of a mitochondrial glutathione transporter. *J Pharmacol Exp Ther.* 303, 476-486
29. Ayer, A., Tan, S.-X., Grant, C. M., Meyer, A. J., Dawes, I. W., and Perrone, G. G. (2010) The critical role of glutathione in maintenance of the mitochondrial genome. *Free Radic. Biol. Med.* 49, 1956-1968

## CHAPTER 4

### OVEREXPRESSION OF THE YEAST HIGH AFFINITY GLUTATHIONE TRANSPORTER, HGT1, RESCUES GROWTH IN CELLS LACKING $\gamma$ - GLUTAMYL-CYSTEINE SYNTHETASE

#### **Abstract**

In *Saccharomyces cerevisiae*, depletion of glutathione (GSH) leads to increased sensitivity to oxidants and other toxic compounds, disruption of Fe-S cluster maturation, and eventually cell death. Subcellular GSH pools are maintained by intracellular biosynthesis and import of GSH from the extracellular environment. The physiological implications of disrupting the *GSH1* gene encoding  $\gamma$ -glutamylcysteine synthetase, causing low levels of GSH, have been very well characterized. Recent studies have also demonstrated the effects of GSH overaccumulation via overexpression of the high affinity GSH transporter, Hgt1. However, it has not been determined how cells that shuttle between GSH deplete and replete conditions respond to extreme fluctuations in GSH pools. To study this, our lab employed a GSH deplete (*gsh1* $\Delta$ ) yeast strain engineered to overexpress *HGT1*. Interestingly, we find that *HGT1* overexpression partially rescues growth in the absence of GSH in *gsh1* $\Delta$  strains. This result was dependent on the availability of cysteine in the growth media; however, overexpression of the high affinity cysteine transporter Yct1 did not rescue growth in the *gsh1* $\Delta$  strain in a similar manner as Hgt1. Furthermore, cysteine levels are not significantly increased in *HGT1* overexpression strains. Another

thiol containing molecule, dithiothreitol, also partially restored growth in *gsh1Δ* cells overexpressing *HGT1*, suggesting that the rescue involves redox-dependent pathways. Previous studies have shown that GSH limitation in yeast leads to an iron starvation response that is mediated by the low iron sensing transcription factor, Aft1. Analysis of subcellular iron and mRNA expression of Aft1-regulated genes reveal that *HGT1* overexpression partially alleviates the iron starvation-like response of *gsh1Δ* cells. Taken together, these results suggest that *HGT1* overexpression may facilitate import of other small thiol-containing compounds that can sustain cell growth without GSH supplementation in GSH-depleted yeast. These data also suggest that both thiol-redox regulation and iron metabolism may be important for the rescue of *gsh1Δ* cells by Hgt1. However, the specific mechanisms whereby *HGT1* overexpression compensates for the lack of GSH are still unclear.

## **Introduction**

Glutathione (L- $\gamma$ -glutamyl-L-cysteinylglycine, GSH) is an essential low molecular weight thiol in eukaryotic cells. Its ability to serve as a reducing equivalent in several biological reactions offers protection against reactive oxygen species (ROS), xenobiotics, and heavy metals. Additionally, GSH serves as an iron ligand for some Fe-S binding proteins involved in iron regulation and the synthesis and maturation of Fe-S cluster proteins. The importance of GSH is highlighted by the fact that depletion of GSH pools is detrimental to the health and viability of eukaryotes. In yeast, low GSH levels result in oxidant sensitivity, mitochondrial dysfunction, disruption of iron regulation, and limited cell growth (1). Similarly, elevated GSH triggers the unfolded protein response (UPR) in

the ER and disrupts iron homeostasis, leading to cell death (2). Hence, the homeostatic maintenance of GSH is critical.

Two ways in which GSH pools are sustained is through intracellular synthesis and import from the extracellular environment. The biosynthesis of GSH occurs via a two-step ATP-dependent enzymatic process. In the first reaction,  $\gamma$ -glutamylcysteine is formed by  $\gamma$ -glutamylcysteine synthetase (Gsh1). In the second step, glycine is added to the peptide via GSH synthetase (Gsh2). Previous studies by Grant et al. found that  $\gamma$ -glutamylcysteine can partially compensate for GSH as an antioxidant. However, poor growth of yeast lacking Gsh2 (*gsh2* $\Delta$ ) in minimal media is evidence that  $\gamma$ -glutamylcysteine cannot fully substitute for the essential function of GSH (3).

Biochemical evidence for GSH transport from the extracellular environment has been demonstrated in a variety of organisms ranging from bacteria to yeast and mammalian cells. However, the only high affinity GSH transporter identified is the plasma membrane-localized Hgt1/Opt1 of *S. cerevisiae* (4). Recent reports show that overexpression of *HGT1* in media supplemented with 100  $\mu$ M GSH leads to overaccumulation of both reduced (GSH) and oxidized glutathione (GSSG) (2). Studies using either *gsh1* $\Delta$  or *HGT1* overexpression strains have characterized the effects of low and high levels of intracellular GSH separately. However, no studies have been reported how fluctuation from GSH depletion to GSH overaccumulation affects subcellular redox homeostasis as well as cellular health and viability.

To understand how yeast respond to GSH deplete and replete conditions, we overexpressed the Hgt1 transporter in a *gsh1* $\Delta$  strain. Surprisingly, we find that GSH-depleted cells overexpressing *HGT1* are viable when grown in synthetic complete media

without GSH supplementation. Since the dithiol reducing agent 1,4-dithiothreitol (DTT) was found to partially rescue *gsh1Δ* cells, we set out to determine if the thiol or thioether containing amino acids cysteine and methionine in synthetic complete media were responsible for this rescue (5). Our results show that cysteine was indeed able to sustain growth of *gsh1Δ* + *HGT1* strains, both aerobically and anaerobically. This led us to investigate further the findings by Bourbonloux et al. in which cysteine was shown to marginally inhibit the uptake of GSH from the extracellular environment by Hgt1, suggesting that Hgt1 can import cysteine with low specificity (4). We hypothesized that *HGT1* overexpressing *gsh1Δ* cells selectively uptake cysteine from the extracellular environment to sustain growth. To determine if increased cysteine uptake restores growth, we overexpressed the high affinity cysteine transporter, Yct1, in a *gsh1Δ* strain. Previous studies demonstrated that cells overexpressing *YCT1* result in a spike of intracellular cysteine and cystine within an hour after addition to the medium (6, 7). Cysteine treated cells expressing *YCT1* also display a delayed increase of key metabolites in the sulfur amino acid pathway, with GSH increasing 3-fold after 5 hours (7). Since only trace amounts of GSH are needed to sustain growth, we set out to determine if enhanced cysteine uptake by Yct1 can rescue *gsh1Δ* cells as seen with Hgt1 (8). Our results suggest that the rescue witnessed in *HGT1* strains depleted of GSH does not involve a significant increase in intracellular cysteine.

GSH has also been identified as a key player in the maturation of extra-mitochondrial Fe-S clusters. Iron-sulfur (Fe-S) clusters are essential for a wide range of biological processes and disruption of Fe-S cluster biogenesis has been linked to pathologies such as anemia, Friedreich's ataxia, and myopathy (9). The biogenesis of Fe-

S clusters begins in the mitochondrial matrix by a set of proteins termed the Fe-S cluster assembly (ISC) machinery. The maturation of cytosolic Fe-S clusters is dependent on the ISC machinery. The ISC machinery is proposed to produce an unknown sulfur-containing substrate that is exported from the mitochondrial matrix with the help of GSH and the GSH-persulfide exporter, Atm1 (10). Depletion of GSH in yeast results in impaired maturation of cytosolic Fe-S proteins, iron accumulation, and the constitutive activation of the iron regulatory transcription factor, Aft1 (2, 5, 11). Similarly, iron regulation is disrupted with increased GSH in *HGT1*-overexpressing cells (2). Studies evaluating extreme changes in GSH concluded that the essential role of GSH is its involvement in Fe-S cluster biogenesis. To investigate if rescue by Hgt1 involves iron regulation, we measured subcellular iron and RNA expression of Aft1-regulated genes. Interestingly, our data suggests that the limited rescue of *gsh1Δ* by *HGT1* overexpression may be partly due to restored regulation of iron metabolism.

## **Experimental Procedures**

*Yeast Strains, Media, and Growth Conditions*-*Saccharomyces cerevisiae* used in this study were derived from the wild type (WT) strain BY4741 (*MATa his3Δ1 leu2Δ0 met15Δ0 ura3Δ0*). The *glr1::kanMX4* deletion strain was purchased from Open Biosystems. Strains were grown in synthetic complete (SC) selection media (0.671% yeast nitrogen base without amino acids and ammonium sulfate, 2% glucose, with appropriate drop-out mix) (US Biological) or in supplemented minimal media, termed 6AA/B media (0.671% yeast nitrogen base without amino acids and ammonium sulfate, 2% glucose, supplemented with six essential amino acids and bases at the following concentrations: 20

mg/L adenine, 60 mg/L leucine, 30 mg/L lysine, 20 mg/L histidine, 20 mg/L tryptophan, and 20 mg/L methionine). Where required, media was solidified using 2% agar. All assays were done using exponentially grown cells.

*Plasmid Construction and Transformation*-The *gsh1Δ* strain was created by chromosomal replacement of *GSH1* with an amino acid marker gene. Briefly, the *GSH1* deletion plasmid (pGSH1KO) was prepared by cloning upstream and downstream regions of the *GSH1* gene using the primers listed in Table 3.1 (see Chapter 3). The upstream PCR product was digested with BamHI and EcoRI and the downstream with Sall and EcoRI. Both digested PCR products were ligated in a trimolecular reaction into the BamHI and Sall sites of the yeast integrating plasmid pRS403 (*HIS3* selection). After linearization with EcoRI, the integrating deletion plasmid was inserted into the genome of WT BY4741 yeast via homologous recombination. The pTEF-416-*HGT1* plasmid described earlier (*CEN URA3, TEF1* promoter driving *HGT1* expression) was used for *HGT1* overexpression (4). Yeast transformations were performed by standard lithium acetate protocols (12). GSH deplete (*gsh1Δ*) strains were selected on 25 μM GSH SC (-HIS) plates after transformation with pGSH1KO and 0.1 μM GSH SC (-HIS, -URA) when the pTEF-416 and pTEF-416-*HGT1* plasmids were transformed.

*Subcellular fractionation*-Yeast cells were grown aerobically to mid-log phase in SC selection medium with 2% glucose. Mitochondrial and post-mitochondrial supernatant (PMS) fractions were obtained as previously described by converting cells to spheroplasts followed by gentle lysis using a loose-fitting Dounce homogenizer and differential centrifugation. Incubation with DTT was omitted from fractionation steps to avoid

reduction of endogenous disulfides and protease inhibitors were not included in buffers (13).

*GSH/GSSG Assay*-Total GSH (reduced GSH and oxidized GSSG) was measured in whole cell, PMS, and mitochondrial extracts using the 5,5-dithiobis(2-nitrobenzoic acid)-GSSG reductase cycling assay as previously described (14). For whole cells measurements,  $2 \times 10^7$  cells (or  $2 \times 10^9$  cells for GSH deplete strains) were harvested via centrifugation at 12000 rpm for 10 seconds. Cell pellets were washed twice with water. Lysis was performed by vigorous vortexing using 1% 5-sulfosalicylic acid (wt/vol) and glass beads. The resulting supernatant containing GSH was incubated on ice for 30 minutes and cleared via centrifugation. PMS and mitochondrial fractions were prepared as described above. Protein content was measured using the Bradford method with bovine serum albumin as a calibration standard. Subcellular fractions were incubated with 1% 5-sulfosalicylic acid on ice for 30 minutes, fractions were spun at 13000 g at 4 °C, and the supernatant containing total GSH was transferred to sterile microcentrifuge tubes.

*Western blots*- Immunoblotting was used to check gene expression within yeast extracts. Recombinant yeast Gsh1 was expressed in *E. coli* and the purified enzyme was used to create the monoclonal Gsh1 (1:1000, rabbit IgG, IRDye, LI-COR, Lincoln, NE) antibody used in this study (15). The Pkg1 (1:10,000, mouse IgG monoclonal, Invitrogen) antibody was used as a loading control.

*Growth Curves in Liquid Media and Solid Media Spot Tests*-To determine the growth pattern of yeast strains in liquid media, cells were plated on SC(-URA) 2% glucose plates containing 0.05  $\mu$ M GSH for 2-3 days. Each strain was later inoculated into fresh SC or 6AA/B selection media at an OD<sub>600</sub> of 0.05. Growth phenotypes of yeast strains were

determined in sterile 96-well plates using a Synergy H1 plate-reader and Gen5 Software 2.09. For growth on plates, strains were harvested from SC(-URA) 2% glucose plates containing 0.05  $\mu\text{M}$  GSH and resuspended in sterile water to  $\text{OD}_{600}$  of 1. The cells were serially diluted to 1:10, 1:100, and 1:1000. The resuspended cells were spotted on SC or 6AA/B selection plates and incubated at 30 °C aerobically or anaerobically for 2 days.

*Intracellular Iron Analysis-* Intracellular iron of cytosolic and mitochondrial extracts was measured using a PerkinElmer PinAAcle 900T graphite furnace atomic absorption spectrometer according to the manufacturer's instructions. Yeast cells were grown on SC(-URA) 2% glucose plates containing 1  $\mu\text{M}$  GSH for 2-3 days. Cells were inoculated into fresh SC(-URA) 2% glucose media with or without GSH and grown overnight until reaching mid-log phase. Cytosolic and mitochondrial fractions were prepared as described above. Extracts were diluted in Milli-Q water and measurements performed. Protein content was measured by standard Bradford analysis and iron content was standardized per mg protein (15).

## **Results**

*Confirmation of  $gsh1\Delta$  + vector and  $gsh1\Delta$  +  $HGT1$  phenotypes-* To study the effects of GSH fluctuations, we created a  $gsh1\Delta$  strain that constitutively uptakes GSH from the extracellular environment via  $HGT1$  overexpression. Due to the essential nature of GSH,  $gsh1\Delta$  strains were pre-grown on SC plates supplemented with 0.1  $\mu\text{M}$  GSH and cultured in SC liquid medium with 0.1  $\mu\text{M}$  GSH until reaching mid-log phase. Western blot analysis confirmed that  $GSH1$  was knocked out of both  $gsh1\Delta$  + vector and  $gsh1\Delta$  +  $HGT1$  strains (Fig. 4.1A). Because  $HGT1$  expressing strains have been shown to

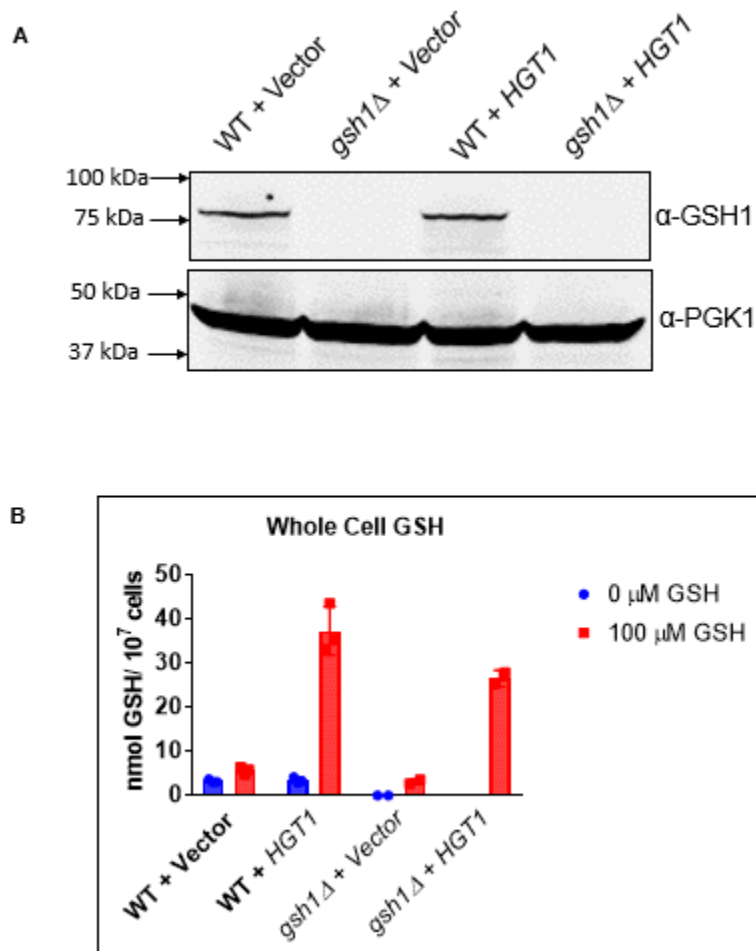


**Figure 4.1. Confirmation of *gsh1* $\Delta$  + vector and *gsh1* $\Delta$  + *HGT1* phenotypes.** (A) Western blot analysis of whole cell extracts (75  $\mu\text{g}$  protein loaded) shows that Gsh1 is not expressed in *gsh1* $\Delta$  strains. (B) Whole cell GSH depletion is confirmed via the DTNB spectrophotometric assay in *gsh1* $\Delta$  + vector and *gsh1* $\Delta$  + *HGT1* strains pre-grown on SC + 0.1  $\mu\text{M}$  GSH plates and cultured in SC + 0.1  $\mu\text{M}$  GSH medium overnight. Data shown are the means and standard deviation (SD) of 2-3 biological replicates. ND, not detected due to values lower than the assay detection limit.

overaccumulate GSH when exposed to GSH, we measured the steady state levels of total GSH in *gsh1Δ* + vector and *gsh1Δ* + *HGT1* with or without GSH treatment (Fig. 4.1B) (2).

As expected, GSH was depleted in both *gsh1Δ* + vector and *gsh1Δ* + *HGT1* untreated strains. Incubation with 100  $\mu$ M GSH for 30 minutes resulted in GSH overaccumulation in *gsh1Δ* + *HGT1* in a similar manner as WT + *HGT1*. However, total intracellular GSH was lower in treated *gsh1Δ* + *HGT1* compared to WT. Taken together, we successfully created a yeast genetic model to monitor extreme GSH fluctuations.

*HGT1 overexpression rescues the growth defect of gsh1Δ cells and causes increased sensitivity to GSH and GSSG-* After confirming the phenotypes of *gsh1Δ* + vector and *gsh1Δ* + *HGT1*, we assessed the requirement of GSH for growth. All strains were pre-grown in SC medium containing 0.05  $\mu$ M GSH. Serial dilution and spotting onto SC plates showed that *gsh1Δ* + *HGT1* grows without added GSH (Fig. 4.2A). These results suggest that overexpression of *HGT1* rescues the growth defect of *gsh1Δ* strains. The rescue was also apparent when cells were grown in liquid media (Fig. 4.2B). Kumar et al. report that GSH concentrations higher than 20  $\mu$ M impedes growth of *HGT1* expressing cells (2). We confirmed this phenotype in WT + *HGT1*. Interestingly, we see that concentrations as low as 5  $\mu$ M are toxic for *gsh1Δ* + *HGT1*. We also tested the sensitivity of WT + *HGT1* and *gsh1Δ* + *HGT1* to GSSG. GSSG is equal to two molecules of GSH (16). Our data suggests that *HGT1* strains are slightly less sensitive to GSSG in liquid media (compare 2.5  $\mu$ M GSSG in Fig 4.3B with 5  $\mu$ M GSH in Fig. 4.2B). This may be due to Hgt1 having a higher affinity for GSH compared to GSSG leading to lower GSSG uptake at comparable media concentrations (Fig. 4.3A-B) (17).

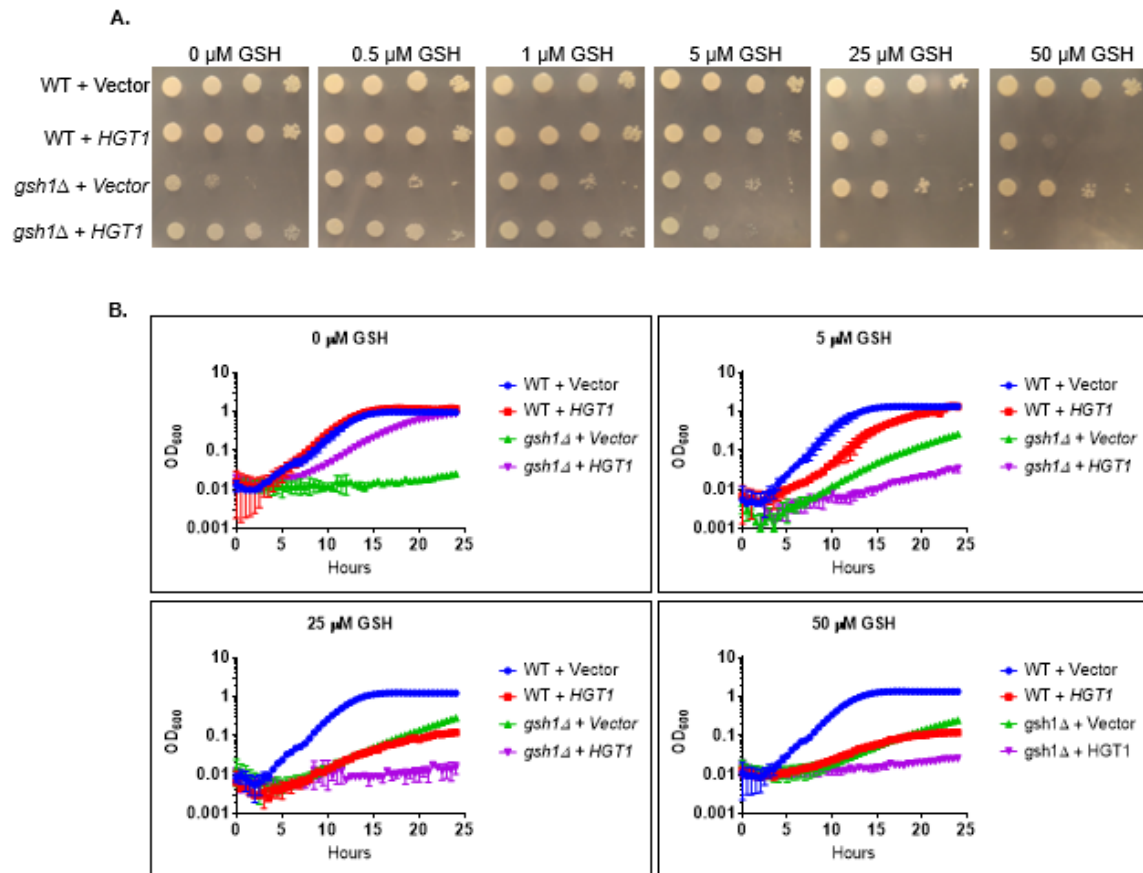


**Figure 4.2. *HGT1* overexpression rescues the growth defect of *gsh1* $\Delta$  cells and causes increased sensitivity to GSH.** (A) WT and *gsh1* $\Delta$  strains were pre-grown on SC + 0.05  $\mu$ M GSH selection plates. Yeast strains were serially diluted and spotted on SC glucose media with increasing GSH concentrations and grown anaerobically for 2 days at 30  $^{\circ}$ C (B) Growth and sensitivity to GSH was analyzed by using a Synergy H1 plate-reader. The growth curves are reported as means of 2 independent experiments with error bars representing the SD.

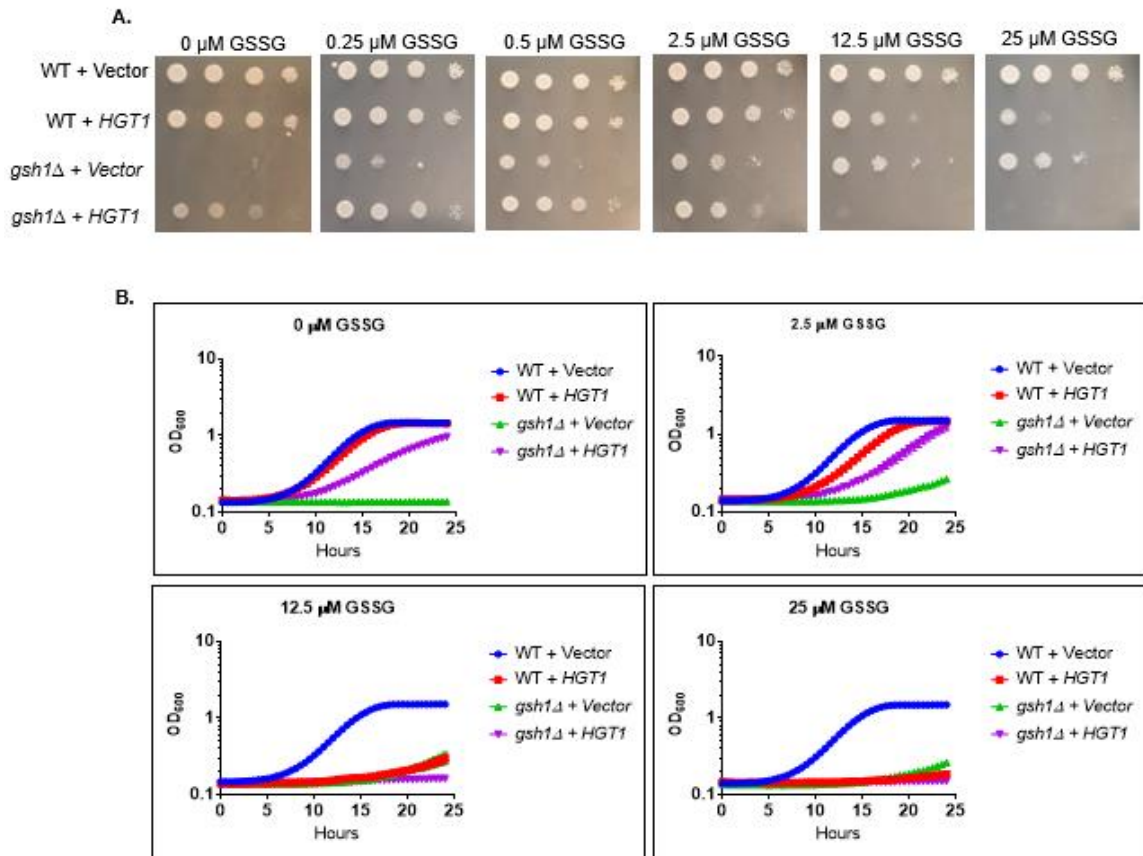


**Figure 4.3. WT and *gsh1* $\Delta$  strains overexpressing *HGT1* are sensitive to extracellular GSSG.** (A) WT and *gsh1* $\Delta$  strains were pre-grown on SC + 0.05  $\mu$ M GSH selection plates. Yeast strains were serially diluted and spotted on SC glucose media with increasing GSSG concentrations and grown anaerobically for 2 days at 30 °C (B) Growth and sensitivity to GSSG was analyzed by using a Synergy H1 plate-reader. Growth curves are reported as the means of 2 independent experiments with error bars representing SD.

*Overnight incubation of gsh1Δ strains with increasing GSH concentrations led to less GSH accumulation in gsh1Δ + HGT1-* Due to the unexpected growth patterns of *gsh1Δ + HGT1*, intracellular GSH was assessed in cells grown with various GSH concentrations. In this study, the minimum amount of GSH necessary for growth of both *gsh1Δ + vector* and *gsh1Δ + HGT1* cells cultured from SC + 0.05 μM GSH plates was 0.1 μM GSH. When grown with increasing, relatively low GSH concentrations, *HGT1* overexpression had no effect on intracellular GSH in WT strains (Fig. 4.4A). While GSH levels were difficult to detect in *gsh1Δ* cells cultured in concentrations less than 1 μM, detectible GSH measurements show that *gsh1Δ + HGT1* accumulate less GSH in overnight growth than the vector control (Fig. 4.4B). As shown by Kumar et al., *HGT1* cells treated with GSH increase shortly after adding GSH to the growth media and decrease over time. The authors contributed the decrease to the degradation of GSH by the γ -glutamyl transpeptidase (γ-GT)-independent Dug1–Dug2–Dug3 pathway (2). Therefore, our data for WT + *HGT1* coincide with the published literature. It is possible that the low level of GSH rapidly imported by *HGT1* overexpression is degraded quickly by the Dug pathway, while slower controlled import with native *HGT1* expression avoids this degradation.

*Kinetic measurements of GSH content in gsh1Δ + vector and gsh1Δ + HGT1-* To determine if GSH catabolism is responsible for low intracellular GSH measurements in *gsh1Δ + HGT1*, we monitored GSH levels over time for cells treated with 100 μM GSH (Fig. 4.5). As seen in previous reports using WT yeast, GSH levels in *gsh1Δ* strains overexpressing *HGT1* accumulate high levels of GSH within one hour of treatment and drop after two hours (2). GSH levels in *gsh1Δ + vector* increase slightly and stay constant over time. *HGT1* overexpressing cells return to basal levels at four hours. At six and eight

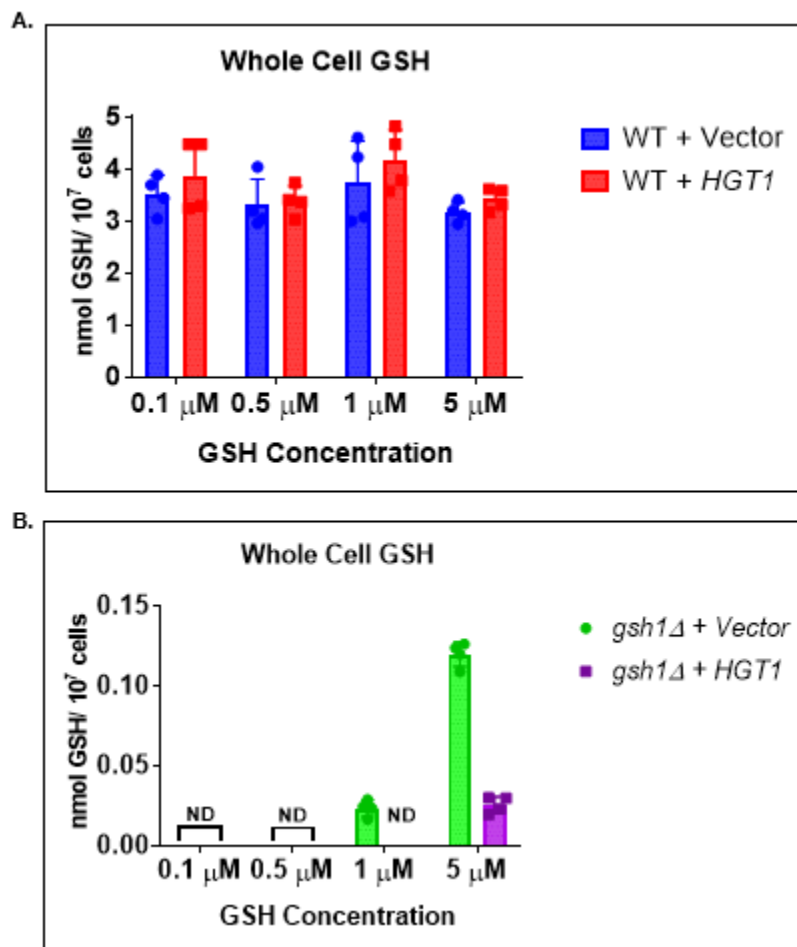


**Figure 4.4. Overnight incubation of *gsh1* $\Delta$  strains with increasing GSH concentrations led to less GSH accumulation in *gsh1* $\Delta$  + *HGT1*.** Yeast strains were pre-grown on SC + 0.05  $\mu$ M GSH selection plates and inoculated in SC media with various concentrations of GSH. Cells were acidified with 1% SSA and whole cell GSH in (A) WT and (B) *gsh1* $\Delta$  strains containing vector and *HGT1* plasmids was measured using the DTNB cycling assay. Data shown are means for four independent experiments with error bars representing SD. ND, not detected due to values lower than the assay detection limit.

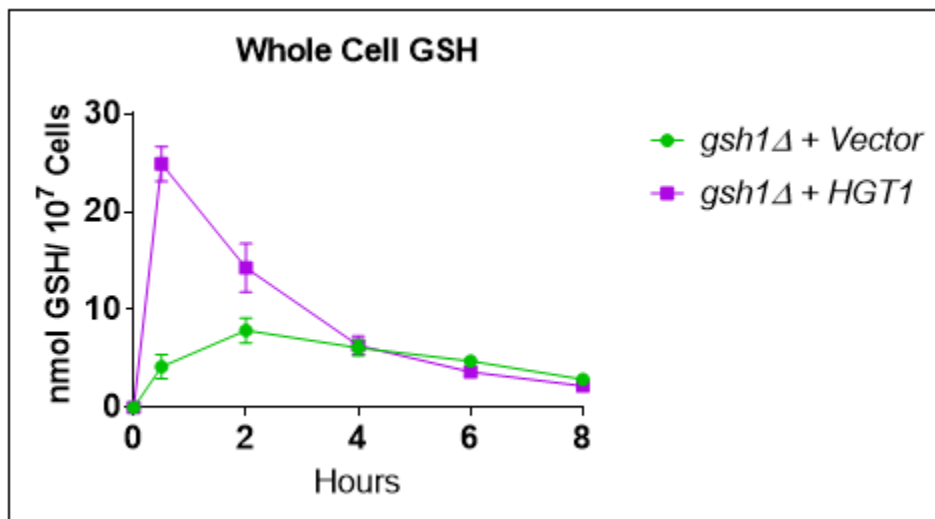


**Figure 4.5. Kinetic measurements of GSH content in *gsh1Δ* + vector and *gsh1Δ* + *HGT1*.** Kinetics of cellular GSH accumulation was monitored in cells grown using SC + 0.05  $\mu$ M GSH selection plates and liquid cultures overnight in SC media with 0.1  $\mu$ M GSH. 100  $\mu$ M GSH was added to exponentially growing cells at time 0 and cell aliquots were collected over eight hours. Values are the means of 3 independent experiments with error bars representing SD.

hours GSH levels in *gsh1Δ* + *HGT1* were similar, if not slightly lower than the vector control. This observation could explain the reduced GSH levels after overnight growth for *gsh1Δ* + *HGT1* vs. *gsh1Δ* + vector strains. However, additional experiments over a longer time course and possibly lower GSH concentrations are required to determine if these differences between strains after overnight growth are significant.

*HGT1 overexpression partially rescues the growth defect of gsh1Δ strains-* Due to its cellular abundance ranging from 3 mM to 10 mM and its ability to serve as a cofactor in many redox reactions, GSH is thought to be an important redox buffer in the cell. Therefore, we wanted to investigate the rescue of *gsh1Δ* by *HGT1* overexpression in different redox and nutrient environments. We observed that the *gsh1Δ* + *HGT1* strain can grow almost as well as WT in aerobic and anaerobic conditions (Fig. 4.6A). Therefore, the potential for oxidant production under aerobic conditions has little effect on the ability of *HGT1* to restore growth in *gsh1Δ*. Next, we wanted to see if the availability of amino acid played a role in viability of *gsh1Δ* + *HGT1*. We therefore monitored growth of strains on 6AA/B medium, defined as minimal medium with only six amino acids and nucleobases that are essential for yeast growth added at relatively low concentrations. In comparison, SC medium only lacks a single or a few amino acids that allows maintenance of transformed plasmids (see methods section) (18). Consistent with previous reports neither *gsh1Δ* + vector nor *gsh1Δ* + *HGT1* are able to grow. Therefore, it seems that *HGT1* only partially rescues *gsh1Δ* and this rescue is related to nutrient availability (Fig. 4.6B-C).

*Cysteine is a key amino acid for rescue of gsh1Δ when HGT1 is overexpressed-* Of the twenty common amino acids, cysteine is one of the least abundant. Yet, the free sulfhydryl group serves as a redox center for many enzymes, regulatory proteins, and

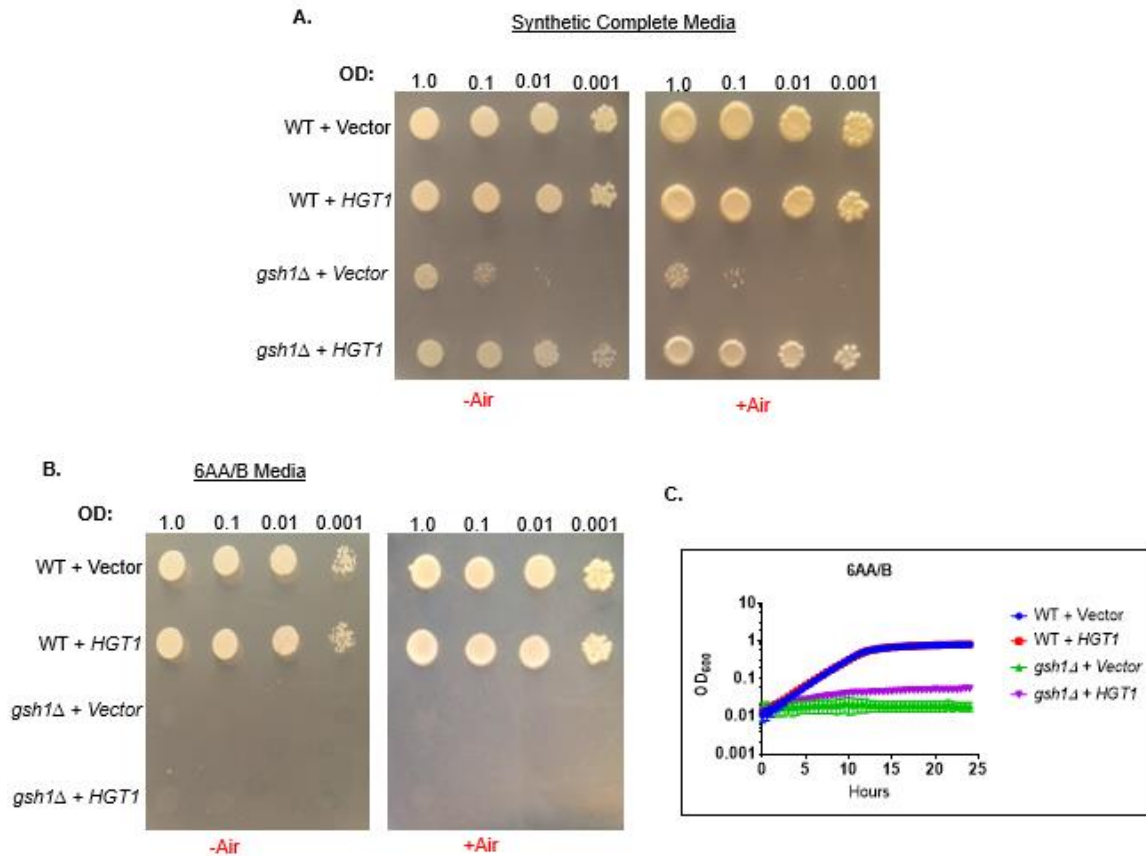


**Figure 4.6 *HGT1* overexpression partially rescues the growth defect of *gsh1* $\Delta$  strains.** (A) *HGT1* overexpression in GSH depleted (*gsh1* $\Delta$ ) cells are fully viable without GSH supplementation on SC plates under both aerobic and anaerobic conditions. GSH depleted strains expressing either an empty vector or an *HGT1* overexpression plasmid are unable to grow on 6AA/B plates after 48 hours (B), nor in liquid media after 24 hours of growth (C). Data shown in (C) are the means of 2 independent experiments with error bars representing SD.

cofactors, including GSH (19). Since SC medium contains cysteine, we set out to determine if cysteine is responsible for the rescue of *gsh1Δ* by *HGT1*. Indeed, cysteine resulted in improved growth of *gsh1Δ + HGT1* strains on 6AA/B media under anaerobic conditions. However, this rescue did not occur under aerobic conditions, suggesting that cysteine alone cannot replace the function of GSH in minimal media under mild oxidative stress conditions (Fig. 4.7A). Of the additional amino acids found in SC media tested, no other individual amino acid alone could partially restore growth, including the thioether-containing amino acid methionine (Fig. 4.7B). However, *gsh1Δ + HGT1* cells grew better on SC medium compared to 6AA/B + Cys medium, particularly in aerobic conditions, suggesting that the other amino acids, nucleobases, and other nutrients in SC medium collectively improve the viability of *gsh1Δ + HGT1* cells independently of cysteine. To test this, we used SC media lacking uracil, the amino acid selection marker, and cysteine (Fig. 4.8). The *gsh1Δ + HGT1* was able to grow in SC media lacking cysteine, although at a slower rate compared to SC media with cysteine added back. These results further confirm that nutrient availability is important for growth of *gsh1Δ* cells expressing *HGT1*, with cysteine playing a key role. To further test a redox-dependent mechanism of rescue, we investigated the effects of the sulfhydryl-containing reducing agent dithiothreitol (Fig. 4.9). Dithiothreitol was able to partially restore growth under aerobic conditions but was toxic to all strains under anaerobic conditions at the same concentration (data not shown). Thus, our results suggest that the requirement for GSH is partially redox-dependent and *HGT1* overexpression helps meet the redox needs of the cell.

*gsh1Δ + HGT1 strains are viable after 48 hours without GSH supplementation.* To test the efficiency of rescue during prolonged growth, viability was

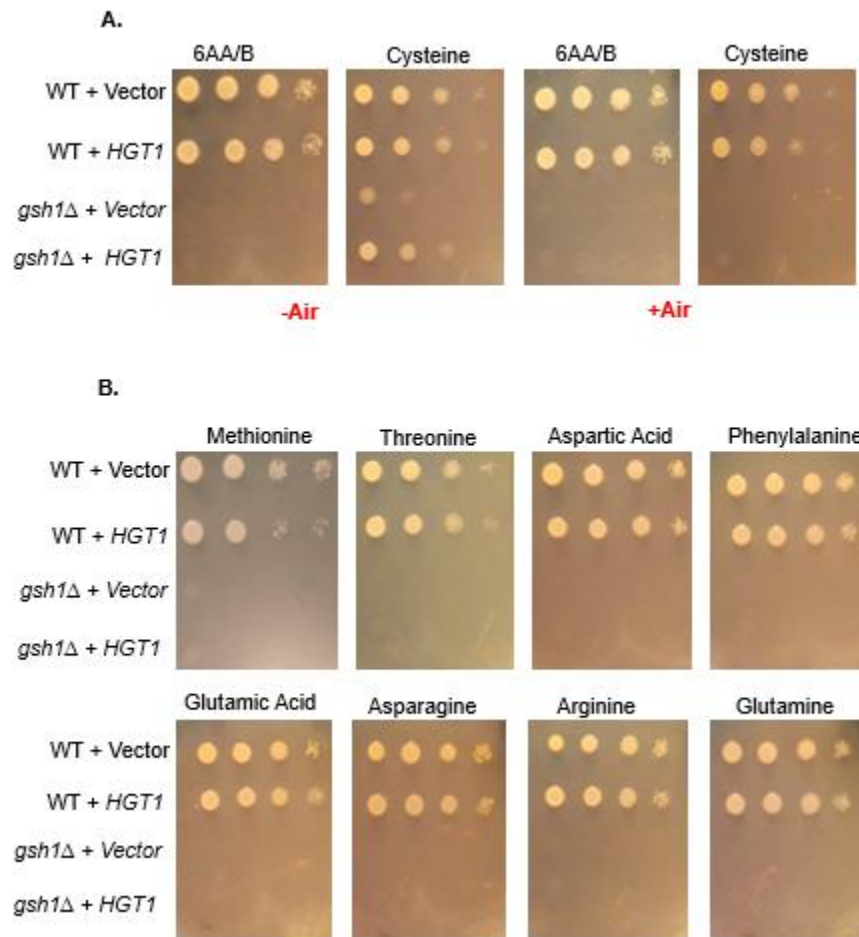


**Figure 4.7 Cysteine is a key amino acid for rescue of *gsh1*Δ when *HGT1* is overexpressed.** Yeast cells pre-grown on SC plates with 0.05 μM GSH for 2 days were spotted on (A) 6AA/B plates with or without 85.6 mg/L cysteine under aerobic and anaerobic conditions (B) or 85.6 mg/L additional non-essential amino acids.

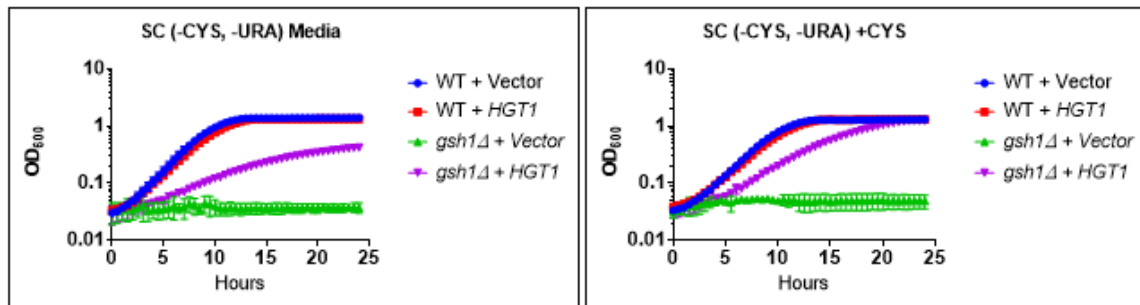


**Figure 4.8 Cysteine improves growth of *gsh1Δ* + *HGT1* cells in SC media.** Growth curve analysis in SC media shows that cysteine is a key amino acid for rescue in SC media. Growth curves are reported as the means of 2 independent experiments with error bars representing SD

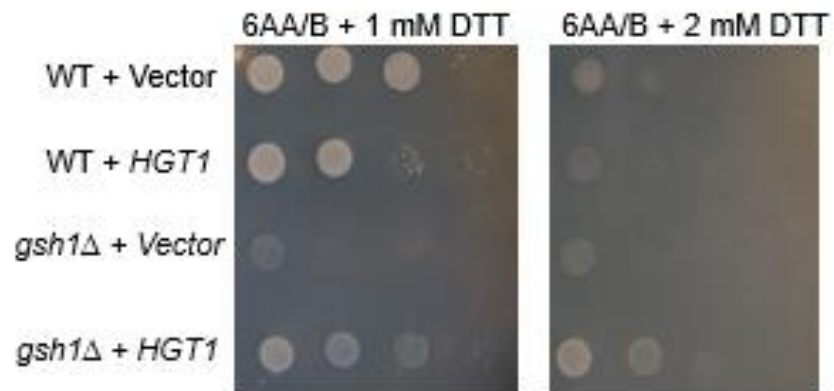


**Figure 4.9. DTT partially restores growth of *gsh1*Δ + *HGT1* strains on minimal 6AA/B media.** (A) Yeast cells pre-grown on SC plates with 0.05 μM GSH for 2 days were spotted on 6AA/B plates with increasing concentrations of DTT under aerobic conditions.

monitored for 48 hours at different starting ODs. Ayer et al. reported that *gsh1Δ* cells switched to GSH-deficient media undergo 8-10 cell divisions before GSH pools are too diluted to support further growth (1). Therefore, we tested if *gsh1Δ + HGT1* cells would continuously grow for longer than 24 hours with >10 divisions without GSH addition. Cells harvested from SC plates supplemented with 0.05 μM GSH were grown for 48 hours in SC media without GSH. Here, we show that *gsh1Δ + HGT1* cells grow similar to WT and growth exceeds 10 divisions regardless of the starting OD (Fig. 4.10A). After growth in SC media for 48 hours, *gsh1Δ + HGT1* cells and the WT control were plated on 6AA/B minimal media with or without cysteine. We confirm that cysteine can still rescue cells completely devoid of GSH (Fig. 4.10B).

*Cysteine uptake is not responsible for growth of gsh1Δ + HGT1 strains in SC media-* Our findings that cysteine is able to render *gsh1Δ + HGT1* viable in minimal media was not surprising as previous studies have shown that *gsh1Δ* growth can be partially restored by reducing agents (20). Furthermore, cysteine marginally inhibits Hgt1 uptake of GSH, suggesting that it may serve as a weak-binding Hgt1 substrate (4). Thus, we hypothesized that *HGT1* overexpression leads to increased cysteine import in the absence of extracellular GSH. To test this hypothesis, we measured intracellular cysteine levels of strains grown overnight in SC media. However, we find that cysteine levels in *gsh1Δ + HGT1* were similar or only slightly higher than *gsh1Δ + vector* and WT controls (Fig. 4.11A). To further our studies, we determined if cysteine availability played a role in *gsh1Δ* rescue by overexpressing the Yct1 transporter in WT and *gsh1Δ* strains. We show that *YCT1* overexpression is not able to rescue *gsh1Δ* in SC media as seen with *HGT1*

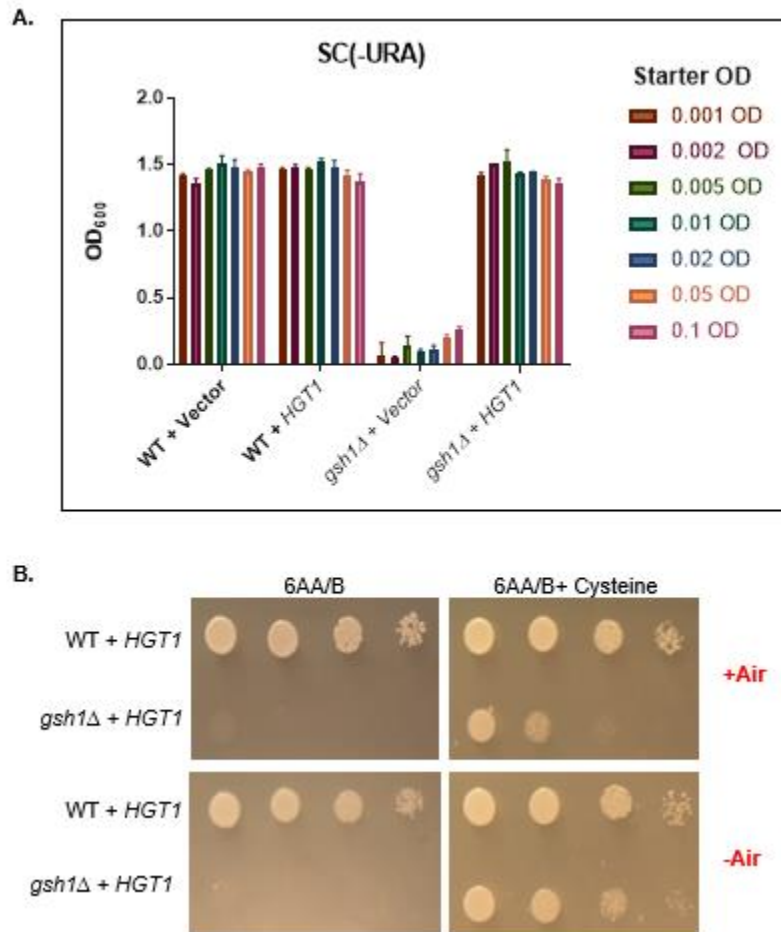
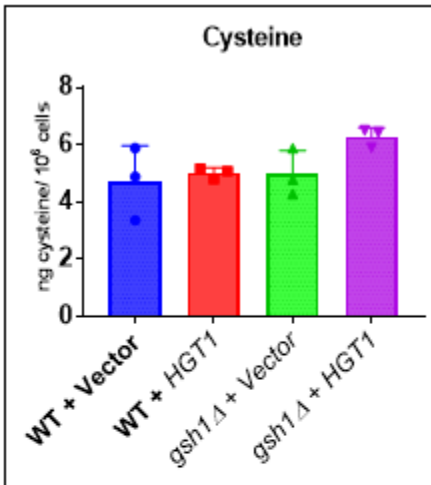


**Figure 4.10 *gsh1Δ* + *HGT1* strains are viable after 48 hours without GSH supplementation.** (A) Yeast cells were pre-grown on SC plates with 0.05  $\mu$ M GSH for 2 days, diluted to various starting ODs in sterile water, and grown in SC selection media for 48 hours. Growth is represented as the mean and standard deviation of 2 biological replicates. (B) After growing WT and *gsh1Δ* strains for 48 hours in SC selection media with repeated dilutions to maintain exponential growth, cells were spotted on 6AA/B plates with or without 85.6 mg/L cysteine and incubated for 2 days under aerobic and anaerobic conditions.

A.



B.

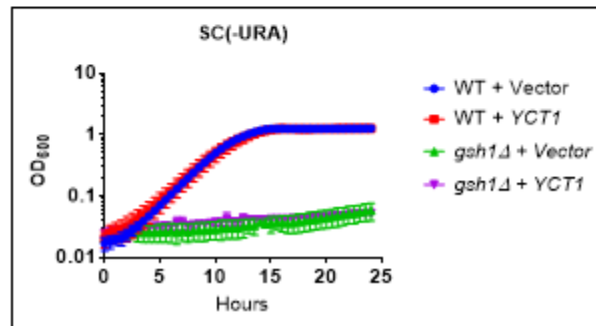


**Figure 4.11. Cysteine uptake is not responsible for growth of *gsh1*Δ + *HGT1* strains in SC media.** (A) Yeast strains were pre-grown on synthetic complete plates with 1 μM GSH for 2 days. Cells were cultured overnight in SC selection media. Intracellular cysteine was measured by liquid chromatography-tandem mass spectrometry (measurements were done by Michel Toledano's group). (B) *YCT1* strains and controls were pre-grown on SC + 0.05 μM GSH selection plates and growth was assessed in liquid SC media with no GSH. Data shown represent the means of 2-3 independent experiments with error bars representing SD.

(Fig. 4.11B). Taken together, these results suggest that increased cysteine availability is not the cause of *gsh1Δ + HGT1* rescue in media without GSH.

*Subcellular GSH measurements of gsh1Δ + vector and gsh1Δ + HGT1 strains grown in various GSH concentrations-* During oxidative phosphorylation, ROS are generated as by-products due to the incomplete reduction of molecular oxygen to water. This process occurs in the mitochondria, making this organelle subject to oxidative stress. Mitochondrial GSH is thought to play a protective role against the deleterious effects of oxidants. Evidence for the vital role of GSH to mitochondrial function in yeast is shown in research conducted by Ayer et al. The authors report that after one to two divisions *gsh1Δ* cells become irreversibly respiratory incompetent and after 5 divisions approximately 75% of mitochondrial DNA is lost. Despite these effects, GSH depleted cells still can undergo approximately 8-10 divisions. This growth is associated with the consumption of pre-accumulated reserves of GSH (1). Given the importance of mitochondrial GSH and our data showing that *gsh1Δ + HGT1* have less intracellular GSH than *gsh1Δ + vector* after overnight growth, we hypothesized that pre-accumulated reserves of GSH are stored in the mitochondria aiding in cell growth. To test this hypothesis, we grew *gsh1Δ + vector* and *gsh1Δ + HGT1* overnight in various concentrations of GSH. Cytosolic and mitochondrial fractions were tested for subcellular GSH. We find that steady-state levels of cytosolic GSH are similar in *gsh1Δ + vector* and *gsh1Δ + HGT1* strains in low and high concentrations of external GSH (Fig. 4.12A). Similarly, mitochondrial GSH is not significantly different for cells cultured with increasing GSH concentrations (Fig. 4.12B). These data suggest that *gsh1Δ + HGT1* viability is not due to the re-distribution of GSH to the mitochondria.

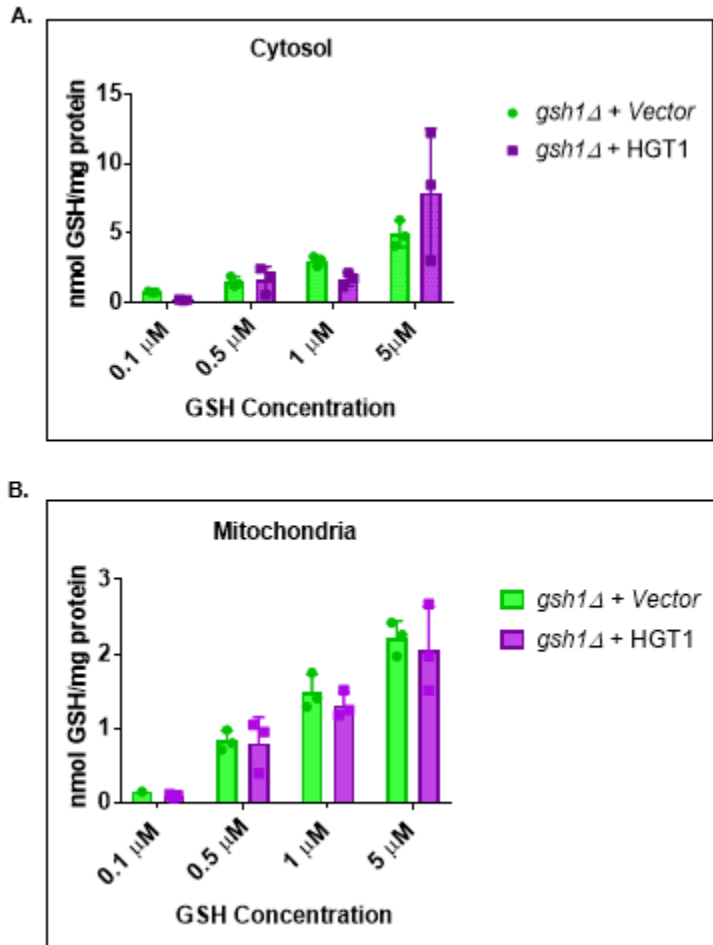


**Figure 4.12. Subcellular GSH measurements of *gsh1Δ* + vector and *gsh1Δ* + *HGT1* strains grown in various GSH concentrations.** Yeast strains were pre-grown on SC + 0.05  $\mu$ M GSH selection plates and inoculated in SC media with various concentrations of GSH. Cells were acidified with 1% SSA. (A) Cytosolic and (B) mitochondrial GSH levels of *gsh1Δ* strains were measured using the DTNB cycling assay. Data shown are the means of 3 independent experiments with error bars representing SD.

*gsh1Δ + HGT1 cells can grow on fermentable, partially fermentable, and non-fermentable carbon sources*— Previous studies assessing mitochondrial respiration and cell growth found that *gsh1Δ* undergo fewer divisions when grown using glycerol and ethanol as a carbon source (1). These data suggest that there is a greater need for GSH when *gsh1Δ* cells are grown under non-fermentative conditions. Therefore, we tested if carbon source affects the growth of *gsh1Δ + HGT1* in the absence of GSH supplementation. We find that *HGT1* rescues *gsh1Δ* cells irrespective of carbon source. Yet, *gsh1Δ + HGT1* appears to grow somewhat slower in glycerol (Fig. 4.13A). Divisions cannot be measured using spot tests. Therefore, growth was also analyzed in liquid media. Cells were grown in SC liquid media for 48 hours containing 2% glucose and SC containing 3% glycerol + 1% ethanol. In fermentative conditions, *gsh1Δ + HGT1* cells reach a final OD<sub>600</sub> similar to that of WT after 48 hours. Non-fermentative conditions resulted in decreased growth of all cells and *gsh1Δ + HGT1* grew slower than the WT controls (Fig. 4.13B). Nevertheless, *HGT1* expressing cells did not stop dividing after 48 hours. These results imply that external GSH is not absolutely required for continued growth under non-fermentative conditions.

*Deletion of GLR1 does not impact the rescue of gsh1Δ by HGT1 overexpression*— GSSG reductase (Glr1) is a cytosolic and mitochondrial-localized oxidoreductase that converts oxidized GSSG to reduced GSH using NADPH as a reducing equivalent (21). Deletion of *GLR1* results in mild oxidative stress due to elevated GSSG. Gostimskaya et al. found that Glr1 is important for *gsh1Δ* strains to recover from GSH depletion and mitochondrial Glr1 is more critical for growth restoration than the cytosolic isoform (22). Therefore, we set out to determine if deletion of *GLR1* affected the rescue of *gsh1Δ* strains by *HGT1* overexpression. On the contrary, our results show that *HGT1* can restore growth

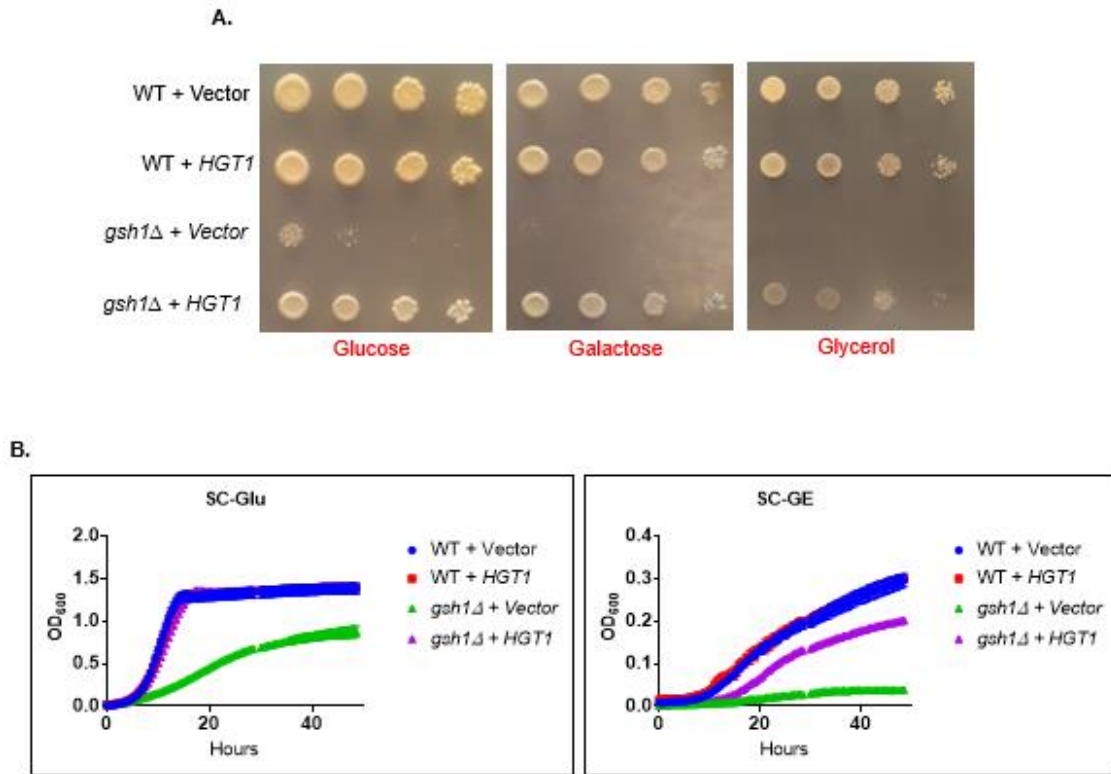


**Figure 4.13. *gsh1*Δ + *HGT1* cells can grow on fermentable, partially fermentable, and non-fermentable carbon sources.** Yeast cells were pre-grown on synthetic complete plates with 0.05 μM GSH for 2 days. (A) Strains were then serially diluted and spotted on SC plates containing 2% glucose, 2% galactose, or 3% glycerol and placed in a 30 °C incubator aerobically for 2 days. (B) Growth was monitored for 48 hours for cells grown in SC media containing 2% glucose (SC-Glu) and SC media containing 3% glycerol + 1% ethanol (SC-GE). Growth curves are the means of 2 independent experiments with error bars representing SD.

of *glr1Δgsh1Δ* as efficiently as *gsh1Δ* (Fig. 4.14). These data suggest that maintaining a high GSH:GSSG ratio is not critical for viability of *gsh1Δ + HGT1*.

*Defects in iron regulation are partially rescued by HGT1 overexpression in a gsh1Δ strain-* Iron regulation in *Saccharomyces cerevisiae* is controlled by the paralogous transcriptional activators, Aft1 and Aft2. Iron deficiency activates Aft1 and Aft2, causing the proteins to move from the cytosol to the nucleus. Inside the nucleus, the transcription factors induce the expression of iron regulon genes involved in the uptake of iron (*FET3*, *FTR1*, *FRE1*, and *FRE2*), and siderophores (*ARN1-4* and *FIT1-3*) (23–25). Defective Fe-S cluster biogenesis leads to the constitutive activation of Aft1(26, 27). GSH depletion in cells causes Aft1 activation, iron accumulation, and upregulation of iron regulatory genes. Overaccumulation of GSH results in a phenotype much like that of *gsh1Δ* (2). Therefore, we wanted to determine the impact that *HGT1* overexpression has on iron metabolism in GSH depleted cells. To test this, cells were grown in SC + 1 μM GSH plates and transferred to SC media for overnight growth without GSH. We find that cytosolic iron is increased about 2X in *gsh1Δ + vector* while *gsh1Δ + HGT1* has similar iron as WT strains (Fig. 4.15A). As seen in previous studies, mitochondrial iron increases significantly with GSH depletion (15). Here, we report a ~16X increase in mitochondrial iron in *gsh1Δ + vector* compared to WT. While the *gsh1Δ + HGT1* strain also accumulates mitochondrial iron, levels are significantly lower than *gsh1Δ + vector* having a ~10X increase compared to WT (Fig. 4.15B). These results imply that *HGT1* overexpression helps *gsh1Δ* cells regulate iron more efficiently. To further test this theory, mRNA levels were measured for *FET3* and *FIT3* genes. As expected, mRNA levels for both genes are increased in *gsh1Δ + vector* cells due to constitutive activation by Aft1. However, these mRNA levels are reduced

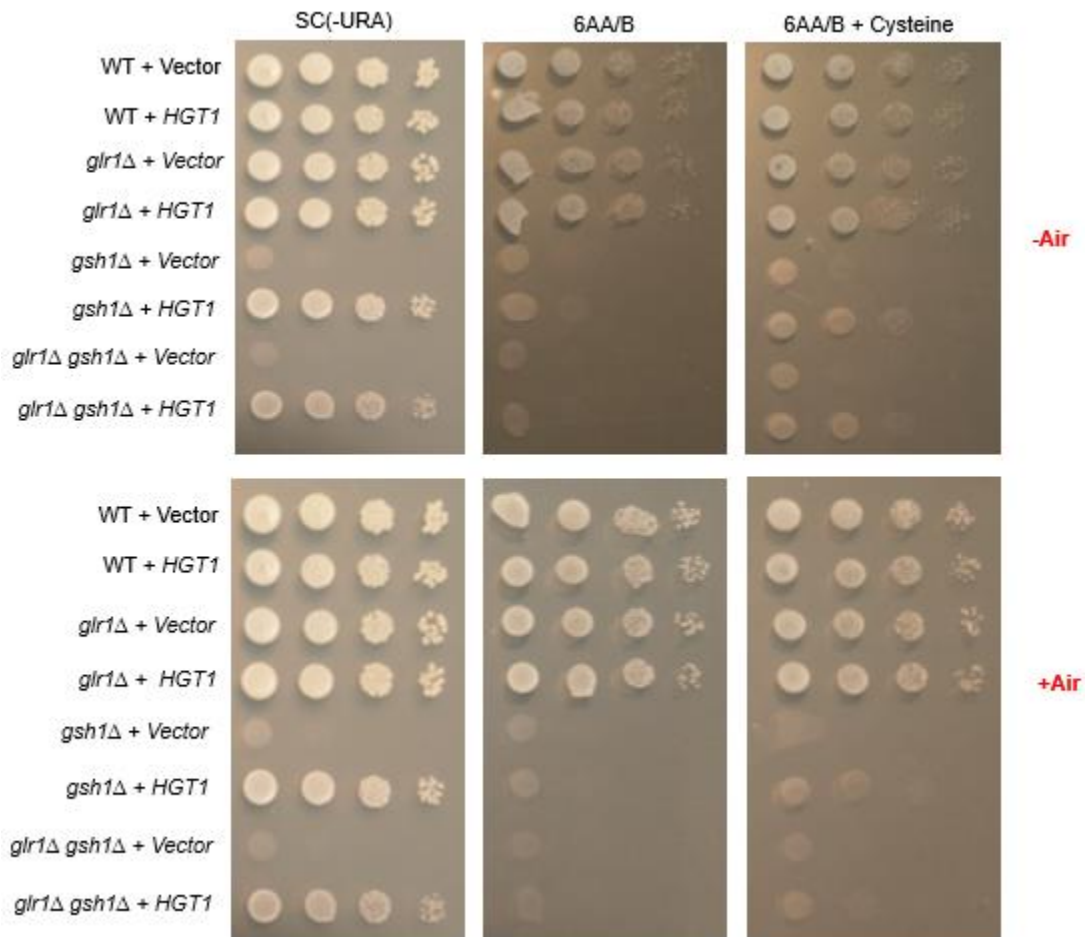


**Figure 4.14 Deletion of *GLR1* does not impact the rescue of *gsh1Δ* by *HGT1* overexpression.** Yeast cells were pre-grown on synthetic complete plates with 0.05  $\mu$ M GSH for 2 days. The indicated strains were then serially diluted and spotted on SC, 6AA/B, and 6AA/B + 85.6 mg/L cysteine plates. Cells were allowed to grow for 2 days.

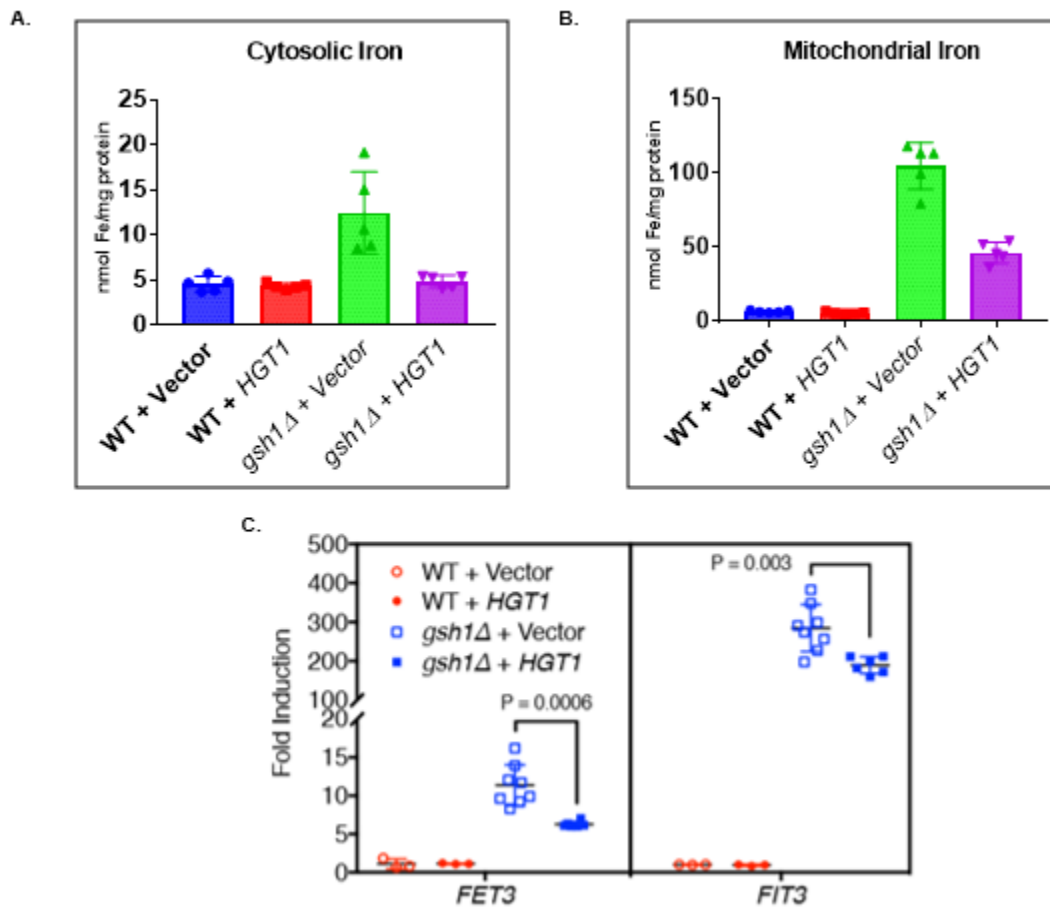


**Figure 4.15. Defects in iron regulation are partially rescued by *HGT1* overexpression in a *gsh1Δ* strain.** Yeast were pre-grown on SC plates with 1  $\mu$ M GSH for 2 days and cultured overnight in SC selection media. (A) Cytosolic and (B) mitochondrial iron was measured by atomic absorption spectroscopy. (C) Quantitative RT-PCR results for *FET3* and *FIT3* mRNA levels were measured in WT and *gsh1Δ* strains. Data shown represents 3-8 independent experiments with error bars representing SD. RT-qPCR measurements were performed by Evan Talib.

in *gsh1Δ* + *HGT1* compared to *gsh1Δ* + vector. Nevertheless, mRNA levels are still relatively high compared to WT (Fig. 4.15C). Thus, iron measurements together with RT-qPCR results confirm that the mechanism of rescue by *HGT1* is partly due to modest recovery of iron regulation.

## **Discussion**

The dependency of eukaryotic cells on intracellular GSH has been very well characterized using *gsh1Δ* strains. These studies have shown that GSH is critical for maintaining mitochondrial integrity and the maturation of extra-mitochondrial Fe-S cluster proteins (4, 11, 26). After the discovery of Hgt1, the consequence of high intracellular GSH was also accessed (2, 4). Nevertheless, these extreme changes in GSH were studied using different strains. Here, we present for the first time a model that explores the ability of cells to fluctuate between low and high GSH by overexpressing *HGT1* in *gsh1Δ*. We report that *HGT1* overexpression can rescue the growth defect of GSH deficiency. This rescue was seen in SC media, which contains all amino acids and nucleobases except ones needed for plasmid selection. We also looked at the ability of *gsh1Δ* + *HGT1* strains to grow on minimal 6AA/B media. Interestingly, *gsh1Δ* + *HGT1* was not viable in 6AA/B media without added GSH. This observation prompted us to investigate which component of SC media amino acids were responsible for the growth of *gsh1Δ* + *HGT1* strains. Since the function of GSH is dependent on the redox-active cysteine, we tested the influence of cysteine on growth (19). We find that cysteine rescues both *gsh1Δ* + vector and *gsh1Δ* + *HGT1*, anaerobically. However, cysteine more effectively restores growth of *gsh1Δ* + *HGT1*. Since cysteine was unable to rescue *gsh1Δ* strains aerobically, we looked at cell

growth using the sulfur-containing amino acid methionine. Neither methionine or other amino acids found in SC media were able to restore growth of *gsh1Δ* + vector or *gsh1Δ* + *HGT1*. Therefore, we conclude that the rescue observed by *HGT1* is dependent on nutrient availability and is only a partial rescue.

To understand the mechanism of rescue, we first considered that growth in SC media could be fulfilling the thiol-redox needs of the cell. Thus, in addition to looking at cysteine we determined how well *gsh1Δ* + vector and *gsh1Δ* + *HGT1* respond to DTT. Contrary to our results with cysteine, DTT was able to rescue cells under aerobic conditions while cysteine restores growth anaerobically in 6AA/B media. These results can be explained by the fact that DTT is a stronger reductant than cysteine due to the second sulfhydryl group. DTT can, therefore, offer greater protection against oxidants. However, when grown anaerobically DTT may create an overly reducing intracellular environment leading to cell death. The restoration of growth using reducing agents in 6AA/B was more profound in *gsh1Δ* + *HGT1* than *gsh1Δ* + vector. Thus, the mechanism for rescue may be partly due to enhanced thiol-redox control.

GSH is thought to be essential due to its involvement in maintaining mitochondrial integrity (11, 22). Therefore, we proposed that pre-accumulated GSH may be redistributed into the mitochondria offering protection against the deleterious effects of GSH limitation. To test this idea, subcellular GSH levels were measured. We did not see a significant difference in cytosolic and mitochondrial GSH. Since GSH depletion leads to respiratory incompetency which has been associated with less cell divisions in *gsh1Δ*, we tested the ability of *gsh1Δ* + vector and *gsh1Δ* + *HGT1* to grow under fermentative and non-fermentative conditions. Using glycerol and ethanol as carbon sources does not stop *gsh1Δ*

+ *HGT1* from dividing in SC media. Thus, we do not believe that the rescue of *gsh1Δ* by *HGT1* is specific to its involvement in mitochondrial function.

The role of GSH in Fe-S cluster assembly has been proposed as its primary function and the reason GSH is essential for viability (2). A characteristic phenotype of GSH depletion is iron accumulation, particularly in the mitochondria. Therefore, we measured subcellular iron in *gsh1Δ* strains grown overnight without GSH. We found that overexpression of *HGT1* in *gsh1Δ* cells results in reduced iron in both the cytosol and mitochondria. However, iron levels in *gsh1Δ + HGT1* are still higher than WT strains. We also measured the mRNA levels of *FET3*, encoding a multicopper oxidase required for ferrous iron uptake and *FIT3*, encoding a mannoprotein responsible for retention of siderophore-iron in the cell wall. The mRNA levels of both genes were lower in *gsh1Δ + HGT1* than the vector control. Yet, *FET3* and *FIT3* mRNA expression was still upregulated in the *gsh1Δ + HGT1* strain. These data imply that *HGT1* overexpression helps *gsh1Δ* cells regulate iron metabolism. Taken together with our studies showing that reductants more efficiently rescued the *gsh1Δ + HGT1* strain in minimal 6AA/B, we conclude that *HGT1* overexpression helps *gsh1Δ* meet the redox and iron homeostatic needs of the cell. Nevertheless, more work is required to define the specific molecular mechanisms at play in the *gsh1Δ + HGT1* strain that compensate for the lack of GSH.

## References

1. Ayer, A., Tan, S.-X., Grant, C. M., Meyer, A. J., Dawes, I. W., and Perrone, G. G. (2010) The critical role of glutathione in maintenance of the mitochondrial genome. *Free Radic. Biol. Med.* 49, 1956-1968
2. Kumar, C., Igarria, A., D'Autreaux, B., Planson, A. G., Junot, C., Godat, E., Bachhawat, A. K., Delaunay-Moisan, A., and Toledano, M. B. (2011) Glutathione revisited: A vital function in iron metabolism and ancillary role in thiol-redox control. *EMBO J.* 30, 2044-2056
3. Grant, C. M., Maciver, F. H., and Dawes, I. W. (1997) Glutathione Synthetase Is Dispensable for Growth under Both Normal and Oxidative Stress Conditions in the Yeast *Saccharomyces cerevisiae* Due to an Accumulation of the Dipeptide  $\gamma$ -Glutamylcysteine. *Mol. Biol. Cell.* 8, 1699-1707
4. Bourbouloux, A., Shahi, P., Chakladar, A., Delrot, S., and Bachhawat, A. K. (2000) Hgt1p, A high affinity glutathione transporter from the yeast *Saccharomyces cerevisiae*. *J. Biol. Chem.* 275, 13259–13265
5. Sipos, K., Lange, H., Fekete, Z., Ullmann, P., Lill, R., and Kispal, G. (2002) Maturation of cytosolic iron-sulfur proteins requires glutathione. *J. Biol. Chem.* 277, 26944-26949
6. Kaur, J., and Bachhawat, A. K. (2007) Yct1p, a novel, high-affinity, cysteine-specific transporter from the yeast *Saccharomyces cerevisiae*. *Genetics.* 176, 877–890
7. Deshpande, A., Bhatia, M., Laxman, S., and Bachhawat, A. (2017) Thiol trapping and metabolic redistribution of sulfur metabolites enable cells to overcome

- cysteine overload. *Microb. Cell.* 4, 112-126
8. Spector, D., Labarre, J., and Toledano, M. B. (2001) A genetic investigation of the essential role of glutathione. Mutations in the proline biosynthesis pathway are the only suppressors of glutathione auxotrophy in yeast. *J. Biol. Chem.* 276, 7011-7016
  9. Rouault, T. A., and Tong, W. H. (2008) Iron-sulfur cluster biogenesis and human disease. *Trends Genet.* 24, 398-407
  10. Outten, C. E., and Albetel, A. N. (2013) Iron sensing and regulation in *Saccharomyces cerevisiae*: Ironing out the mechanistic details. *Curr. Opin. Microbiol.* 16, 662-668
  11. Ayer, A., Tan, S.-X., Grant, C. M., Meyer, A. J., Dawes, I. W., and Perrone, G. G. (2010) The critical role of glutathione in maintenance of the mitochondrial genome. *Free Radic. Biol. Med.* 49, 1956-1968
  12. Gietz, R. D., and Schiestl, R. H. (1991) Applications of high efficiency lithium acetate transformation of intact yeast cells using single-stranded nucleic acids as carrier. *Yeast.* 7, 253-263
  13. Daum, G., Böhni, P. C., and Schatz, G. (1982) Import of proteins into mitochondria. Cytochrome *b*<sub>2</sub> and cytochrome *c* peroxidase are located in the intermembrane space of yeast mitochondria. *J. Biol. Chem.* 257, 13028-13033
  14. Anderson, M. (1985) Glutathione and glutathione disulfide in biological samples. *Methods Enzymol.* 113, 548-555
  15. Ozer, H. K., Dlouhy, A. C., Thornton, J. D., Hu, J., Liu, Y., Barycki, J. J., Balk, J., and Outten, C. E. (2015) Cytosolic Fe-S cluster protein maturation and iron

- regulation are independent of the mitochondrial Erv1/Mia40 Import System. *J. Biol. Chem.* 290, 27829-27840
16. Guedouari, H., Gergondey, R., Bourdais, A., Vanparis, O., Bulteau, A. L., Camadro, J. M., and Auchère, F. (2014) Changes in glutathione-dependent redox status and mitochondrial energetic strategies are part of the adaptive response during the filamentation process in *Candida albicans*. *Biochim. Biophys. Acta - Mol. Basis Dis.* 1842, 1855-1869
  17. Bachhawat, A. K., Thakur, A., Kaur, J., and Zulkifli, M. (2013) Glutathione transporters. *Biochim. Biophys. Acta - Gen. Subj.* 1830, 3154-3164
  18. Sherman, F. (2002) Getting Started with Yeast • Contents • *Methods Enzymol.* 194, 3-21
  19. Poole, L. B. (2015) The basics of thiols and cysteines in redox biology and chemistry. *Free Radic. Biol. Med.* 80, 148-157
  20. Grant, C. M., MacIver, F. H., and Dawes, I. W. (1996) Glutathione is an essential metabolite required for resistance to oxidative stress in the yeast *Saccharomyces cerevisiae*. *Curr. Genet.* 29, 511-515
  21. Outten, C. E., and Culotta, V. C. (2004) Alternative Start Sites in the *Saccharomyces cerevisiae* GLR1 Gene Are Responsible for Mitochondrial and Cytosolic Isoforms of Glutathione Reductase. *J. Biol. Chem.* 279, 7785-7791
  22. Gostimskaya, I., and Grant, C. M. (2016) Yeast mitochondrial glutathione is an essential antioxidant with mitochondrial thioredoxin providing a back-up system. *Free Radic. Biol. Med.* 94, 55-65
  23. Protchenko, O., Ferea, T., Rashford, J., Tiedeman, J., Brown, P. O., Botstein, D.,

- and Philpott, C. C. (2001) Three Cell Wall Mannoproteins Facilitate the Uptake of Iron in *Saccharomyces cerevisiae*. *J. Biol. Chem.* 276, 49244-49250
24. Rutherford, J. C., Jaron, S., and Winge, D. R. (2003) Aft1p and Aft2p mediate iron-responsive gene expression in yeast through related promoter elements. *J. Biol. Chem.* 278, 27636-27643
25. Rutherford, J. C., Ojeda, L., Balk, J., Mühlenhoff, U., Lill, R., and Winge, D. R. (2005) Activation of the iron regulon by the yeast Aft1/Aft2 transcription factors depends on mitochondrial but not cytosolic iron-sulfur protein biogenesis. *J. Biol. Chem.* 280, 10135-10140
26. Lill, R., Diekert, K., Kaut, A., Lange, H., Pelzer, W., Prohl, C., and Kispal, G. (1999) The essential role of mitochondria in the biogenesis of cellular iron-sulfur proteins. *Biol. Chem.* 380, 1157-1166
27. Chen, O. S., Hemenway, S., and Kaplan, J. (2002) Inhibition of Fe-S cluster biosynthesis decreases mitochondrial iron export: Evidence that Yfh1p affects Fe-S cluster synthesis. *Proc. Natl. Acad. Sci.* 99, 12321-12326

## CHAPTER 5

### SUPPLEMENTARY METHODS

#### **Introduction**

This chapter describes experimental details used to obtain results specifically for this dissertation. Here, you will find tips for analyzing genetically modified strains and information about plasmids used for this study. All procedures were adapted from published protocols to obtain results for our purposes. Techniques discussed in detail are small-scale mitochondria isolation, the glutathione (GSH)/ glutathione disulfide (GSSG) assay, GSH uptake into isolated yeast mitochondria, mitochondrial purification, construction of deletion plasmids, and monitoring growth of yeast using the Synergy H1 plate reader. Isolation of mitochondria from other subcellular fractions was based on previously described methods (1). Depending on the subsequent analysis of organelles, the fractionation process was altered for data interpretation. To measure GSH and GSSG from whole cell and subcellular compartments, we utilized the 5,5'-dithiobis(2-nitrobenzoic acid) (DTNB) colorimetric enzyme cycling assay (2, 3). Localization studies on purified mitochondria were done using methods published by Meisinger et al. (4). GSH uptake into yeast mitochondria was modified from the Shertzer group (5). Construction of gene disruption plasmids was accomplished by standard cloning procedures. Lastly, the method developed for monitoring yeast growth using a plate reader was created using the manufacturer's instructions.

## **Small Scale Mitochondria Isolation**

Isolation of cytosolic and mitochondrial fractions was routinely used in conjunction with other assays to analyze biological changes in each compartment. To prepare extracts for analyzing glutathione and iron content, the mitochondrial isolation protocol from Daum et al. was modified (1). For instance, protease inhibitors were omitted prior to separation of cytosolic and mitochondrial fractions since prevention of protein hydrolysis was not critical for GSH and iron measurements. In addition, the culture volume was increased when growing *gsh1Δ* strains for GSH:GSSG analysis because the concentrations of GSH and GSSG are very low in these strains. The resuspension volume for isolated mitochondria in buffer was also adjusted for *gsh1Δ* samples used for GSH analysis.

Buffers Needed (sterile filter or autoclave buffers and store at 4°C):

**SOR buffer:** 1.2 M sorbitol, 20 mM Hepes, pH 7.5

**SM buffer:** 250 mM sucrose, 10 mM MOPS, pH 7.2

Enzyme Stocks

**Zymolyase 20T:** 20 mg/mL in H<sub>2</sub>O (zymolyase was prepared before use and stored at –20 °C. The enzyme is more effective if it is thawed from a frozen stock)

Fractionation Protocol

1. Grow cells overnight in 50-100 mL culture (SC or YPD) to mid-log phase. (Larger cultures of approximately 300-500 mL were used when working with *gsh1Δ* strains to obtain enough mitochondria to measure GSH.)

2. Harvest cells at 3000 rpm for 5 min.
3. Pre-weigh 1.5 mL microcentrifuge tubes and record values.
4. Pour off supernatant (SN), wash cell pellet in 1 mL H<sub>2</sub>O and transfer to pre-weighed microcentrifuge tubes.
5. Spin 10 s at 12000 rpm. Aspirate off SN.
6. Wash cells with 1 mL SOR and spin 10 s at 12000 rpm.
7. Aspirate off the SN and measure the net weight of the cell pellet.
8. Resuspend pellet in SOR buffer (1 mL / 150 mg cells).
9. Add 3 mg of zymolyase per gram of cells.
10. Mix by inverting 5 times and incubate in 30 °C water bath for 30 min to 1 hr.
11. Check spheroplasts after 45-50 min by adding 10 µL into a plastic cuvette and flush with 1 mL H<sub>2</sub>O. In another cuvette, flush 10 µL with 1 mL SOR buffer. If the cell wall of the yeast is no longer intact, the spheroplasts should lyse in H<sub>2</sub>O but not in SOR buffer. Therefore, the sample should look clear in water and cloudy in SOR.
12. Spin samples at 3500 rpm for 5 min at 4 °C. Aspirate off the SN.
13. Wash spheroplasts with 1 mL SOR buffer. (Care should be taken at this step in order to avoid bursting the spheroplasts.)
14. Spin for 5 min at 3500 rpm at 4 °C and aspirate off the SN.
15. Resuspend the spheroplasts in SM buffer (2 µL SM buffer per mg cells). Samples should be kept on ice from this step forward to prevent protein degradation.
16. Add phenylmethanesulfonyl fluoride (PMSF) to a final concentration of 0.5 mM and protease inhibitors at 1:100 dilution to the SM buffer of samples used for

- western blot analysis. (This step is omitted when fractions are used to measure intracellular GSH/GSSG and iron.)
17. Disrupt the plasma membrane of the spheroplasts with 30 strokes in a 1-mL Dounce homogenizer using a loose-fitting pestle.
  18. Spin 5 min at 3000 rpm at 4 °C and carefully transfer SN to a new tube.
  19. Repeat step 18 with the SN to completely remove all pellet debris.
  20. Measure the volume of SN extract after the second spin and record.
  21. Save some of this SN extract (total extract) for western blot analysis if desired.
  22. Spin remaining total extract at 12000 rpm for 10 min at 4 °C.
  23. Transfer SN containing the post-mitochondrial supernatant to a new tube.
  24. Gently wash the pellet comprised of crude mitochondria with 500  $\mu$ L SM buffer.
  25. Spin at 12000 rpm for 10 min at 4 °C and aspirate off the SN.
  26. Resuspend crude mitochondrial pellet in desired volume of SM buffer. (For western blot analysis mitochondria were resuspended in 1/5 volume of the total extract and protease inhibitors were included in the SM buffer.)
  27. Measure protein concentration of subcellular extract using the Bradford assay.

**Note:** When measuring GSSG in the mitochondria of *gsh1* $\Delta$  strains, more concentrated mitochondria are needed. Therefore, mitochondria were resuspended in a final volume of 25  $\mu$ L.

### **GSH/GSSG Assay using Synergy H1 Plate reader**

The GSH/GSSG assay described here was developed with the help of Malini Gupta to measure GSH and GSSG using a Synergy H1 Plate reader. Here, we successfully measured yeast lysates using the procedures outlined by Rahman et al. (2). Whole cell lysates were made according to published methods by Cuozzo et al. (6). In order to accurately measure GSSG, we used undiluted 2-vinylpyridine according to Cuozzo et al. and Anderson et al., (3, 6) rather than the 1:10 dilution recommended by Rahman et al. Another notable difference in the methods published by Rahman et al. was the use of sodium phosphate buffer with 1 mM EDTA (NaPE), while the Rahman protocol suggested potassium phosphate buffer with 5 mM EDTA (KPE). This change was made so that all reagents were the same as previously published methods by the C. Outten group (7, 8). The combined protocols and changes produced results comparable to published data from the lab.

Reagents in this method:

**0.1 M NaPE buffer**- 100 mM sodium phosphate, 1 mM EDTA sodium salt, pH 7.5

**1 mM NADPH** (prepared in NaPE buffer)- Make fresh and keep out of light

**2 mM DTNB** (prepared in NaPE buffer) – Make fresh and keep out of light

**3 U/mL GSSG reductase (GLR)** (prepared freshly in NaPE buffer)

**5-sulfosalicylic acid (SSA)**

**2-vinylpyridine**- do not dilute this product and use under fume hood

**25% triethanolamine** (prepared freshly in NaPE buffer)

#### Whole Cell GSH Sample Preparation:

1. Grow cells in YPD or SC selection media until mid-log phase in desired volume.
2. Collect  $2 \times 10^7$  cells (2 mL at 1 O.D.) by spinning at 12000 rpm for 30 s at room temperature. This amount is assuming 1 O.D. =  $1 \times 10^7$  cells. (For *gsh1Δ* strains harvest  $2 \times 10^9$  cells since [GSH] is low.)
3. Wash cells twice with water and aspirate off SN. Be careful not to disturb pellet.
4. Prepare 1 mL 10% 5-sulfosalicylic acid (SSA) by dissolving 100 mg of SSA into 1 mL of water. Prepare 5-10 mL 1% SSA depending on amount needed for assays.
5. Resuspend cells in 50  $\mu$ L of ice-cold 1% SSA and lyse with approximately 20  $\mu$ L of glass beads in bead beater. (For *gsh1Δ* strains, use 250  $\mu$ L of ice-cold 1% SSA with 100  $\mu$ L of glass beads.)
6. Bring extract to a final volume of 250  $\mu$ L using ice-cold 1% SSA. (Do not dilute *gsh1Δ* extracts.)
7. Allow cells to incubate on ice for 30 min.
8. Spin extract at 13000 x g for 5 min at 4 °C.
9. Samples can be measured immediately or frozen at -80 °C until ready to assay GSH.

#### Enzyme Assay Protocol:

1. Prepare a 100 mM GSH stock solution in NaPE buffer and dilute to 1 mM GSH in 1% SSA.
2. Create GSH standards of 0  $\mu$ M, 1  $\mu$ M, 2.5  $\mu$ M, 5  $\mu$ M, 7.5  $\mu$ M, 15  $\mu$ M, and 25  $\mu$ M GSH using 1% SSA by serially diluting each standard from the 1 mM GSH stock.

3. Mix equal volumes of freshly prepared DTNB and GLR solutions in a reagent reservoir. Keep the reservoir covered with aluminum foil while working with lights on.
4. In a separate reservoir add freshly prepared NADPH solution. Keep covered with aluminum foil while working with lights on.
5. Add 20  $\mu\text{L}$  of the blank, standards, and sample into individual wells of a clear non-sterile 96-well plate.
6. Add 120  $\mu\text{L}$  of the DTNB/GLR mixture into each well and pipet up and down to mix.
7. Allow 30 s for the conversion of GSSG to GSH, then add 60  $\mu\text{L}$  of NADPH and pipet up and down to mix.
8. Read the absorbance at 412 nm every 15 s for 2 min.

Preparation of GSSG samples:

1. Prepare a 50 mM GSSG stock solution in NaPE buffer and dilute to 0.5 mM GSH in 1% SSA.
2. Create GSSG standards of 0  $\mu\text{M}$ , 0.5  $\mu\text{M}$ , 1  $\mu\text{M}$ , 2.5  $\mu\text{M}$ , 5  $\mu\text{M}$ , 7.5  $\mu\text{M}$ , and 12.5  $\mu\text{M}$  GSH in 1% SSA by serially diluting each standard from the 0.5 mM GSSG stock.
3. Transfer 50  $\mu\text{L}$  of the acidified cell extract into a 1.5 mL Eppendorf tube (for mitochondrial samples use 25  $\mu\text{L}$ ).

4. Add 1  $\mu\text{L}$  2-vinylpyridine to the 50  $\mu\text{L}$  acidified cell extract and vortex the mixture (for mitochondrial samples use 0.5  $\mu\text{L}$  for 25  $\mu\text{L}$ ). Use the fume hood when working with 2-vinylpyridine.
5. To the 2-vinylpyridine treated samples add 1  $\mu\text{L}$  of 25% triethanolamine (for mitochondrial samples use 0.5  $\mu\text{L}$ ).
6. Incubate under the fume hood for 1 hour at room temperature.
7. Prepare reagents and read GSSG samples as described above for GSH.

### **Large Scale Mitochondria Isolation and Purification**

The Large Scale Mitochondria Isolation Protocol described in this dissertation was adapted from previously described methods (4, 9). In this protocol, I have outlined details about wash and resuspension volumes that worked well. Notes for how to obtain mitochondria without ER and vacuole contamination are also included. Unfortunately, our data suggested that plasma membrane cannot be completely separated from mitochondria via density gradient ultracentrifugation.

Reagents for this method: (sterile filter or autoclave buffers and store at 4 °C):

**Zymolyase buffer:** 1.2 M sorbitol, 20 mM potassium phosphate, pH 7.4

**SEM buffer:** 250 mM sucrose, 1mM EDTA, 10 mM MOPS-KOH, pH 7.2 (stable for 1 month)

**DTT buffer:** 100 mM Tris- $\text{H}_2\text{SO}_4$ , pH 9.4, 10 mM dithiothreitol (DTT) (add DTT just prior to use)

**Homogenization buffer:** 0.6 M sorbitol, 10 mM Tris-HCl, pH 7.4, 1 mM EDTA, 1 mM PMSF, 0.2% BSA (add PMSF from a freshly prepared 100 mM stock in ethanol just prior to use)

#### Enzyme Stocks

**Zymolyase 20T** (ICN Biochemical): 20 mg/mL in H<sub>2</sub>O – store at - 20°C. (Note: zymolyase works better after stock is stored at -20°C then thawed – NOT freshly made)

#### Sucrose Gradient Buffer

**EM buffer:** 1 mM EDTA, 10 mM MOPS-KOH, pH 7.2 (used for making various concentrations of sucrose at the mitochondrial purification step)

#### Isolation of Crude Mitochondria Fraction Protocol

1. Patch single colony from freezer stock onto plates and grow at 30 °C until patch is thick enough to start overnight cultures.
2. Grow cells in 100 mL YPG (3% glycerol) or SC (synthetic complete) selection media using a 500 mL flask at 30 °C overnight to exponential phase. Mitochondria will be more abundant in non-fermentative medium (e.g. glycerol).
3. The next morning, dilute cells into 1.5 L of media using 5-L flasks to O.D. of 0.03 (or required O.D.).

4. Grow cells until an O.D. of 2 is reached.
5. Harvest cells at 3000 x g for 5 min at 4 °C. All centrifugation during the isolation of crude mitochondria was done using the Avanti J-E Centrifuge (Consult Dr. Wayne Outten's group for use).
6. Pre-weigh 50-mL centrifuge tubes.
7. Pour off SN and resuspend cell pellet in 30 mL H<sub>2</sub>O.
8. Spin at 3000 x g for 5 min at 4 °C. Pour off SN. Repeat steps 7 and 8.
9. Measure net wt. of cell pellet in 50-mL centrifuge tubes. (typical weight is 3-4 g/L)
10. Resuspend pellet in pre-warmed DTT buffer (2 mL/g cells). Shake at 80 rpm at 30 °C for 20 min.
11. Centrifuge cells at 3000 x g for 5 min at 4 °C.
12. Resuspend the pellet in zymolyase buffer (7 mL/g) without zymolyase. Centrifuge at 3000 x g for 5 min at 4 °C.
13. Resuspend the pellet in zymolyase buffer (7 mL/g). Add 3 mg of zymolyase per g of cells. Shake at 80 rpm at 30 °C for 30-45 min.
14. Centrifuge cells at 3000 x g for 5 min at 4 °C and remove SN.
15. Gently wash pellet in zymolyase buffer (7 mL/g).
16. Centrifuge cells at 3000 x g for 5 min at 4 °C and remove SN.
17. Resuspend pellet in ice-cold homogenization buffer (6.5 mL/g + 1:100 protease inhibitors). Samples should be kept on ice from this step forward to prevent protein degradation.
18. Pestle 15 slow strokes in a pre-chilled homogenizer (use a large Dounce homogenizer with loose fitting pestle).

19. Add 1 equal volume of homogenization buffer. Spin 5 min at 1500 x g at 4 °C. Carefully transfer SN to a new tube (pellet contains unbroken cells and nuclei, SN contains crude cytosolic fraction and mitochondria).
20. Centrifuge the SN at 4000 x g for 5 min at 4 °C. Discard the pellet.
21. Spin remaining total extract at 12000 x g for 10 min at 4 °C and remove SN.
22. Resuspend the pellet in ~ 2 mL SEM buffer and centrifuge again at 4000 x g for 5 min at 4 °C, followed by a second spin of the SN at 12000 x g for 10 min at 4 °C. Remove SN. (This step is optional and used to obtain purer mitochondria.)
23. Gently resuspend pellet (crude mitochondria) in 100 µL of SEM buffer. (Cut 2 mm off a yellow tip to avoid disruption of mitochondria.)
24. Determine the concentration of crude mitochondria.
25. The sample can be flash frozen in liquid nitrogen and stored at -80 °C.

**Note:** Prior to purification, crude mitochondria were placed in a glass-Teflon homogenizer and given 10 strokes using a loose pestle. This step was done to ensure that ER and vacuole contamination was removed during the purification step.

#### Purification of Crude Mitochondria Protocol

1. Prepare sucrose gradient by loading 1.5 mL of 60% sucrose (prepared in EM buffer) onto the bottom of ultra-clear centrifuge tubes (Beckman No. 344059). Pipet carefully without disturbing the phases in a stepwise manner by adding 4 mL of 32% sucrose, 1.5 mL of 23% sucrose, and 1.5 mL of 15% sucrose (all prepared in EM buffer). Keep tubes in the fridge for at least 2-3 hours before use. (A needle syringe was used to create the sucrose gradient.)

2. Carefully load the crude mitochondria (0.2 - 1 mL) on top of the sucrose gradient immediately before centrifugation step.
3. Centrifuge for 1 hour at 2 °C at 134000 x g (33000 rpm). The Beckman SW41 Ti swinging-bucket rotor was used in during this step. (Consult with Dr. Qian Wang's group about using the ultracentrifuge.)
4. Recover the purified mitochondria with a Pasteur pipet between the 60% and 32% sucrose interface.
5. If more than one sucrose gradient was needed, pool all mitochondrial samples and dilute with 2X volume of SEM buffer.
6. Pellet the mitochondria using 10000 x g at 4 °C. (Sorvall™ Legend™ Micro 21R refrigerated microcentrifuge was used for this step.)
7. Resuspend the mitochondrial pellet in a small (100-200 µL) volume of SEM and determine the concentration.
8. The sample can be flash frozen in liquid nitrogen and stored at -80 °C.

### **Extraction of Plasma Membrane Proteins from Whole Cells**

To extract the Hgt1-HA protein out of the plasma membrane of whole cell extracts, the lysis buffer listed below was modified from the total cell extract buffer described by Aggarwal et al. (10). Cell extracts were made using 150 µL glass beads and 250 µL lysis buffer. Samples were lysed by vortexing the sample for one minute and incubating on ice for one minute between vortexing. This step was repeated four times. The resulting SN was spun at 13000 rpm for 5 min at 4 °C and transferred to a sterile microcentrifuge tube.

Plasma membrane lysis buffer:

- 50 mM Tris-CL, pH 7.5
- 1% sodium deoxycholate
- 1% Triton-X-100
- 0.1% sodium dodecyl sulfate
- 0.05% phenylmethylsulfonyl fluoride (PMSF)

### **GSH Uptake in Isolated Yeast Mitochondria**

Mitochondrial samples were prepared using the Small Scale Mitochondria Isolation Protocol described above. Uptake of GSH was adapted from the protocol described by Shen et al. (5). Incubation temperature was adjusted to 30 °C which is conducive for yeast. The concentration of GSH added was determined experimentally so that uptake could be measured using the GSH/GSSG assay described above. Incubation time was determined using data reported by Kumar et al. that showed GSH levels spike within an hour of *HGT1* overexpression strains treated with GSH (11).

Reagents used for this assay:

**SM buffer:** 250 mM sucrose, 10 mM MOPS, pH 7.2 (sterile filter or autoclave)

**EM buffer:** 1 mM EDTA, 10 mM MOPS-KOH, pH 7.2

**27% sucrose:** To make 100 mL, dissolve 27 g sucrose in about 70 mL EM buffer; once dissolved, make up volume to 100 ml total by adding EM buffer. (Sterile filter and store at 4 °C.)

### GSH Uptake Protocol:

1. Make freshly prepared mitochondria according to the Small Scale Mitochondria Isolation Protocol. During step 15 do not use protease inhibitors or PMSF, because mitochondria will be used for the GSH/GSSG assay.
2. Resuspend mitochondria in 1/5 of the total extract volume using SM buffer and take the protein concentration via the standard Bradford assay.
3. Resuspend the mitochondria in 1.5 micro-centrifuge tubes at 2 mg/mL and treat with 15 mM GSH prepared in SM buffer.
4. Using a needle syringe, pipette 250  $\mu$ L of 27% sucrose under the mitochondria slowly, creating a cushion.
5. Place the tubes in the 30 °C incubator for 30 min to allow GSH uptake into mitochondria.
6. Centrifuge mitochondria through the sucrose cushion at 14000 x g for 10 min at 4 °C.
7. Aspirate off the SN and wash mitochondria very carefully with 500  $\mu$ L SM.
8. Centrifuge at 14000 x g for 10 min at 4 °C.
9. Aspirate off the SN and add 50  $\mu$ L of 1% SSA.
10. Incubate on ice for 30 min.
11. Spin 5 min at 13000 x g and transfer to new tube.
12. Sample can be frozen at -80 °C until ready to assay total GSH.

## **Chromosomal Replacement- Cloning of the *GSH1* Deletion Plasmid**

Creation of the *GSH1* deletion plasmid (pGSH1KO) was prepared using integrating plasmid vectors pRS403 and pRS406. Upstream and downstream regions of the *GSH1* gene were cloned into the empty vectors using standard cloning procedures. The resulting yeast integrating plasmids were linearized with EcoRI prior to transformation into yeast (Fig 5.1). *GSH1* is knocked out of strains containing pGSH1KO via homologous recombination.

1. Choose an empty vector with the selection marker of choice and look for restriction enzyme sites in the vector that can be used for cloning in fragments. (The upstream and downstream regions of the *GSH1* gene was cloned into the pRS403 and pRS406 vectors at the BamHI and Sall sites).
2. Create primers to amplify the upstream and downstream regions of *GSH1* that will include portions of the gene. In the case of pGSH1KO, restriction enzymes sites were engineered into the primers so the two PCR fragments are ligated together with EcoRI and cloned into the vector with BamHI and Sall (see Chapter 3 for primer sequences).
3. Ligate both the upstream and downstream PCR fragments into the yeast integrating plasmid containing an amino acid selectable marker using T4 DNA Ligase (NEB) at 16 °C overnight or at room temperature with various ratios of vector to fragments. Transform the ligation reactions into DH5 $\alpha$  cells using 10  $\mu$ L of each reaction ratio using the standard *E. coli* transformation protocol. (LB-amp plates were used when

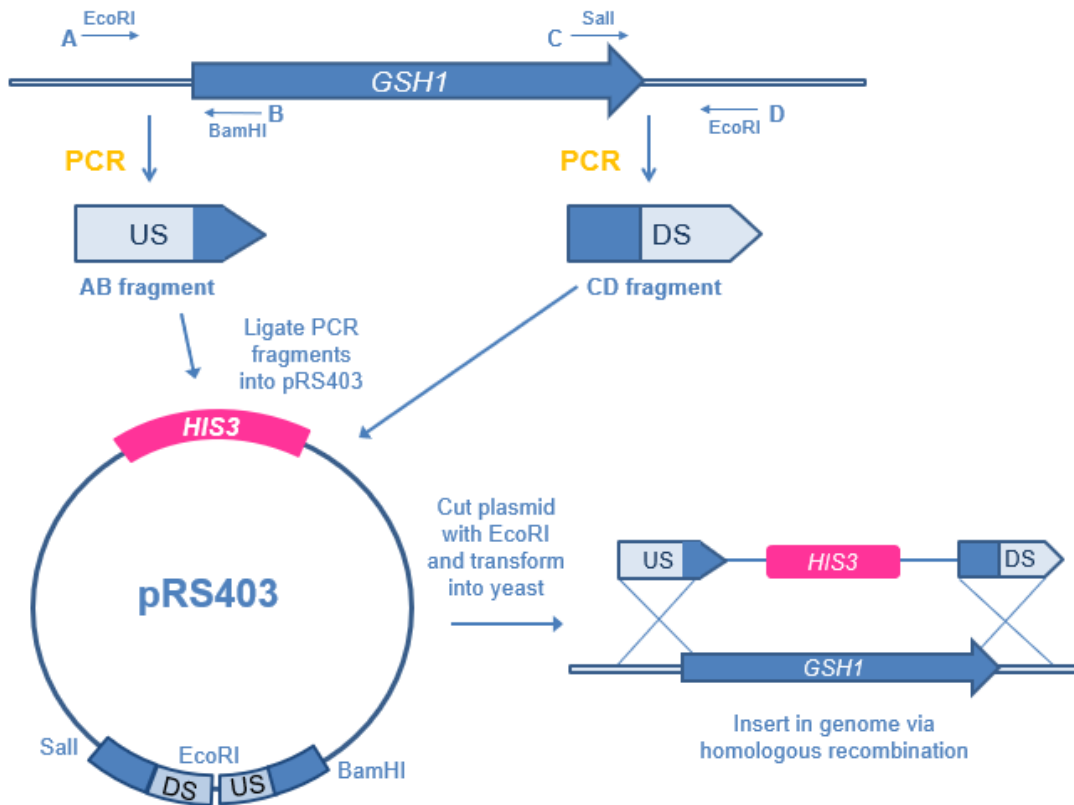


**Figure 5.1 Diagram of steps for creating the pGSH1KO plasmid.** This illustration represents the PCR products and ligation into the empty vector pRS403 by engineering restriction sites into primers. The subsequent digestion and integration in the yeast genome is also depicted.

- creating the *GSHI* deletion plasmid since the pRS403/406 vectors confer ampicillin resistance)
4. Confirm formation of the correct deletion plasmid by restriction mapping and DNA sequencing.
  5. Linearize the yeast integrating plasmid overnight at 37 °C via restriction enzyme digest. (EcoRI restriction digest was performed on the *GSHI* deletion plasmid)
  6. After linearization, the integrating deletion plasmid can be inserted into the genome of yeast strains via homologous recombination using standard lithium acetate transformation protocols.
  7. *GSHI* deletion can be confirmed via PCR colony screening, GSH assay, and Gsh1 western blot analysis.

### **Growth Curve Assay- Synergy H1 Plate reader**

Yeast cell growth was analyzed using a Synergy H1 plate reader. The manufacturer's instructions were followed to establish the protocol. The procedure outlined below details the assay and subsequent analysis of growth. We found that yeast started at O.D. lower than 0.05 could not be detected. Thus, all strains grown using this method were blank corrected from cells started at O.D. = 0.05 (12, 13).

Procedure:

1. Grow cells on a plate until a patch of cells form. This normally takes about 2-3 days.

2. Resuspend a loopful of cells into 1 mL of sterile water and take O.D. in a clear 96 well plate using the plate reader. (This 96-well plate does not have to be sterile)
3. After taking the O.D., dilute each strain to 0.5 O.D. in new sterile micro-centrifuge tubes.
4. Add 20  $\mu$ L of the 0.5 O.D. of cell stock into a sterile flat bottomed clear 96-well microplate (Corning 96-well plates, catalog number 3596 were used in this study)
5. To the cells, add 180  $\mu$ L of autoclaved media so that the starter O.D. is 0.05 (starting cells at O.D. of less than 0.05 is difficult to detect using this method and may yield negative values when subtracted from blank)
6. Leaving the clear plastic top off, seal the top of the 96-well plate with a clear membrane. This allows cells to have aeration during growth while reducing contamination and evaporation. (The Breath Easy sealing membranes from Sigma-Aldrich (catalog # Z380059) were used for all growth curves)
7. Place sealed 96-well plate in the plate reader without the lid.
8. Select wells to be read in the procedure and plate layout sections. (The software used for this experiment is Gene5 2.09.)
9. Allow temperature to reach 30  $^{\circ}$ C before taking initial readings. Measurements were taken every 30 min with the continuous orbital shaking mode set over a course of 24 hrs. The shaking speed was set to slow and frequency set at 559 (1 mm amplitude).
10. Analyze growth curves by plotting the blank corrected OD<sub>600</sub> values of each strain over time on a logarithmic scale.

## References

1. Daum, G., Böhni, P. C., and Schatz, G. (1982) Import of proteins into mitochondria. Cytochrome *b*<sub>2</sub> and cytochrome *c* peroxidase are located in the intermembrane space of yeast mitochondria. *J. Biol. Chem.* 257, 13028-13033
2. Rahman, I., Kode, A., and Biswas, S. (2006) Assay for quantitative determination of glutathione and glutathione disulfide levels using enzymatic recycling method. *Nat. Protoc.* 1, 3159-3165
3. Anderson, M. (1985) Glutathione and glutathione disulfide in biological samples. *Methods Enzymol.* 133, 548-555
4. Meisinger, C., Sommer, T., and Pfanner, N. (2000) Purification of *Saccharomyces cerevisiae* mitochondria devoid of microsomal and cytosolic contaminations. *Anal. Biochem.* 287, 339-342
5. Shen, D., Dalton, T. P., Nebert, D. W., and Shertzer, H. G. (2005) Glutathione redox state regulates mitochondrial reactive oxygen production. *J. Biol. Chem.* 280, 25305-25312
6. Cuozzo, J. W., and Kaiser, C. A. (1999) Competition between glutathione and protein thiols for disulphide-bond formation. *Nat. Cell Biol.* 1, 130-135
7. Outten, C. E., and Culotta, V. C. (2004) Alternative Start Sites in the *Saccharomyces cerevisiae* GLR1 Gene Are Responsible for Mitochondrial and Cytosolic Isoforms of Glutathione Reductase. *J. Biol. Chem.* 279, 7785-7791
8. Hu, J., Dong, L., and Outten, C. E. (2008) The redox environment in the mitochondrial intermembrane space is maintained separately from the cytosol and matrix. *J. Biol. Chem.* 283, 29126-29134

9. Meisinger, C., Pfanner, N., and Truscott, K. N. (2006) Isolation of mitochondria. *Methods Mol. Biol. Clift. Nj.* 313, 33-39
10. Aggarwal, M., and Mondal, A. K. (2006) Role of N-terminal hydrophobic region in modulating the subcellular localization and enzyme activity of the bisphosphate nucleotidase from *Debaryomyces hansenii*. *Eukaryot. Cell.* 5, 262-271
11. Kumar, C., Igarria, A., D'Autreaux, B., Planson, A. G., Junot, C., Godat, E., Bachhawat, A. K., Delaunay-Moisan, A., and Toledano, M. B. (2011) Glutathione revisited: A vital function in iron metabolism and ancillary role in thiol-redox control. *EMBO J.* 30, 2044-2056
12. Quigley, T. (2008) Monitoring the Growth of *E. coli* With Light Scattering Using the Synergy™ 4 Multi-Mode Microplate Reader with Hybrid Technology™. *BioTek*
13. Held, P. (2010) Monitoring Growth of Beer Brewing Strains of *Saccharomyces Cerevisiae*-The utility of synergy H1 for providing high quality kinetic data for yeast growth applications. *Biotek Appl. Note.* 10.1109/IEMDC.2009.5075199